CNSOPB

CANADA-NOVA SCOTIA
OFFSHORE PETROLEUM BOARD

Deep Panuke Resource Management Study

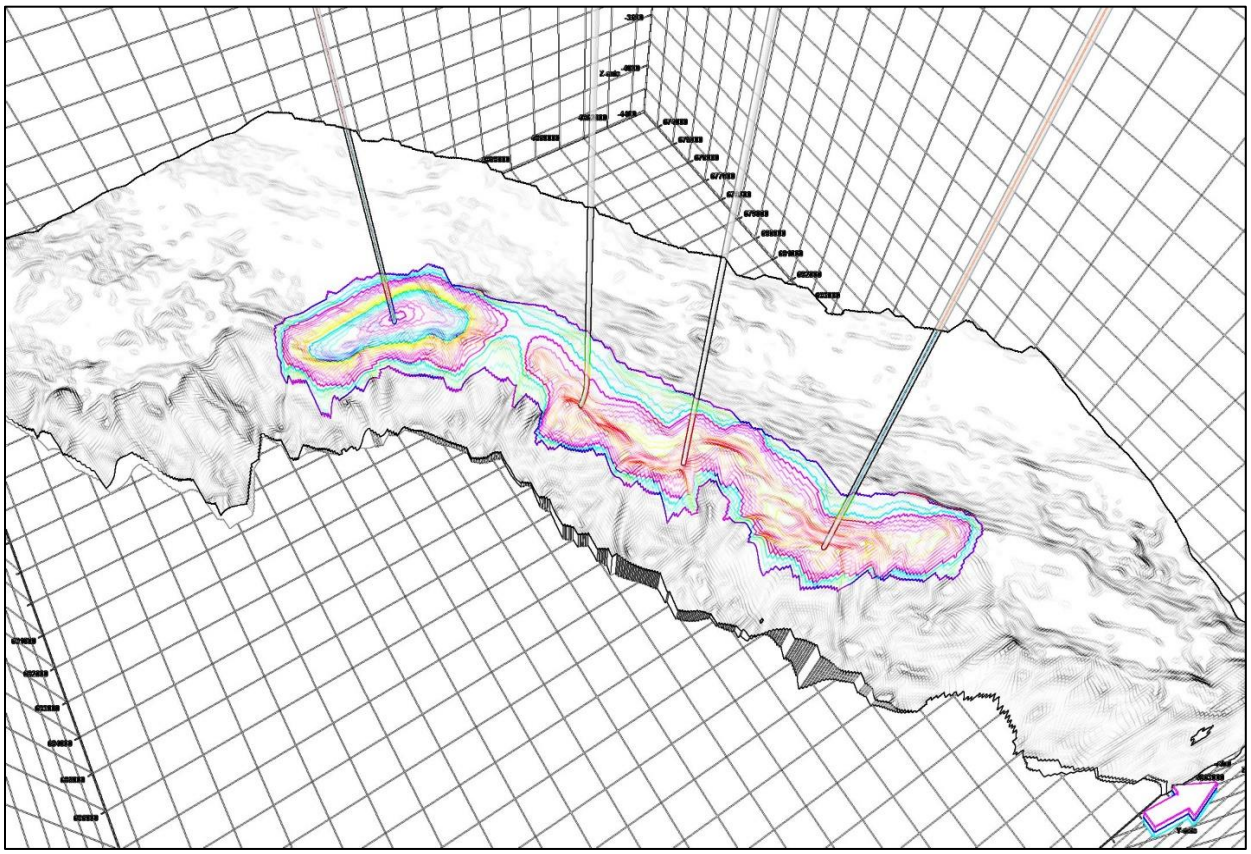

Ehsan Belghiszadeh, Carl Makrides, Brent Smith

December 16, 2020

Contents

Executive Summary

The Deep Panuke gas field was discovered in 1998 by PanCanadian Energy Corporation's Panuke PP3C J-99 (PP3C) well. The PP3C well encountered sour natural gas in the fractured and porous limestones of the Baccaro Member within the Abenaki Formation. The field was delineated by eight additional wells, including sidetracks, that were drilled between 1999 – 2003.

Four of the original Deep Panuke delineation wells were re-completed as production wells (Panuke H-08, Panuke M-79A, Margaree F-70 and MarCoh D-14). These four production wells were tied back, via subsea flowlines, to an offshore production platform for processing. The processed sales ready gas was then exported to landfall in Goldboro, Nova Scotia via a 22" export pipeline. Production from Deep Panuke started in August 2013 and was permanently shut down in May 2018. The peak gas rate was 8.5 E6m3/d (300 MMscf/d). The project operated seasonally from 2015 to 2018 to maximize economic recovery by only producing during the winter months when gas prices were higher.

Studies of gas fields, similar to Deep Panuke, indicate that the recovery factors of naturally fractured carbonate reservoirs with active aquifers are typically low (in some cases as low as 20% of the original gas in place) as the fractures can act as conduits into the water leg.

In November 2006, Encana, as operator of the project, submitted the final Deep Panuke Development Plan Application (2006 DPA) to the Canada Nova Scotia Offshore Petroleum Board (CNSOPB). Based on the 2006 DPA, the Deep Panuke gas field was expected to recover 18.6 E9m3 (659 Bcf) of gas. Original Gas in Place (OGIP), recovery efficiency, aquifer drive potential, reservoir compartmentalization, fracture heterogeneity and well completion challenges were identified as the main subsurface uncertainties by the operator.

The CNSOPB conducted independent geological, geophysical and petrophysical interpretations and studies of the Deep Panuke field. The results of these interpretations and studies were used to create an independent dynamic simulation model of the Deep Panuke reservoir. For the duration of the Deep Panuke project, the simulation model was the primary tool used to evaluate the operator's production strategies to ensure waste of the resource did not occur and economic hydrocarbon recovery from the field was maximized. The CNSOPB's simulation model was also used to evaluate a number of sensitivities such as vertical matrix and fracture permeability, perforation length, rate variability and drilling of additional wells. CNSOPB regulatory oversight of the Deep Panuke project included but was not limited to the following: daily monitoring and surveillance of production data, review of daily, monthly and annual reports, review of Resource Management Plans (RMP) and other resource management documents and regular audits of the operator's production strategies and practices.

The key conclusions and lessons learned from the CNSOPB's Deep Panuke Resource Management Study appear in Chapter 9 of this report.

1. Introduction

The purpose of the CNSOPB's Deep Panuke Resource Management Study is to describe the resource management practices and strategies used by the operator during the life of the Deep Panuke Offshore Gas Development (Deep Panuke). This report also describes the regulatory oversight activities and analyses conducted by the CNSOPB to ensure waste of the Deep Panuke resources did not occur by ensuring economic hydrocarbon recovery was maximized.

In 1992, LASMO Nova Scotia Limited (LASMO) and Nova Scotia Resources (Ventures) Limited (NSRL) began producing light oil from the Cohasset and Panuke oil fields (Cohasset/Panuke Project). In 1996, PanCanadian Petroleum Ltd (PanCanadian) became the operator of the Cohasset/Panuke Project. While producing oil from the Cohasset/Panuke Project, PanCanadian was also conducting exploration drilling in the area. In 1998, PanCanadian sidetracked and deepened the lower portion of the Panuke PP-3B J-99 production well to penetrate a target in the underlying Abenaki carbonate bank. This new exploration well was named Panuke PP-3C J-99 (PP-3C) and resulted in the discovery of the Deep Panuke gas field. This well encountered sour natural gas in the fractured and porous carbonates of the Baccaro Member of the Abenaki Formation.

In 2002, PanCanadian merged with the Alberta Energy Company Ltd. to form Encana Corporation (Encana). After the PP-3C discovery well was drilled, the operator drilled a number of delineation wells in the Deep Panuke field, some of which were sidetracked. These wells were drilled during 1999 - 2003 and include the following: Panuke PI-1A/PI-1B J-99 (PI-1B), Panuke H-08 (H-08), Panuke F-09 (F-09), Panuke M-79/M-79A (M-79A), Margaree F-70 (F-70), and MarCoh D-41 (D-41). These wells delineated a natural gas reservoir which was estimated to

contain 11.5 – 26.2 E9m3 (407 – 931 Bcf) of recoverable gas based on Encana's 2006 DPA for the Deep Panuke Offshore Gas Development (Deep Panuke).

The Deep Panuke gas field is located approximately 250 km southeast of Halifax and 47 km west of Sable Island. The field development concept described in the operator's 2006 DPA was to convert four of the original Deep Panuke delineation wells (H-08, M-79A, F-70, and D-41) into production wells. The four production wells would be completed and tied back via subsea flowlines to a jack-up type offshore production platform (Production Field Centre or PFC). The produced gas would be processed on the PFC and then exported via subsea pipeline to landfall at Goldboro, Nova Scotia, located approximately 176 km northwest of the PFC. The produced gas would be transported via pipeline from Goldboro to markets in Canada and the United States.

Deep Panuke produced from 2013 to 2018. The project operated seasonally from 2015 to 2018, which allowed gas revenues to be optimized by only producing during the colder months when natural gas prices were higher.

The PFC was designed for a peak gas production rate of 8.5 E6m3/d (300 MMscf/d). The raw gas produced from Deep Panuke contained approximately 0.18% hydrogen sulphide (H2S); therefore, gas sweetening equipment was installed on the PFC. An amine sweetening system was used to remove the H2S and some of the CO2 (acid gas). The Margaree E-70 (E-70) acid gas injection well was drilled in 2010 as part of the Deep Panuke project. The H2S and CO2 removed during gas processing on the PFC were injected into the E-70 acid gas injection well.

2. Literature Review

This section includes a brief summary of the most important papers/studies published by the academic community and industry on the reservoir engineering principles and flow processes of naturally fractured gas reservoirs similar to Deep Panuke.

In fractured reservoirs, the fracture system dominates the flow of fluids; therefore, a description of these inter-connecting networks is essential. These systems can however rarely be defined from direct observation. Production tests would be the most reliable method of estimating the flow characteristics and productivities of fractured reservoirs. Lithology has a considerable impact on fracture density and fracture intensity is generally much higher in carbonate rocks than sandstones. Reservoir characterization and production geology in fractured reservoirs relies heavily on core data however; in many cases, core recovery is very poor due to the fractured nature of these reservoirs.

The physical principles that control recovery are similar for both fractured and non-fractured reservoirs. The main difference is the relative importance of these principles. If the fractures did not exist, many fractured reservoirs could not be produced economically. The combination of high porosity/low permeability matrix and low porosity/high permeability fractures is the key to the productivity of wells drilled in porous fractured reservoirs.

Forecasting the performance of fractured reservoirs is usually more difficult than conventional reservoirs. Simplified models (Figure 2.1) are typically used to predict fluid flow in the reservoir as well as matrix fracture fluid transfer (Heinemann & Mittermeir, 2014).

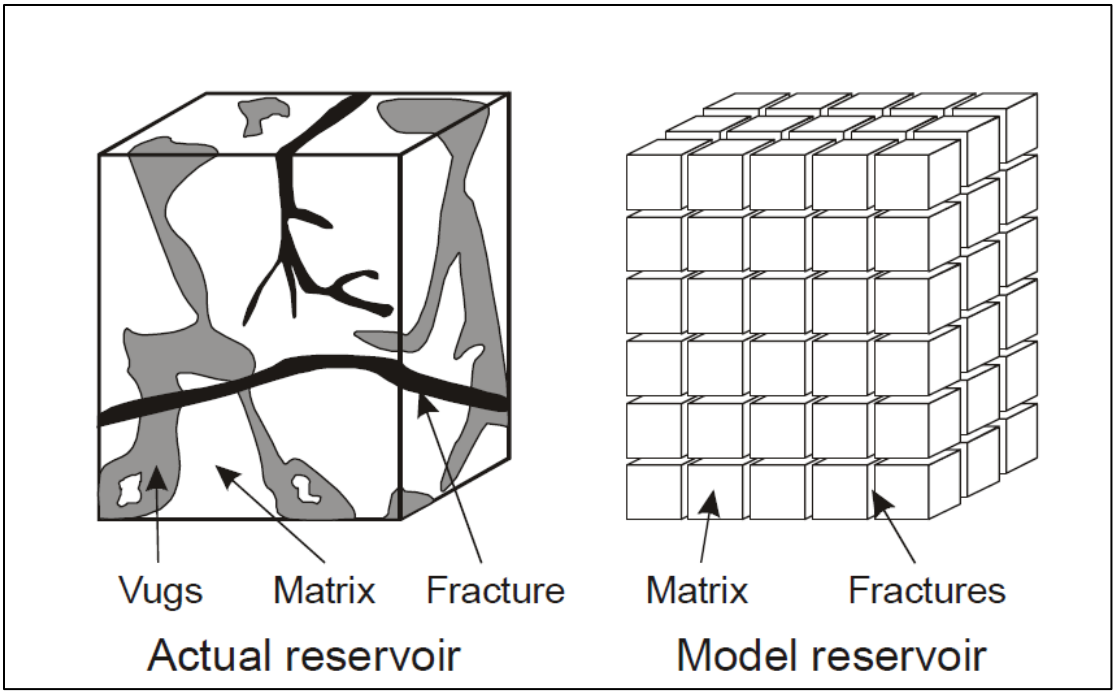

Figure 2.1: Simplified model of fractured reservoirs (Heinemann& Mittermeir, 2014). This figure shows how the matrix and fractures are modeled in the software.

Simulation modeling, as mentioned above is the primary tool in managing fractured reservoirs and predicting their performance. Fractured reservoirs are usually divided into blocks and each block is associated with a set of fractures and matrix properties.

Recovery factors of naturally fractured gas reservoirs with aquifers are typically low (as low as 20% of the original gas in place). Fractures in these reservoirs are seen as conduits into the water leg. In an effort to minimize water production, gel treatments, rate restrictions, and plug backs are often used; however, these methods are not usually successful. Laboratory work, demonstrates that water will continue to imbibe into tight matrix rock submerged under water for months. This implies that the best operating strategy may be to produce the wells at the highest rates possible until water breakthrough, followed by a shut-in period of perhaps several years to allow gas to re-accumulate (Pow, Kantzas, Allan & Mallmes, 1999).

Based on Pow et al, abrupt water production from wells producing from fractured carbonate gas reservoirs is not normally caused by coning or channeling. They mention that due to viscosity of gas typically being two orders of magnitude less than the viscosity of water, and the density of gas being an order of magnitude lower than the density of water at reservoir conditions, extremely high-pressure gradients are required to generate a small cone in a permeable fracture system (Pow et al, 1999).

Aguilera, 1999, showed that recovery factors could range from 12% to 60% in naturally fractured reservoirs with water drive, similar to Deep Panuke, depending on the strength of the water drive.

3. Deep Panuke Analogue Fields

There are numerous examples of naturally fractured gas reservoirs with active aquifers in the foothills of Alberta and northeastern British Columbia. Examples include the Pincher Creek field in Alberta and the Bucking Horse, Pocketknife, Sikanni and Grassy fields in British Columbia.

Gas reservoirs in the Mississippian Debolt Formation in the Buckinghorse, Pocketknife, Grassy and Sikanni fields of northeast British Columbia can be considered analogues to Deep Panuke in terms of reservoir processes. No correlation in these fields was observed between recovery efficiency and production rate. The best production strategy was determined to be producing the wells as quickly as possible until water breakthrough, followed by well shut-ins to allow time for matrix imbibition and gas accumulation in the near-wellbore region.

In the Bucking Horse Debolt fractured A Pool, the original gas in place was approximately 689 E6m3 (24.3 Bcf) and the final recovery was 151.2 E6m3 (5.34 Bcf), resulting in a recovery factor of only 22%. Analyzing this field, Pow et al concluded that matrix imbibition continued for many years even after the wells watered out and production was suspended. They also identified that coning had a minor effect on recovery and the best production strategy was to produce the wells at the highest possible rate until they watered out and then shut them in for gas re-accumulation (Pow et al, 1999).

The Beaver River field on the border of the Yukon and British Columbia (BC) is another fractured carbonate reservoir analogous to Deep Panuke. This field experienced a significant loss of reserves due to vertical permeability issues. This field was once believed to be BC’s largest gas field with estimated recoverable reserves of one Trillion cubic feet (Tcf) of gas. The initial rates of over 5.7 E6m3/d (200 MMscf/d) from six production wells were also promising. The rapid

increase in water production caused the production rate to decline to 85 E3m3/d (3 MMscf/d) after only 5 years. The rapid influx of water was not caused by water coning but was caused by the permeable aquifer in combination with high vertical permeability and the small matrix pore volume.

4. History of the Deep Panuke Development

Panuke PP-3C J-99 (PP-3C) was the discovery well for the Deep Panuke gas field. PP-3C was spudded in July 1998 and reached total depth in April 1999, in the Abenaki Formation. This well was followed by a number of delineation wells drilled to determine the areal extent and resource potential of the field. The initial Deep Panuke Development Plan Application (DPA) was submitted to the CNSOPB in March 2002. This DPA was withdrawn in 2003 to allow the operator to conduct additional evaluations of the project. In November 2006, the operator submitted a revised Deep Panuke DPA, which received approval from the CNSOPB in September 2007.

4.1. Initial Deep Panuke Development Plan Application (March 2002)

PanCanadian Energy Corporation (PanCanadian) submitted the original Deep Panuke DPA in March 2002. The PP-3C well was the Deep Panuke's discovery well and was followed by four delineation wells drilled during 1999 - 2000: PI-1B, H-08, F-09 and M-79A. Based on the available data, PanCanadian estimated that the Deep Panuke gas field contained 34 E9m3 (1.2 Tcf) of gas in place (expected value) and 26.5 E9m3 (935 Bcf) of recoverable gas. The reservoir was estimated to have low associated liquid volumes, 318 m3 (2000 barrels) per day at peak gas rate of 11.3 E6m3/d (400 MMscf/d), and approximately 0.2% hydrogen sulfide.

The initial analysis performed by PanCanadian showed that Deep Panuke would produce natural gas from a porous carbonate reservoir located 3500-4000 meters below the seafloor. The gas field was located on the margin of the carbonate platform in the Abenaki Formation.

The Deep Panuke gas field was determined to be normally pressured and the hydrological review of the logs and well test data indicated a common pressure system with a single field-wide gas-water contact. The majority of the gas was believed to be trapped in the Abenaki 5 sequence,

with the minor gas present in the upper part of the Abenaki 4 sequence. There may also be additional reserves in the lower portion of the Abenaki 6 sequence but no wells had encountered significant porosity development in this interval. The following table (Table 4.1.1) shows a list of the Deep Panuke wells drilled from 1998 to 2000.

Table 4.1.1: Wells drilled by PanCanadian from 1998 to 2000

Well ID	Year Spudded	Total Measured Depth (m)
PP-3C	1998	4163.4
PI-1A	1999	4030
PI-1B	1999	4046.3
H-08	2000	3682
M-79	2000	4598.3
M-79A	2000	3934.7
F-09	2000	3815

Reservoir models were generated by merging well porosity data with seismic attributes in a mathematical process. Permeability were modeled based on core porosity and permeability data. The Archie equation was used to model water saturations. PanCanadian created a simulation model of the Deep Panuke field. This simulation model was used to investigate the main uncertainties as understood at the time of the initial 2002 Development Plan (i.e. pool off-take rates, recovery, water encroachment, well numbers, well locations and completion designs).

An integrated production model, which included reservoir, tubing and pipeline descriptions, was used to model the distribution of resource sizes and reservoir realizations. The most likely scenario required four additional wells to be drilled: two to replace the PP-3C and PI-1B wellbores, and two additional development wells.

Figure 4.1.1 shows PanCanadian's most likely sales gas production forecast.

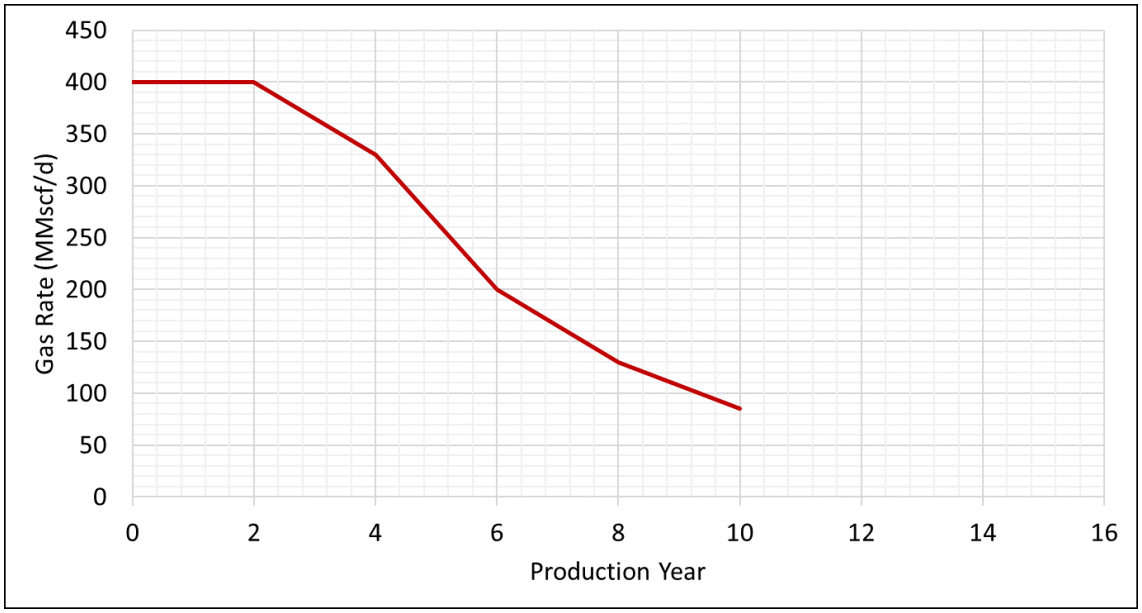

Figure 4.1.1: Sales gas production forecast generated from data in the March 2002 Deep Panuke DPA. This chart shows a production life of 10 years with a maximum production rate of 11.3 E6m3 (400 MMscf)/d.

Table 4.1.2 summarizes probabilistic OGIP and expected Sales Gas in Place (SGIP) for the Abenaki 5.

Table 4.1.2: Initial Development Plan OGIP & SGIP (March 2002 DPA)

Field	P10 OGIP E9m3 (Tcf)	P50 OGIP E9m3 (Tcf)	P90 OGIP E9m3 (Tcf)	Expected OGIP E9m3 (Tcf)	Expected SGIP E9m3 (Tcf)
Abenaki 5	43.3 (1.53)	30.9 (1.09)	21.8 (0.77)	32.8 (1.16)	26.1 (0.92)

4.2. Initial Development Plan Addendum (November 2002)

A Development Plan Addendum for the Deep Panuke field was submitted to the CNSOPB in November 2002. Encana submitted this addendum as PanCanadian had undergone a merger earlier in 2002 and the company name had changed to Encana. The following are the main changes in the operator's November 2002 Addendum compared to the initial March 2002 Deep Panuke DPA submitted by PanCanadian.

- The volume of condensate was increased to 397 m3 (2500 barrels)/day.
- Operator's revised drilling plan was to drill six new production wells. The operator did not plan to reuse any of the suspended Deep Panuke exploration and delineation wells for production.

4.3. Final Development Plan Application (November 2006)

The operator submitted the final Deep Panuke DPA to the CNSOPB in November 2006. Based on the 2006 DPA, the gas field would be produced by re-entering and completing four of the existing Deep Panuke wells as subsea wells and drilling one new production well. These wells were planned to be tied back to a central Production Field Centre (PFC) via subsea flowlines and control umbilicals. The PFC was designed for a peak gas rate of 8.5 E6m3/d (300 MMscf/d). The 2006 DPA indicated that up to three additional subsea production wells might be drilled. These additional wells were planned to be drilled after production start-up and after at least one full year of production. The 2006 DPA indicated the Deep Panuke project was expected to recover between11.5 E9m3 (407 Bcf) to 26.4 E9m3 (931 Bcf) of gas with a mean (expected) recoverable volume of 18.7 E9m3 (659 Bcf). Depending on the recoverable reserves, it was estimated the project would produce from 8 to 18 years with a mean (expected) project life of 13 years.

It was determined that the Deep Panuke gas reservoir contained low volumes of associated gas liquids and approximately 0.18% H2S (sour gas). The mean expected volume of produced condensate was approximately 163.8 m3/d (1030 bbl/d) at a peak gas rate of 8.5 E6m3/d (300 MMscf/d). Peak production was expected to continue for a period of approximately two years. Production was then expected to decline until the cut-off gas rate of 1.1 E6m3/d (40 MMscfd). This cut-off gas rate is a technical limit based on the design of the processing facilities. In the 2006

DPA, the operator described their subsurface development workflow. This workflow began with the application of well and seismic data to create a detailed reservoir description. An "Earth Model" was created using analyses and interpretations of the gas pool's geology, geophysics and petrophysics, as well as fluid and pressure studies. This model was then used to estimate OGIP. A reservoir simulation model was created and used to ensure the "Earth Model" was consistent with well test data. The operator used this model to predict key reservoir performance parameters and gas recovery factors which resulted in Recoverable Gas in Place (RGIP) estimates. Monte Carlo probabilistic simulations were used to study key uncertainties such as OGIP, aquifer size, transmissibility, recovery factors, life after plateau and RGIP.

4.3.1. Geology

The Deep Panuke reservoir consists of porous and variably fractured limestones and dolomites of the Abenaki Formation. The Abenaki Formation is subdivided into four Members (i.e. Artimon, Baccaro, Misaine and Scatarie). The Scatarie Member at the base of the Abenaki Formation marks the onset of widespread, shallow marine carbonate deposition across the Scotian Shelf and is overlain by a succession of open marine shales of the Misaine Member. The Baccaro Member of the Abenaki Formation is a thick carbonate margin succession of limestones, dolomites and minor clastics. The Artimon Member caps the Abenaki Formation.

In the 2006 DPA, the Abenaki Formation along the Deep Panuke platform margin was divided into seven depositional cycles (sequences) based on well correlations. The Baccaro Member of the Abenaki Formation is comprised of the depositional sequences referred to in the 2006 DPA as the Abenaki 2, 3, 4, 5, and 6, each bounded by a sequence boundary (Figure 4.3.1.1). The Artimon Member, referred to in the 2006 DPA as the Abenaki 7, overlies this succession. The Deep Panuke gas field is trapped primarily in porous dolostones and limestones within the Abenaki 4 and

Abenaki 5 sequences. The top seal for the Deep Panuke reservoir are the non-porous limestones of the Abenaki 6 and 7 sequences.

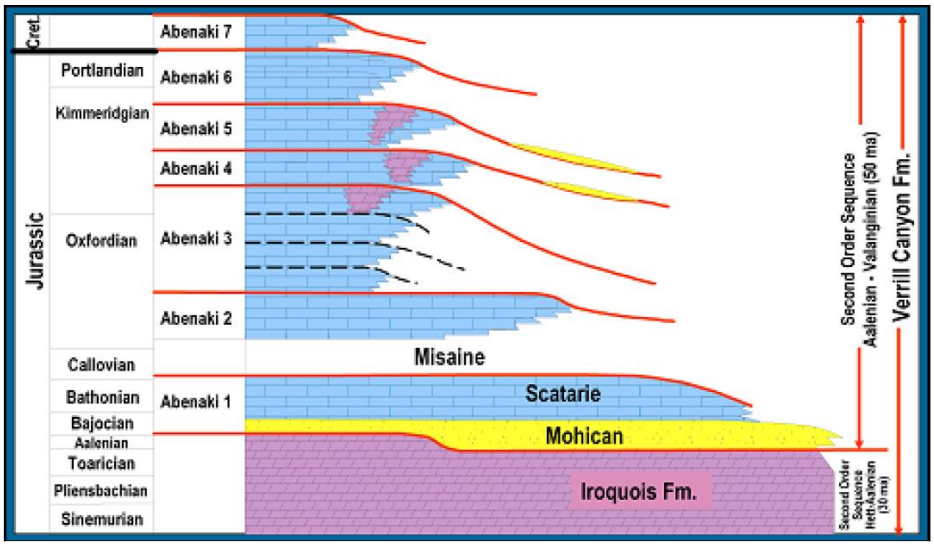

Figure 4.3.1.1: Abenaki Formation Stratigraphic Framework (2006 DPA).

Table 4.3.1.1 shows a list of the Deep Panuke wells and their tested flow rates.

Table 4.3.1.1: Deep Panuke Wells and Their Tested Flowrates (2006 DPA)

Well Name	Well Termination Date	Flow Rate E6m3/d (MMscf/d)
Panuke PP-3C	1999	1.6 (55)
Panuke PI-1A/B	2000	1.5 (52)
Panuke H-08	2000	1.6 (57)
Panuke F-09	2000	0.003 (0.1)
Panuke M-79/A	2000	1.8 (63)
Margaree F-70	2003	1.4 (50)

The F-70 production test showed that 93% of gas production came from a 10 m heavily fractured reservoir interval (Figure 4.3.1.2).

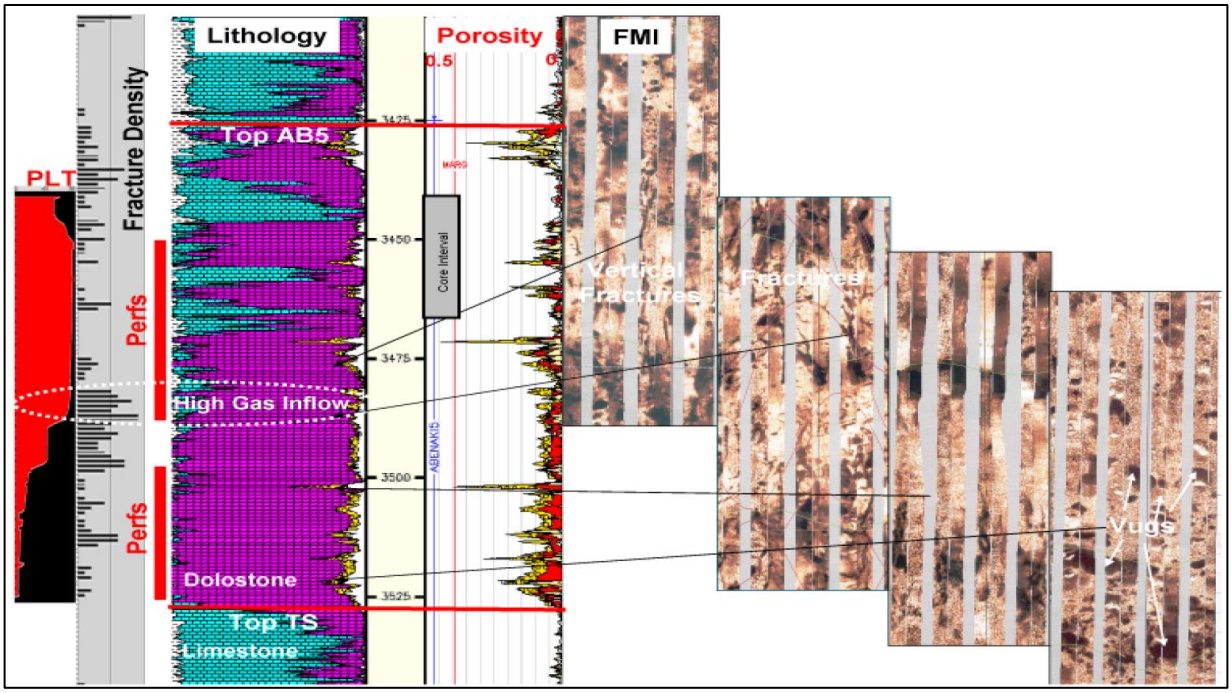

Figure 4.3.1.2: F-70 Flow Test (2006 DPA). FMI log shows fractures and vugs. Note the fracture density in the perforated intervals.

In general, reservoir stratigraphy at Deep Panuke consisted of the porous and permeable limestones and dolomites in the Abenaki 5, low porosity and permeability limestones near the base of Abenaki 5 known as the “Tight Streak” and, porous and permeable limestones and dolomites in the Abenaki 4 (Figure 4.3.1.3).

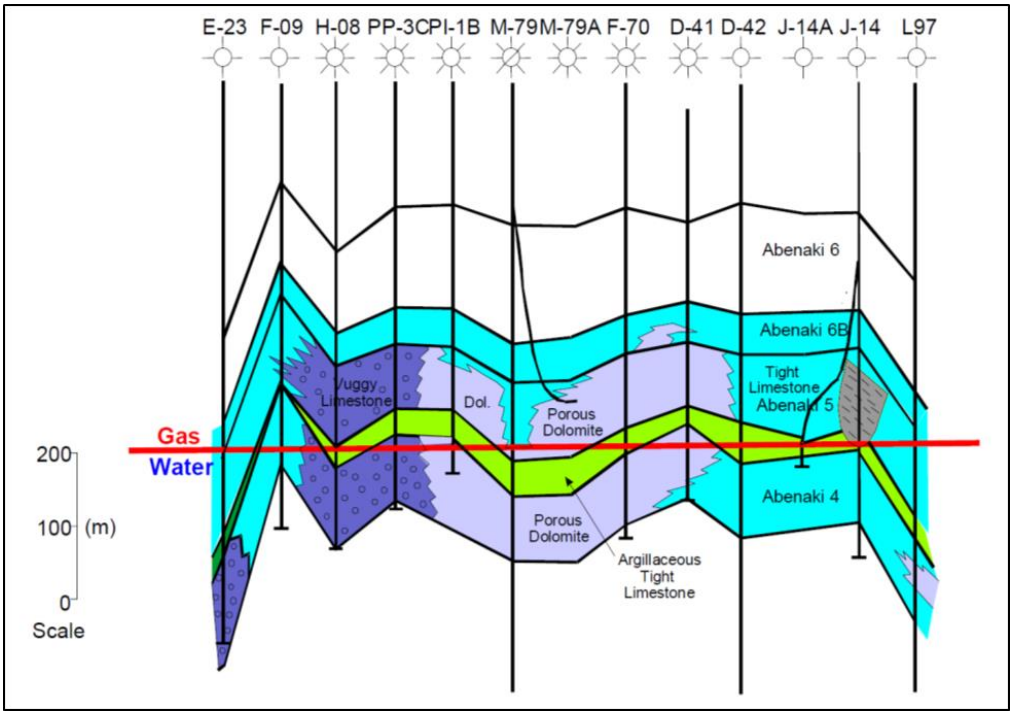

Figure 4.3.1.3: Deep Panuke Stratigraphy (2006 DPA). H-08 production well is drilled in the Vuggy Limestone area and M-79A, F-70 and D-41 production wells were drilled in the porous dolomite reservoir section. The Tight Streak section is also shown in this figure in light green.

4.3.2. Reservoir Characterization

The main Deep Panuke reservoir regions were named by the operator as the High Permeability Reef Front (HPRF) and the Vuggy Limestone (VL) areas (Figure 4.3.2.1). These regions are describe below.

- **High Permeability Reef Front (HPRF):** this region is extensively dolomitized with a high density of fractures. The Deep Panuke production wells M-79A, F-70 and D-41 are located in this region. Due to the extensive fracture network, the majority of the recoverable gas in Deep Panuke is located in the HPRF.
- **Vuggy Limestone (VL):** this region has high porosity and high permeability limestones with a moderate density of fracturing. H-08 and the PP-3C discovery well were drilled in this region.

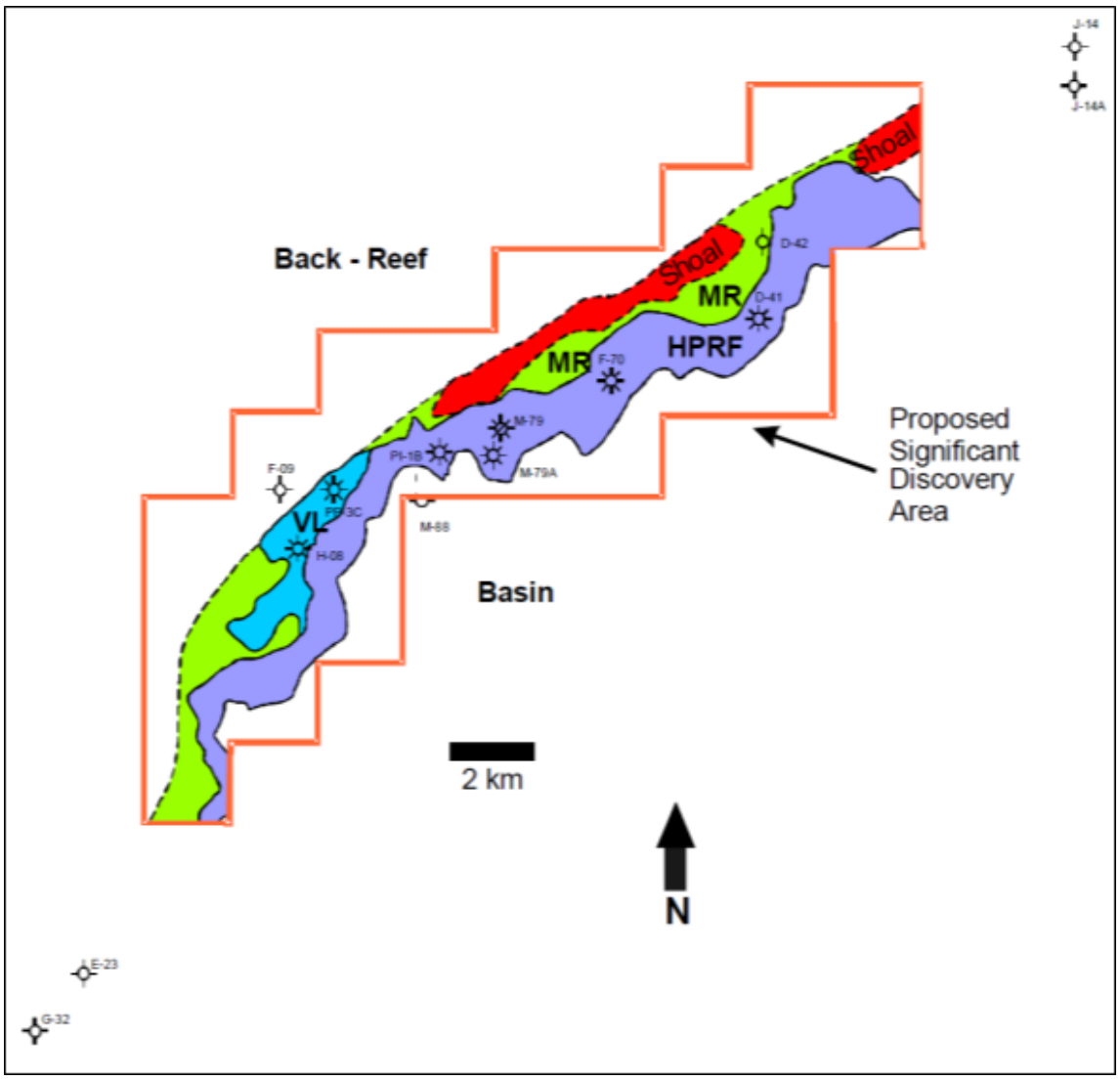

Figure 4.3.2.1: Deep Panuke Reservoir Regions (2006 DPA). The VL and HPRF are the two main Deep Panuke reservoir regions and all production wells are located in these areas.

The operator conducted comprehensive Logging While Drilling (LWD) and wireline logging programs in the Deep Panuke exploration and delineation wells. This included flow testing, production logging, high-resolution image logs, conventional core, rotary sidewall cores, and wireline formation pressures and fluid samples. The large vugs in the VL region and extensive fracturing in the HPRF made the acquisition of conventional and sidewall challenging. As a result, most cores were acquired in the lower porosity "tighter" intervals resulting in under-sampling of the higher quality reservoir intervals. These sampling limitations affected the operator's ability to

fully characterize the Deep Panuke reservoir. Figures 4.3.2.2 and 4.3.2.3 show the porosity-permeability relationships for dolomite and limestone rock types based on the available conventional and sidewall core data.

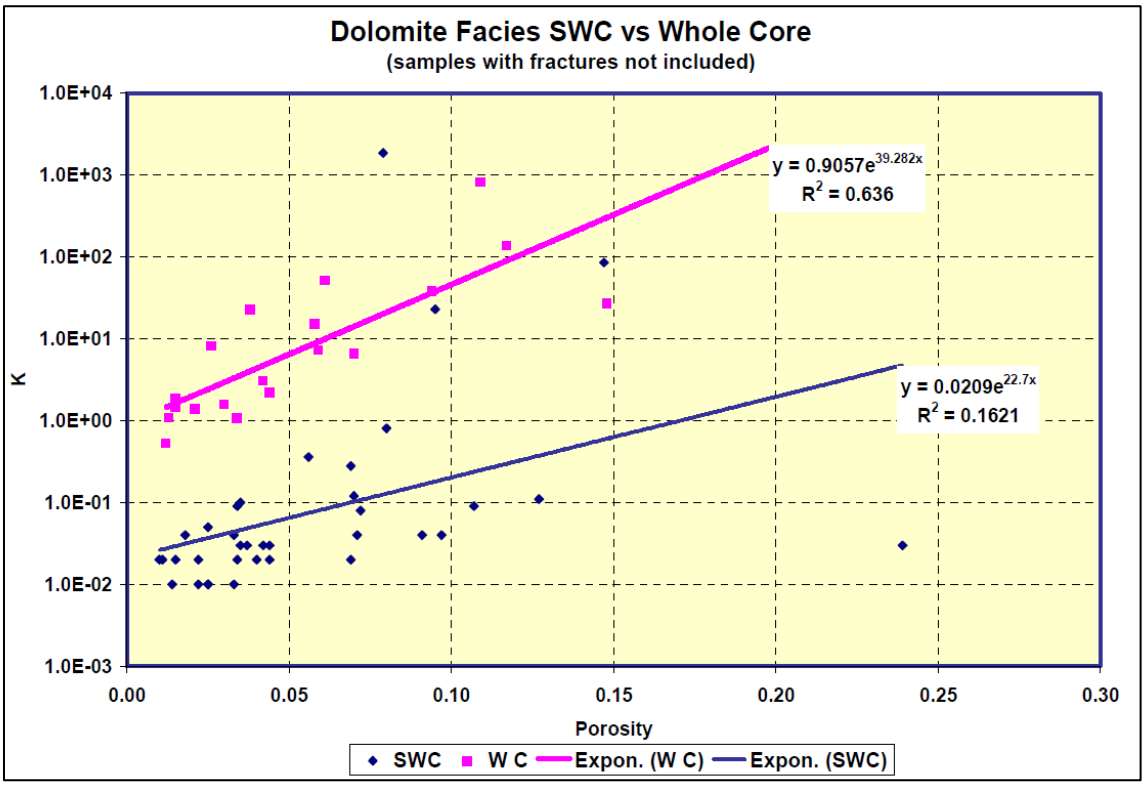

Figure 4.3.2.2: Dolomite Porosity-Permeability Cross-Plot (2006 DPA). Pink points are from conventional core and the blue points are from sidewall core.

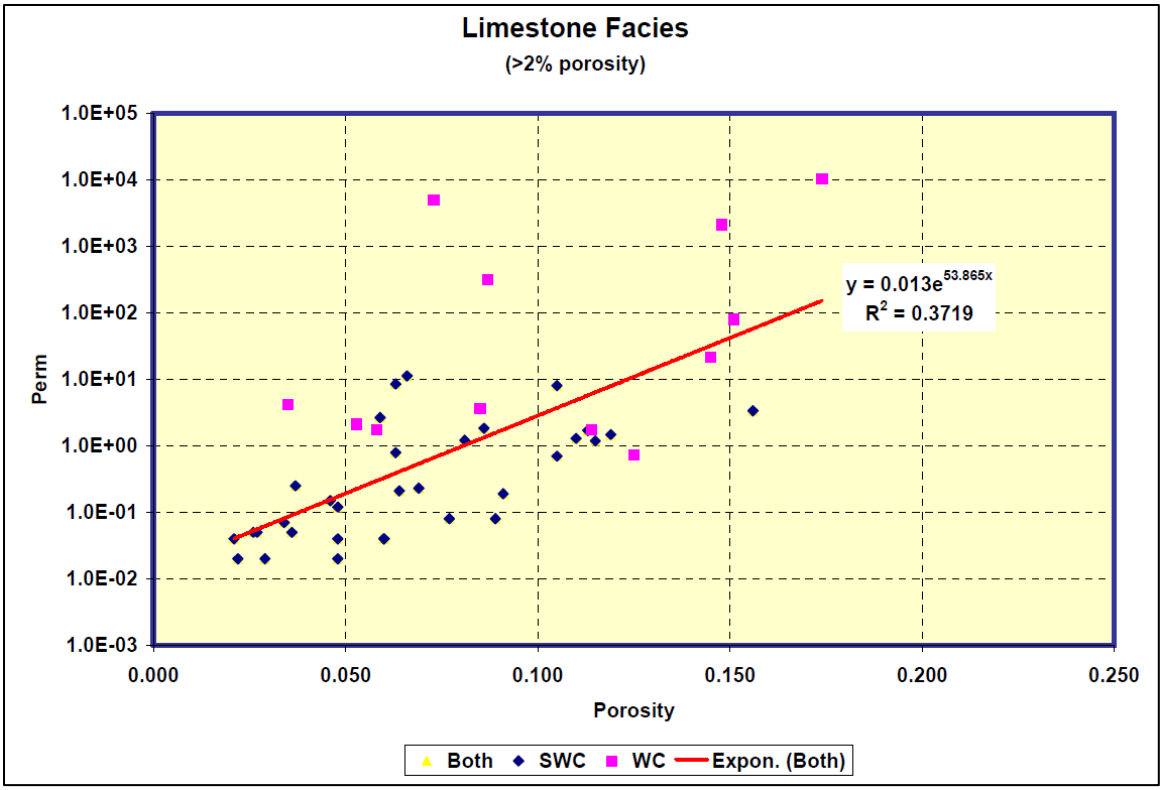

Figure 4.3.2.3: Limestone Porosity-Permeability Cross-Plot (2006 DPA).

Table 4.3.2.1 lists the petrophysical properties included in the 2006 DPA for each Abenaki zone penetrated by the Deep Panuke wells.

Table 4.3.2.1: Average Petrophysical Properties (2006 DPA)

Well	Interval	Top TVDSS (m)	Base TVDSS (m)	Gross Thickness (m)	Net Pay Thickness (m)	Porosity (fraction)	Sw (fraction)
PP-3C	AB6	3313.1	3362	48.9	0		
	AB5	3362	3487.3	125.3	85.4	0.17	0.34
	AB4	3487.3	3575.5	88.2	11.8	0.06	0.78
	Total	3313.1	3575.5	262.4	97.2	0.16	0.36
PI-1A	AB6	3317.4	3369.9	52.4	0		
	AB5	3369.9	3503.7	133.8	6.9	0.04	0.29
	AB4	3503.7	3543.3	39.7	0		
	Total	3317.4	3543.3	225.9	6.9		
PI-1B	AB6	3318.5	3368.7	50.2	0		
	AB5	3368.7	3493.1	124.4	38.6	0.05	0.13
	AB4	3493.1	3521	27.9	10.2	0.06	0.1
	Total	3318.5	3521	202.5	48.8	0.06	0.13
M-79	AB6	3365.5	3417.2	51.7	0		
	AB5	3417.2	3572.8	155.7	13.5	0.04	0.58
	AB4	3572.8	3658.1	85.2	0		
	Total	3365.5	3658.1	292.6	13.5	0.04	0.58
M-79A	AB6	3350.6	3405.4	54.8	4.3	0.04	0.43
	AB5	3405.4	3445.3	37.8	16.2	0.08	0.06
	Total	3350.6	3445.3	92.5	20.6	0.07	0.1
H-08	AB6	3349.7	3394.4	44.7	6.2	0.12	0.23
	AB5	3394.4	3532.1	137.7	105.8	0.23	0.23
	AB4	3532.1	3644.2	112.1	0		
	Total	3349.7	3644.2	294.5	112	0.22	0.23
F-70	AB6	3326.1	3378.1	52	1	0.06	0.26
	AB5	3378.1	3515	136.9	75	0.09	0.06
	AB4	3515	3597	82.1	0		
	Total	3326.1	3597	270.9	76	0.09	0.06
F-09	AB6	3250.9	3295	44.1	0		
	AB5	3295	3412.4	117.3	11	0.05	0.46
	AB4	3412.4	3529.8	117.4	15.8	0.04	0.72
	Total	3250.9	3529.8	278.8	26.8	0.04	0.6
D-41	AB6	3308.4	3364.7	29.4	2.5	0.03	0.61
	AB5	3364.7	3475.6	110.8	91.4	0.09	0.06
	AB4	3475.6	3572.2	96.6	28.2	0.09	0.07
	Total	3308.4	3572.2	236.8	122.1	0.09	0.07

Pressure data acquired by flow testing and wireline formation testing indicated that the Abenaki gas reservoir was normally pressured (hydro-pressured). This data also showed that there was only one gas pool at Deep Panuke, which was underlain by a regional aquifer. The above pressure data was used to define the gas-water contact (GWC) for the field located at -3504 m TVD-SS (Figure 4.3.2.4).

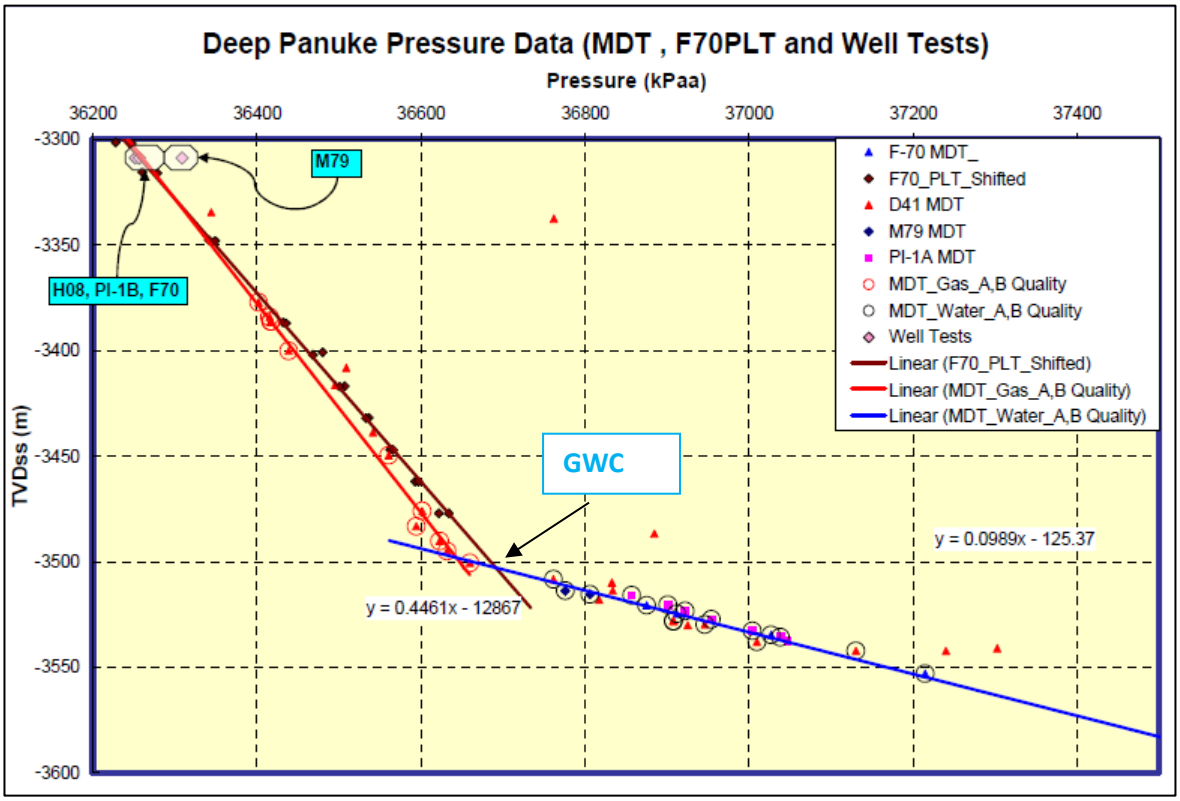

Figure 4.3.2.4: The elevation of the GWC was estimated at -3504 m TVD-SS (2006 DPA).

Based on the 2006 DPA, the vertical and horizontal extent of the aquifer and the degree of connectivity with the Deep Panuke gas pool were not fully understood, prior to the start of production, due to the limited number of wells and the complex nature of the reservoir. The operator identified aquifer size and connectivity to the gas zone as key uncertainties that could have a significant impact on overall recovery. The following Table 4.3.2.2 summarizes the main reservoir properties for the Abenaki gas pool.

Table 4.3.2.2: Reservoir Fluid Properties (2006 DPA)

Reservoir Fluid Parameters	Value
Reservoir Datum Depth	3309 m TVDss
GWC	3504 m TVDss
Temperature at Datum	123 deg. C
Gas Gravity	0.62
Condensate Gas Ratio	3.28 Bbls/MMscf
Formation Volume Factor	0.004 rsm3/sms
Initial Reservoir Pressure at Datum	363 Barsa

When constructing their geological models, the operator used neural network analysis combined with seismic attributes to estimate porosity across the field. A training data set for the neural network was developed which consisted of petrophysical total porosity and seismic attributes extracted from seismic traces at well locations. The neural network model was then trained on seismic attributes to predict porosity across the 3-D seismic volume. This procedure was done separately for the VL and HPRF regions. The operator generated a number of deterministic estimates for OGIP for both HPRF and VL regions. These estimates were developed by using different porosity models and by varying the field's areal extent. Three of these models ("Small", "Mid" and "Large") were selected by the operator to construct their reservoir simulation models. Table 4.3.2.3 shows the OGIP values from these simulation models.

Table 4.3.2.3: Simulation Model OGIP (2006 DPA)

Simulation Model	HPRF OGIP E9m3 (Bcf)	VL OGIP E9m3 (Bcf)	TOTAL OGIP E9m3 (Bcf)
Small	19.8 (700)	2.5 (87.5)	22.3 (787.5)
Mid	26.6 (938)	2.9 (101.5)	29.4 (1039.5)
Large	32.9 (1162)	5.7 (203)	38.7 (1365)

In the simulation model, the HPRF area was modeled as a dual-porosity reservoir. Simulation modeling yielded recovery factors in the range of 0.40 – 0.79 for the HPRF region. In the 2006

DPA, the operator acknowledged that there were additional risks associated with fracture heterogeneity, well completion problems and poor well performance at high water cuts could decrease overall recovery to as low as 20%. The operator also observed that overall Deep Panuke gas recovery was most sensitive to OGIP in the HPRF, recovery factor in the HPRF and VL areas, and aquifer size and transmissibility. The following table shows the estimated RGIP for the VL and HPRF reservoir regions (Table 4.3.2.4).

Table 4.3.2.4: Deep Panuke RGIP by Reservoir Region (2006 DPA)

Reservoir Region	P90 E9m3 (Bcf)	P50 E9m3 (Bcf)	P10 E9m3 (Bcf)	MEAN E9m3 (Bcf)
HPRF	9.8 (345)	16.1 (568)	24.0 (849)	16.5 (584)
VL	1.4 (48)	2.0 (72)	3.0 (106)	2.1 (75)
Total	**11.5 (407)**	**18.3 (645)**	**26.4 (931)**	**18.7 (659)**

The 2006 DPA states that the number of wells required to effectively develop the Deep Panuke reservoir is uncertain primarily due to the uncertainties associated with RGIP, aquifer size, and aquifer connectivity. The operator stated in the 2006 DPA that they would re-use four of the existing Deep Panuke wells H-08, M-79A, F-70, and D-41 and plan to drill one additional producer. The 2006 DPA indicated that there could be a second phase of development, which could include drilling up to three additional production wells. This second phase of development would depend on well and reservoir performance once production had commenced.

The following charts (Figures 4.3.2.5 and 4.3.2.6) show the 2006 DPA probabilistic assessment of forecasted daily sales gas and water production rates.

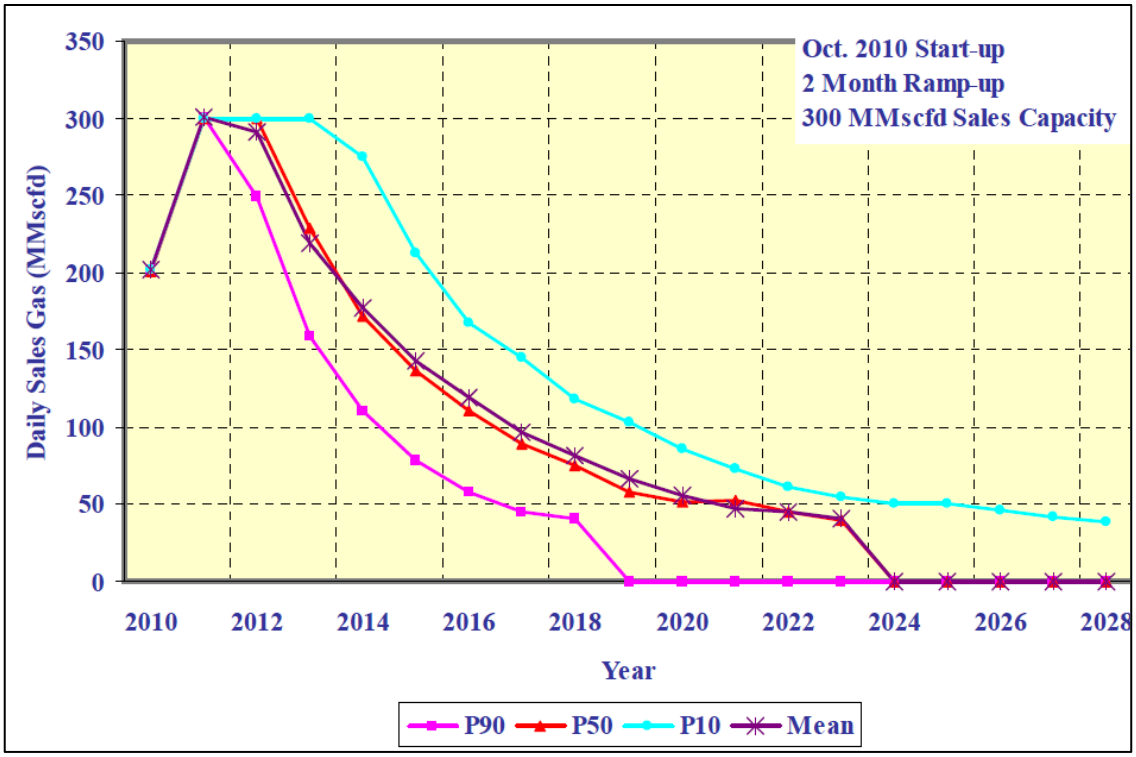

Figure 4.3.2.5: Deep Panuke Forecasted Sales Gas Rate (2006 DPA). The maximum predicted gas rate is 300 MMscf/d.

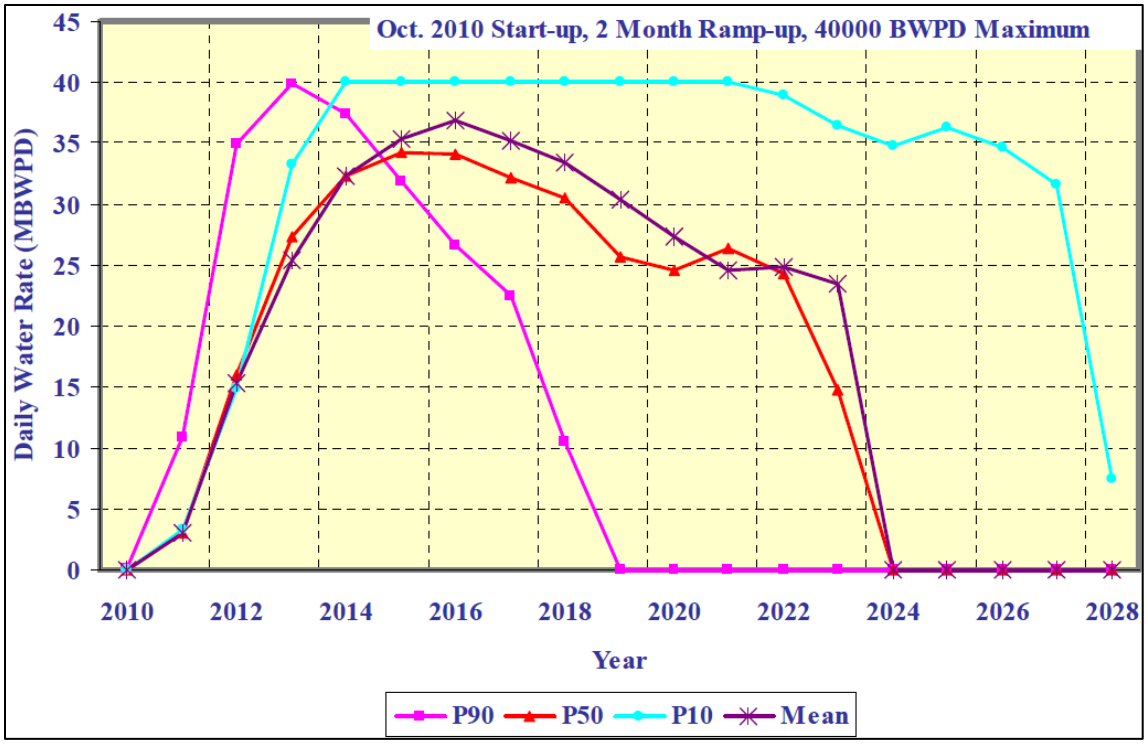

Figure 4.3.2.6: Forecasted Water Production Rate (2006 DPA). The maximum daily water production rate is 40,000 bbl/d.

In the 2006 DPA, the operator identified the following key subsurface risks:

- OGIP range
- Recovery efficiency
- Aquifer drive potential
- Compartmentalization of the VL area
- Fracture heterogeneity in the HPRF
- Well completion problems

4.3.3. Development Economics

In the 2006 DPA, the operator used discounted cash flow analysis with a number of sensitivities. The operator expected significant variability in monthly operating costs mainly due to the impact

of the PFC leasing cost, which was assumed to constitute the single largest component of operating costs. Annual operating costs including the PFC lease cost was estimated to be $150 million $CDN per year +/- 25%. The cost of drilling any future wells including the tie back to the PFC was estimated to be $120 million $CDN.

5. CNSOPB Reservoir Characterization of the Deep Panuke Field

5.1. Seismic Interpretation Overview

The majority of the recoverable gas reserves in the Deep Panuke field are located in the Abenaki 5 sequence. A time structure map of the Abenaki 5 is shown in map view in Figure 5.1.1. Seismic Profile A to A' intersects the Panuke PP-3C discovery well and the Queensland M-88 well which was drilled to evaluate a different play concept on the slope of the carbonate bank.

The trap for the Deep Panuke gas field is a combination structural and stratigraphic trap. The structural elevation increases to the north and northeast and plunges to the southwest where it drops below the GWC. The Abenaki 5 is overlain by tight upper foreslope limestones of the Abenaki 6 sequence, which provides an effective top seal. Slope failure has created a scalloped bank margin, which limits the field's extent to the northeast of the MarCoh D-41 well. The porosity in the dolomitized and leached reef-front limestones of the Abenaki 5 transitions to the north and northwest to tight back-reef oolitic and mudstone facies which provides the lateral seal in the landward direction.

The Abenaki 5 seismic reflection is generally picked as a peak, but transitions to a trough where highly porous and vuggy limestones are encountered. The interpretation becomes more challenging in the seaward direction beyond the slope break. Figures 5.1.2, 5.1.3, 5.1.4, and 5.1.5 are seismic dip lines through the Deep Panuke production wells.

It should be noted that the structure maps produced by the CNSOPB are generally consistent with the maps produced by the operator.

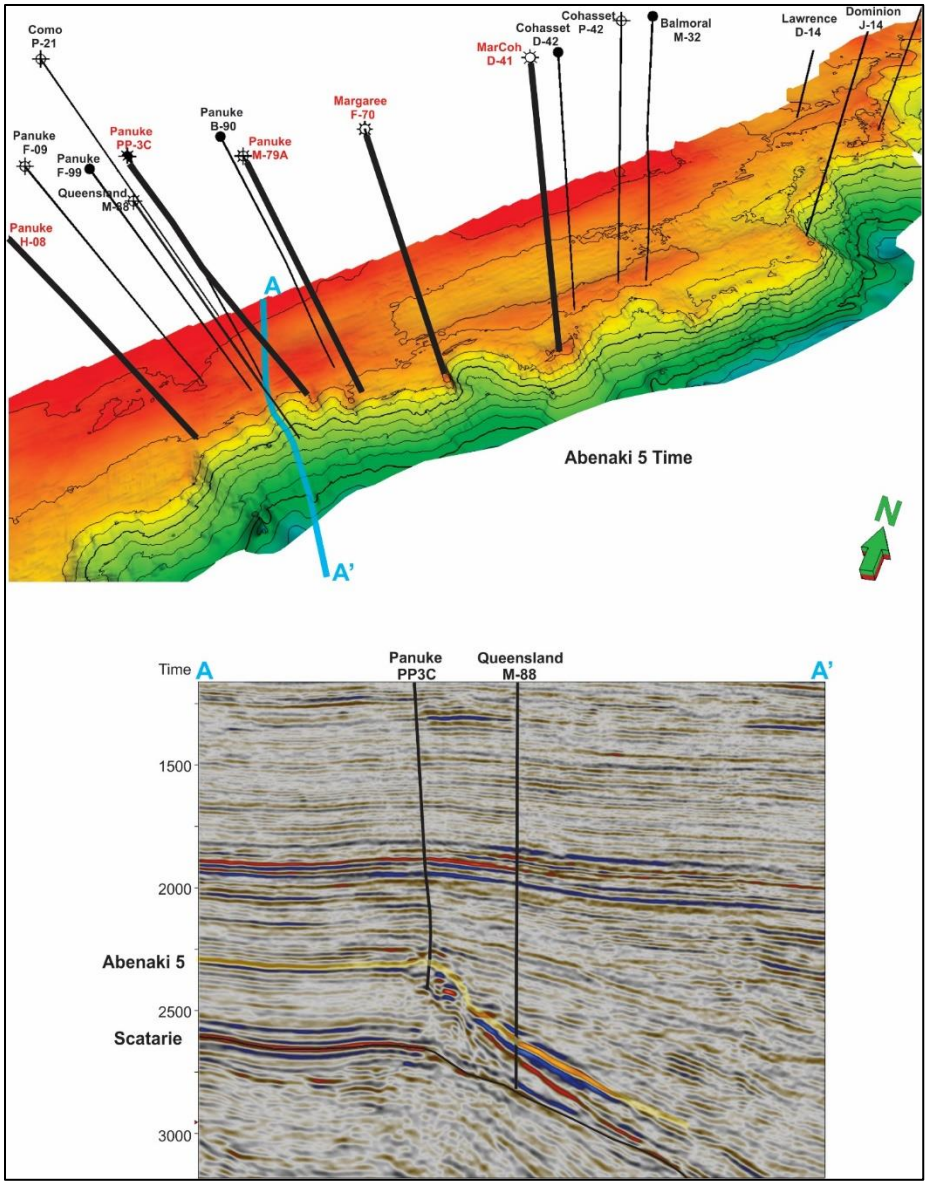

Figure 5.1.1: Top Abenaki 5 Time Structure Map (upper figure) and seismic profile from A to A' (lower figure). On the seismic profile, the top of the Abenaki 5 is shown in yellow and the Scatarie is shown in black.

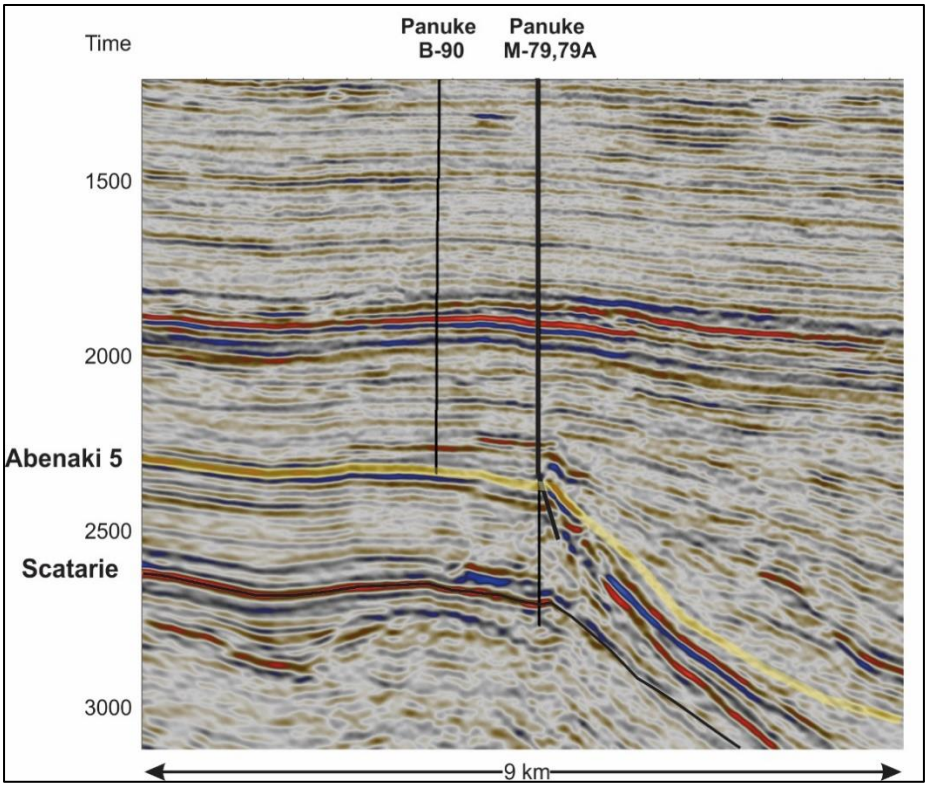

Figure 5.1.2: Seismic dip profile through the Panuke B-90 and Panuke M-79/M-79A wells.

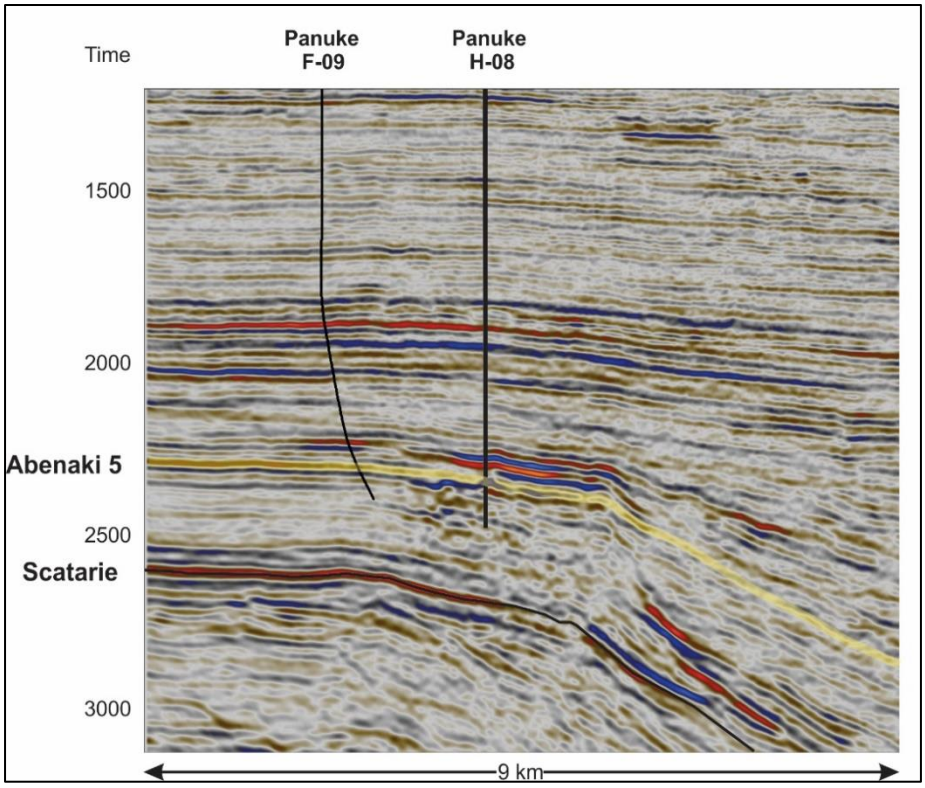

Figure 5.1.3: Seismic dip profile through the Panuke F-09 and Panuke H-08 wells.

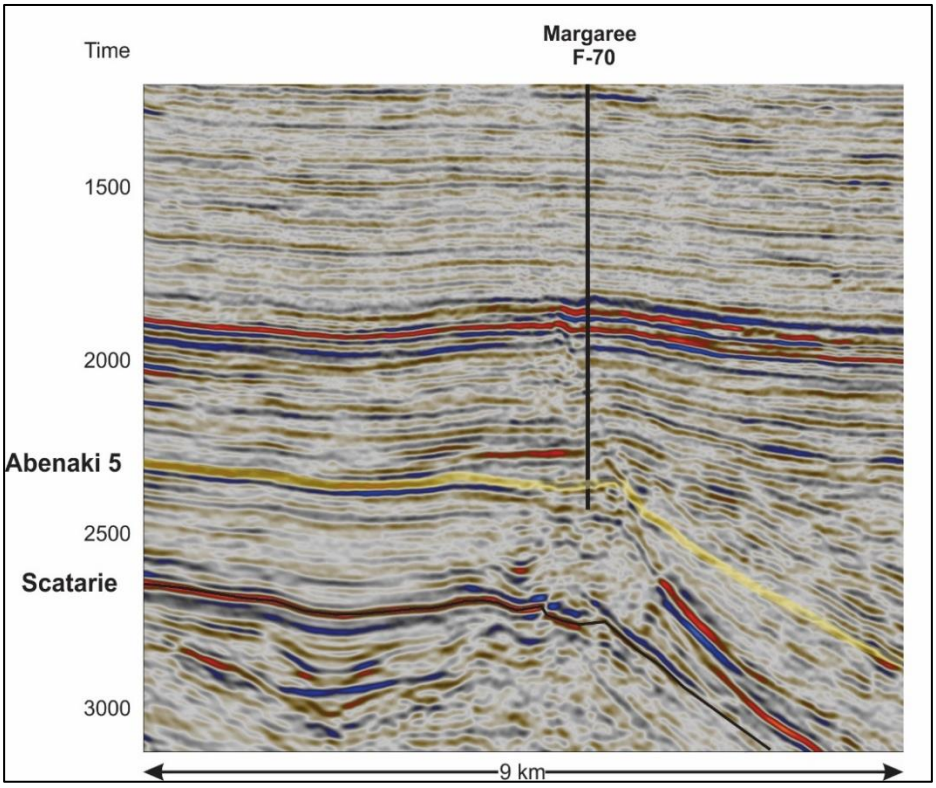

Figure 5.1.4: Seismic dip profile through the Margaree F-70 well.

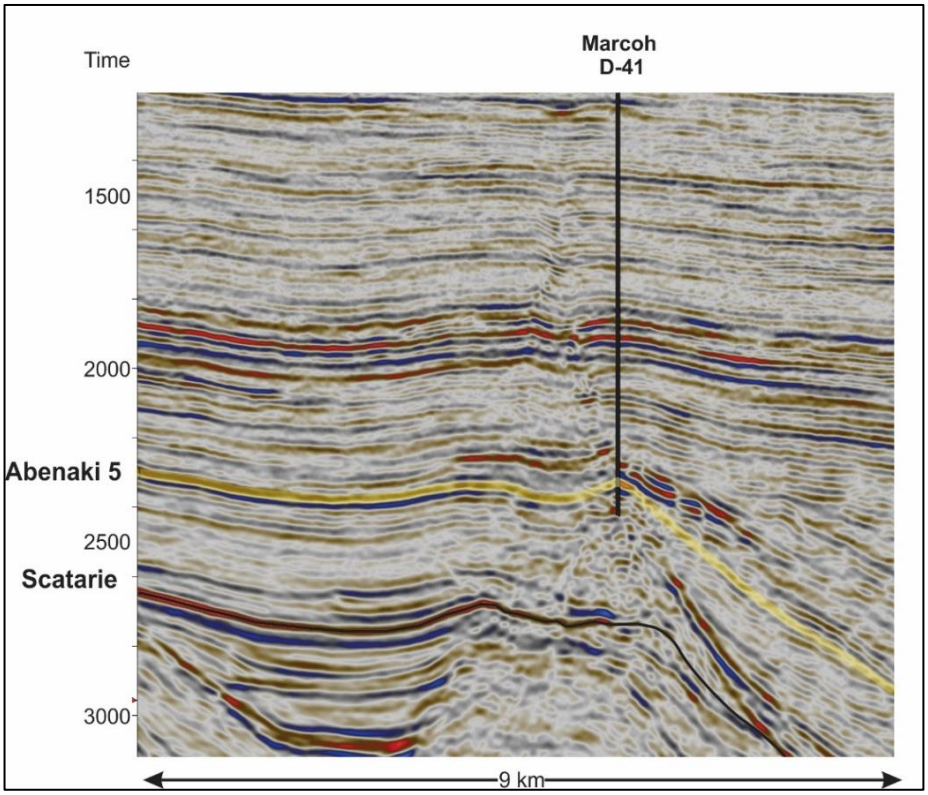

Figure 5.1.5: Seismic dip profile through the MarCoh D-41 well.

5.2. Petrophysical Overview

The CNSOPB conducted an independent petrophysical analysis of the wells in the Deep Panuke field utilizing all available well logs, cores, and pressure data. Porosity was typically calculated using the density-neutron crossplot method. Porosity was calculated from the sonic log in the intervals where the density and/or neutron data was of poor quality or missing. Formation water resistivity (Rw) was determined by analysis of water samples obtained from the Panuke PI-1A well. True formation resistivity (Rt) was determined from the deep resistivity measurement and water saturation (Sw) was calculated using the Archie equation.

Wireline formation pressure data was crossplotted to determine the elevation of the Deep Panuke gas-water contact (GWC). The elevation of the GWC, from wireline pressure data, was consistent with the "gas-down-to" and "water-up-to" elevations determined from well logs and with formation flow test results. The CNSOPB's GWC was consistent with the GWC calculated by the operator.

The Vuggy Limestone (VL) region of the Deep Panuke reservoir consists of cavernous vuggy porosity with some fracture porosity. The VL region has high average porosities in the Abenaki 5 which vary from 0.19 (PP-3C) to 0.23 (H-08). The High Permeability Reef Front (HPRF) reservoir region has fair average porosities in the Abenaki 5 but a moderate to high degree of fracture porosity. The average porosity of the Abenaki 5, in the HPRF, for the Deep Panuke production wells (M-79A, F-70 & D-41) varies from 0.09 - 0.10. However, formation micro-imager logs combined with flow testing and production logging have demonstrated there is a significant network of connected fractures in the HPRF. Due to the extent and permeability of the HPRF fracture porosity system, approximately 83% of the gas produced from the Deep Panuke field was produced from this reservoir region.

Conventional and sidewall core data was used to evaluate the relationship between porosity and permeability. It was determined that a porosity of 0.04 was approximately equivalent to a permeability of 0.l mD, which is the typical permeability cutoff for gas reservoirs. The following cutoffs were used to calculate net pay for the Deep Panuke wells: Porosity >= 0.04, Sw <= 0.70, and Volume of Shale (Vsh) <=0.30. The results of the CNSOPB's petrophysical analysis are summarized in Table 5.2.1.

Table 5.2.1 – CNSOPB Deep Panuke Reservoir Property Summary

Well	Zone	Top (m MD)	Base (m MD)	Net Pay (m TVD)	Net Pay Porosity (fraction)	Sw (fraction)
Panuke PP-3C	Abenaki 6	3714.0	3913.3	20.1	0.05	0.53
	Abenaki 5	3913.3	4050.0	75.8	0.19	0.36
	Abenaki 4	4050.0	Not penetrated	8.0	0.08	0.57
Panuke PI-1A	Abenaki 6	3662.0	3855.5	3.8	0.05	0.55
	Abenaki 5	3855.5	3990.3	2.0	0.06	0.56
	Abenaki 4	3990.3	Not penetrated	wet	N/A	N/A
Panuke PI-1B	Abenaki 6	3662.0	3859.2	3.0	0.05	0.60
	Abenaki 5	3859.2	3993.0	24.5	0.07	0.33
	Abenaki 4	3993.0	Not penetrated	2.0	0.08	0.44
Panuke H-08*	Abenaki 6	3292.0	3424.0	8.6	0.06	0.36
	Abenaki 5	3424.0	3571.5	98.9	0.23	0.25
	Abenaki 4	3571.5	3683.5	wet	N/A	N/A
Panuke M-79	Abenaki 6	3250.0	3446.0	2.6	0.06	0.60
	Abenaki 5	3446.0	3571.0	1.5	0.06	0.61
	Abenaki 4	3571.0	3704.5	wet	N/A	N/A
	Abenaki 3	3704.5	4118.0	wet	N/A	N/A
	Abenaki 2	4118.0	4330.0	wet	N/A	N/A
Panuke M-79A*	Abenaki 6	3250.0	3482.0	1.2	0.04	0.54
	Abenaki 5	3482.0	Not penetrated	14.6	0.09	0.25
Margaree F-70*	Abenaki 6	3222.0	3425.7	7.9	0.05	0.49
	Abenaki 5	3425.7	3562.5	61.80	0.10	0.23
	Abenaki 4	3562.5	Not penetrated	wet	N/A	N/A
MarCoh D-41*	Abenaki 6	3246.5	3405.2	1.1	0.07	0.57
	Abenaki 5	3405.2	3523.4	79.0	0.10	0.25
	Abenaki 4	3523.4	Not penetrated	22.5	0.15	0.21

*****Deep Panuke production well.

5.3.Dynamic Simulation Model

The Deep Panuke dynamic reservoir simulation models were developed by the CNSOPB using all available data. Structural, geological information and reservoir properties were interpreted from seismic data, well logs, well tests and wireline pressure data as described above. This information

was used to develop a series of structural (seismic depth maps) and reservoir property maps (i.e. porosity, gross and net thickness and water saturation) for each Deep Panuke reservoir zone (i.e. Abenaki 6, Abenaki 5, Abenaki 4 etc.). Where necessary the maps were adjusted to ensure they honored the well data. The matrix permeability map was derived by applying a porosity/permeability transform to the porosity maps. These maps were the main geological, geophysical and petrophysical inputs to the CNSOPB's reservoir simulation models. The directional surveys for each well were also loaded to ensure the well penetrations through each reservoir zone were accurate. The above maps and data were gridded to create a simulation flow model.

Fluid models were built from Pressure/Volume/Temperature (PVT) data obtained from well samples. Special core analysis data (e.g. relative permeability, capillary pressure) was also incorporated into the models to better describe fluid flow through the reservoir. Rock mechanics analysis provided information on how the rock properties such as porosity and permeability respond to changes in pressure during production. Analytical aquifer models were added to the simulation model to provide functions that model the influx of water and the resultant pressure support to the reservoir. Information from the fluid models and saturation functions were used together with the observed elevation of the gas water contact to initialize reservoir fluid distributions. Well models were created from the trajectories of drilled wells, which included details of each well's construction (e.g. tubing, perforations, completion equipment etc.). The last stage in building the reservoir model was to incorporate actual production data for each well. This data was used to calibrate the reservoir model during history matching. Once the model was history matched to the observed data, field management strategies were assessed via predictive modeling.

CNSOPB's independent simulation model building process began by converting the Deep Panuke depth structure maps into simulation surfaces. Four separate depth surfaces were generated (Abenaki 6, Abenaki 5, Tight Streak and Abenaki 4). These surfaces were then converted into horizons (Figures 5.3.1). These horizons were gridded (Figure 5.3.2) and were converted into three separate reservoir simulation zones (Table 5.3.1 & Figure 5.3.3).

Table 5.3.1: Reservoir Simulation Zones

Zone	Top Horizon	Bottom Horizon
1	Abenaki 6	Abenaki 5
2	Abenaki 5	Tight Streak
3	Tight Streak	Abenaki 4

The grids provide a detailed 3D model of the subsurface in which the volumetric and dynamic simulation calculations are performed. Grids are used for dynamic simulations and their properties are frequently upscaled from the geological, geophysical and petrophysical inputs to create a model with a coarser resolution to optimize the performance of the simulation model.

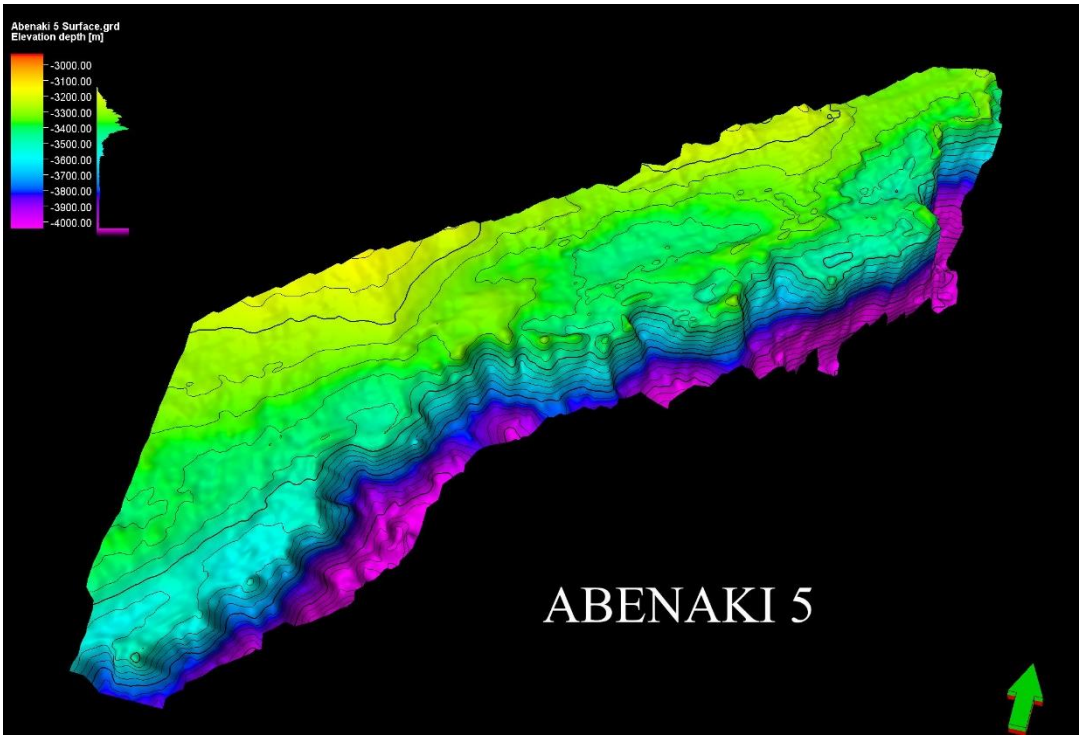

Figure 5.3.1: Depth structure map of the top of Abenaki 5. Warmer colours show structural highs while cooler colours indicate structural lows.

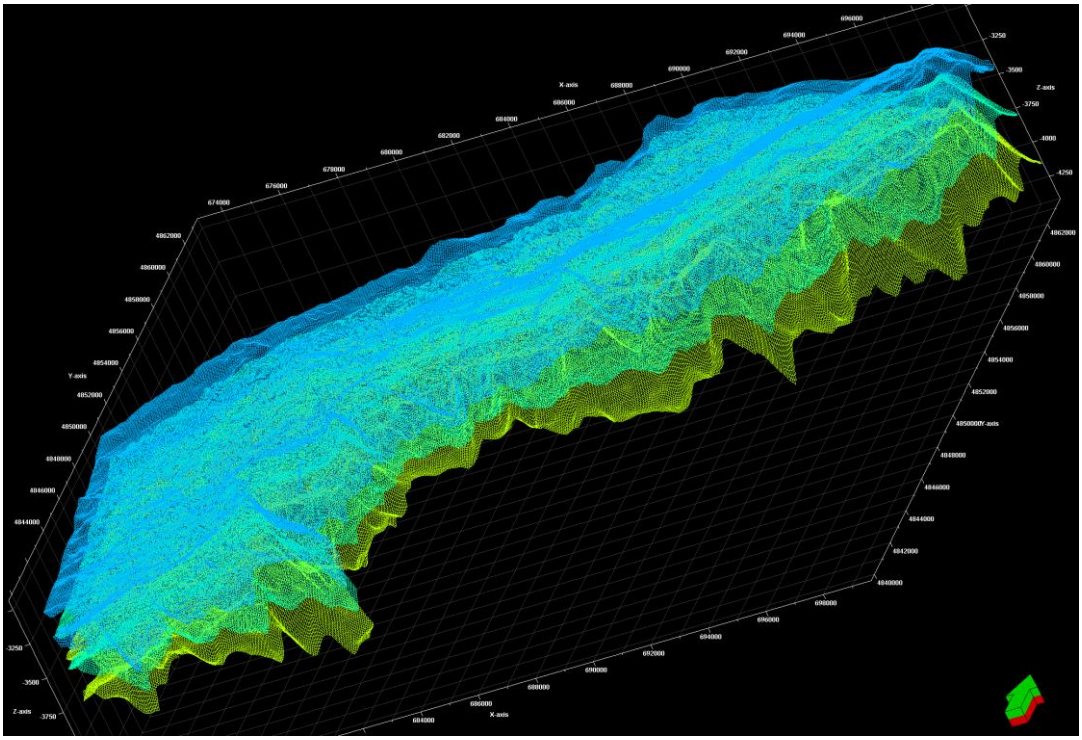

Figure 5.3.2: Simulation model Grid assignment.

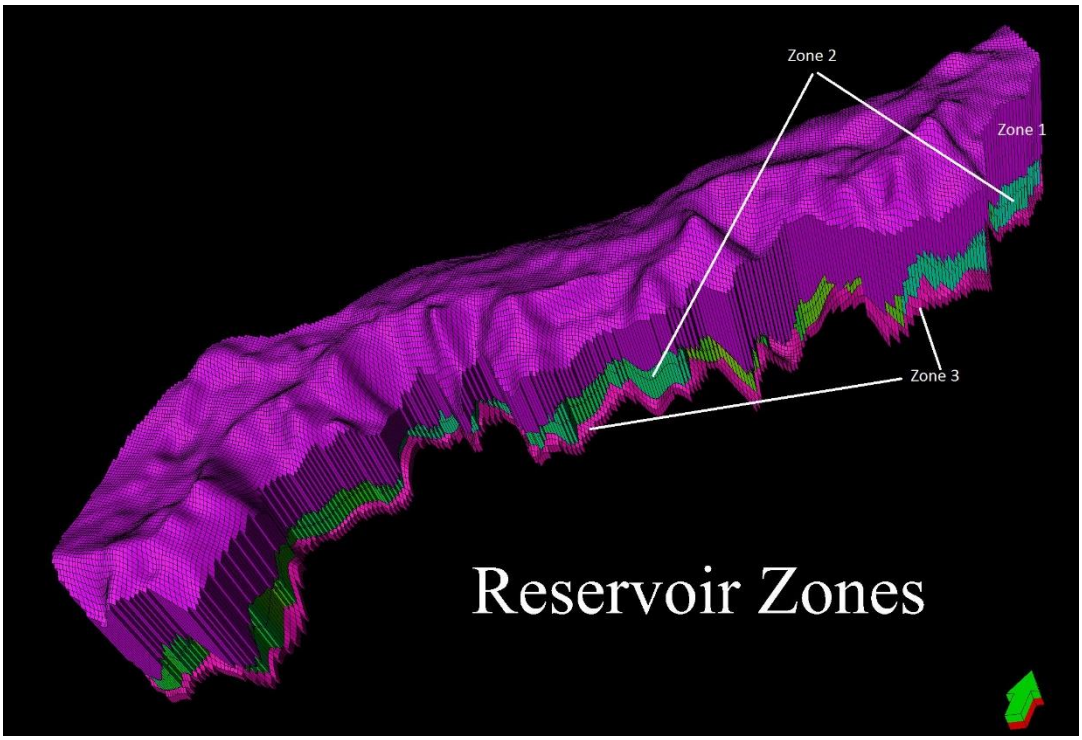

Figure 5.3.3: Three distinct reservoir zones were defined in the simulation model.

The final simulation model consisted of 1,019,520 grid cells. The number of grid cells and cell dimensions were selected to optimize simulation run time while maintaining reasonable accuracy.

As a highly fractured reservoir, Deep Panuke had to be simulated as a dual permeability reservoir. In this method, each grid cell is assigned separate matrix and fracture reservoir properties (Figures 5.3.4 & 5.3.5).

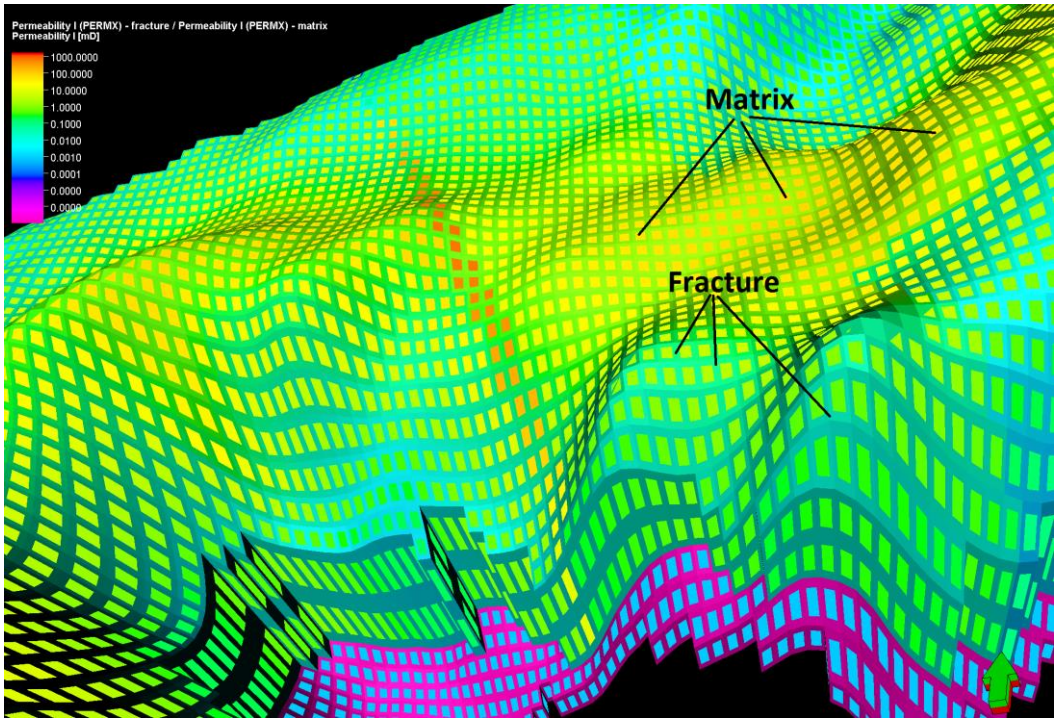

Figure 5.3.4: This figure shows how fracture and matrix is visually represented in the simulation model. Matrix is shown with squares and fractures are shown as channels connecting the matrix blocks.

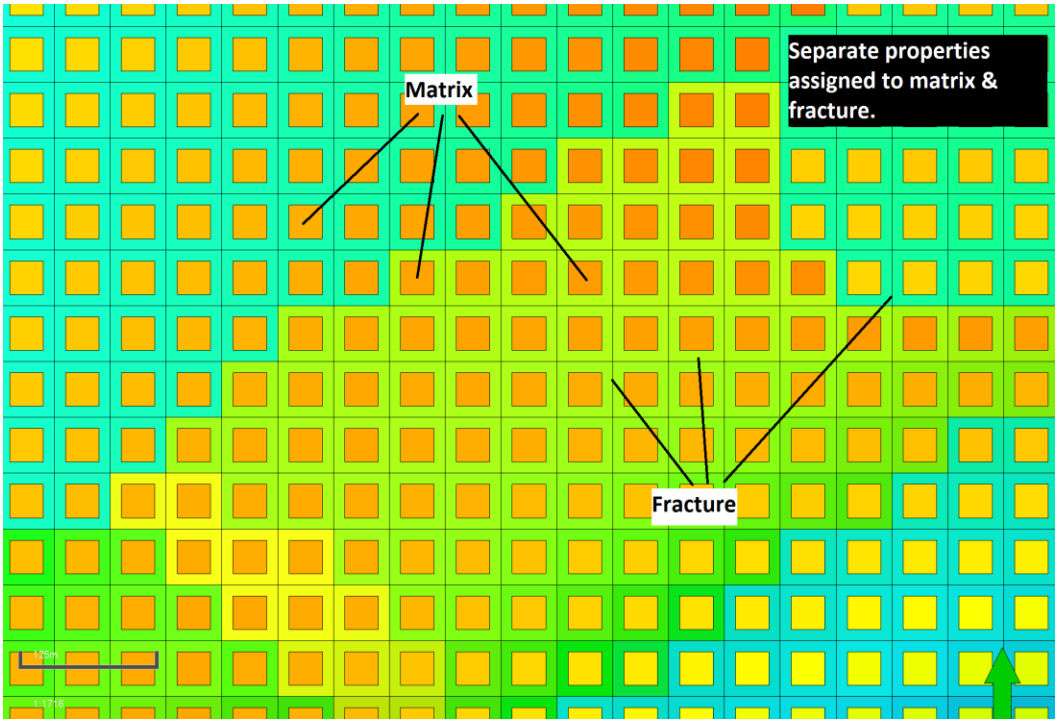

Figure 5.3.5: Matrices are shown with squares and fractures are shown as channels connecting the matrix blocks. Separate properties such as porosities, permeability and saturations were assigned to matrix and fracture.

The Abenaki 6 and Abenaki 4 zones were assumed to have zero porosity in the model. This assumption means, for modeling purposes, these zones were assumed to contain no hydrocarbons. For the Abenaki 5, reservoir properties such as porosity and net to gross were determined from reservoir property maps.

The following Figures 5.3.6 and 5.3.7 show initial porosity and net to gross ratios assigned to the grid cells. The assigned Abenaki 5 porosities ranged from zero to 22.5% and the assigned net to gross ratios ranged from zero to 0.97. Figures 5.3.8 and 5.3.9 show the distribution of these properties in the initial un-calibrated simulation model.

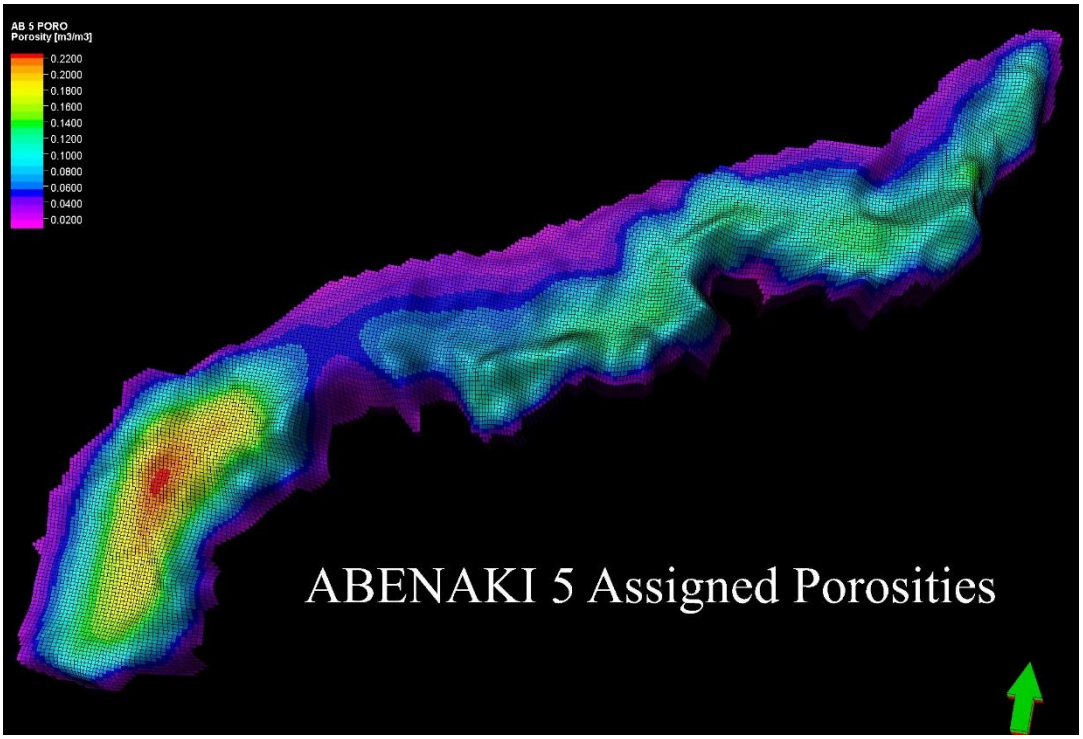

Figure 5.3.6: This figure shows porosities assigned to grid cells that belonged to Abenaki 5 as the main simulation layer. Warmer colours indicate higher porosities.

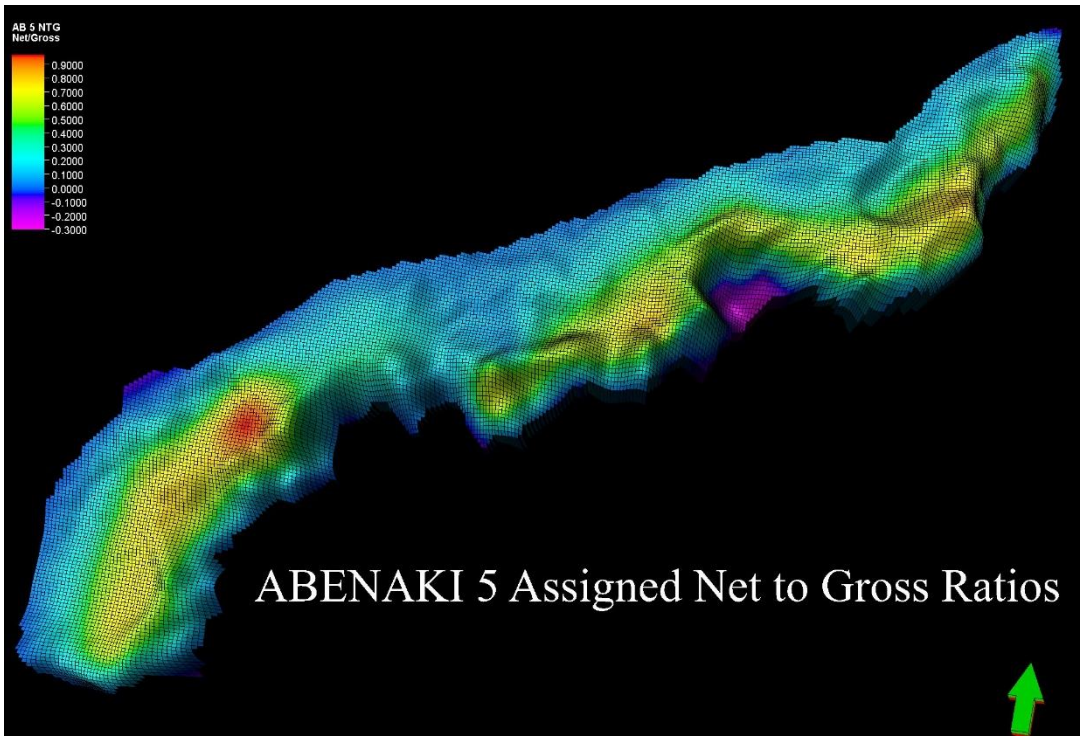

Figure 5.3.7: This figure shows net to gross ratios assigned to grid cells that belonged to Abenaki 5 as the main simulation layer. Warmer colours indicate higher net to gross intervals.

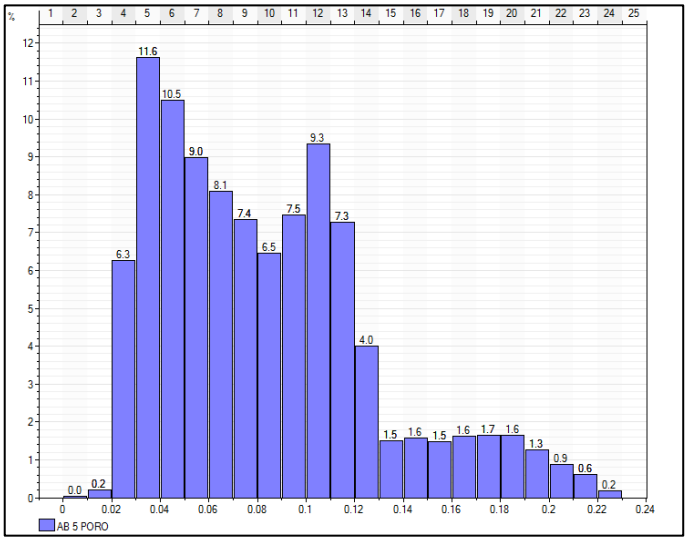

Figure 5.3.8: Abenaki 5 porosity distribution used in the simulation model.

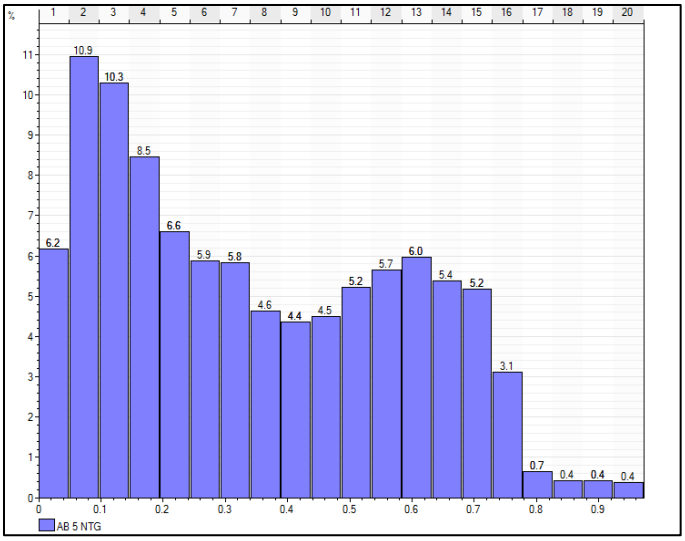

Figure 5.3.9: Net to gross ratio distributions used in the simulation model.

Porosity distribution shows that most assigned cell porosities are below 12%. The net to gross ratio distribution shows that these ratios are assigned more evenly and are generally below 0.75. Wells and perforations were also added to the model as shown in Figure 5.3.10.

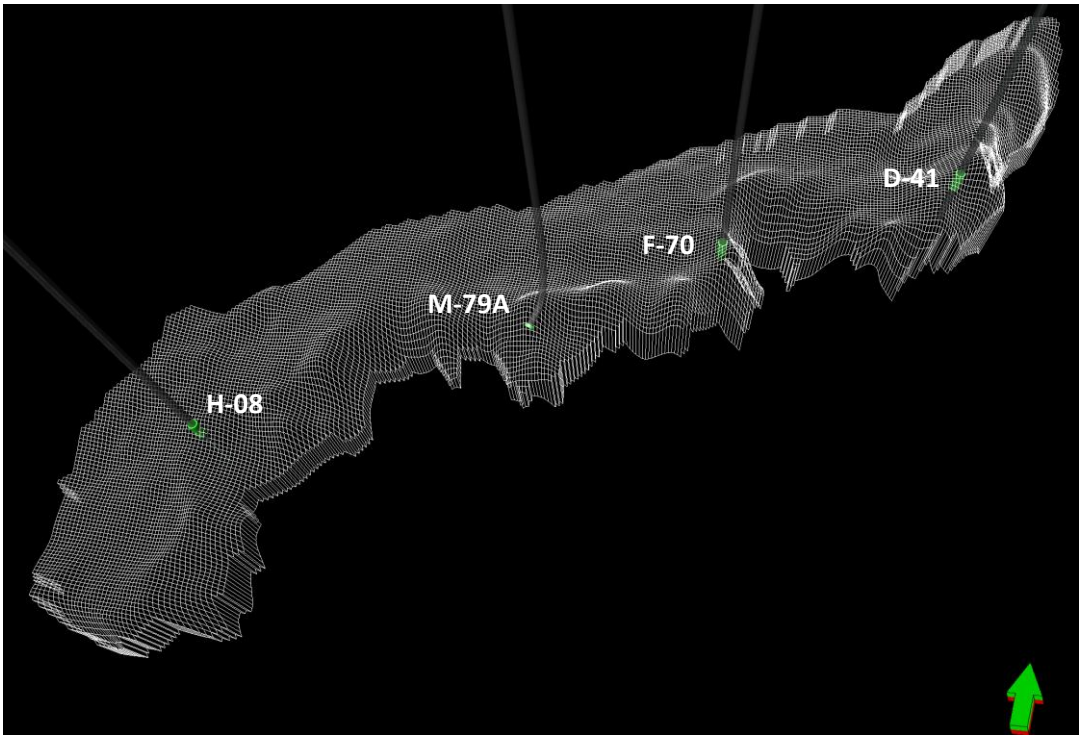

Figure 5.3.10: The four gas production wells shown in the Abenaki 5 layer. Well perforations are also shown in green in the figure.

The main reservoir zone (Abenaki 5) was divided into two separate regions: Limestone (VL) and High Perm Reef Front (HPRF) (Figure 5.3.11). The VL region consisted of 24.3% of the total number of Abenaki 5 grid cells and the remaining 75.7% of grid cells were assigned to the HPRF region. H-08 was the only production well in the VL region. The other three production wells were drilled in the HPRF region. VL to HPRF boundary was modeled as a fault to evaluate the degree of connectivity between the two reservoir regions.

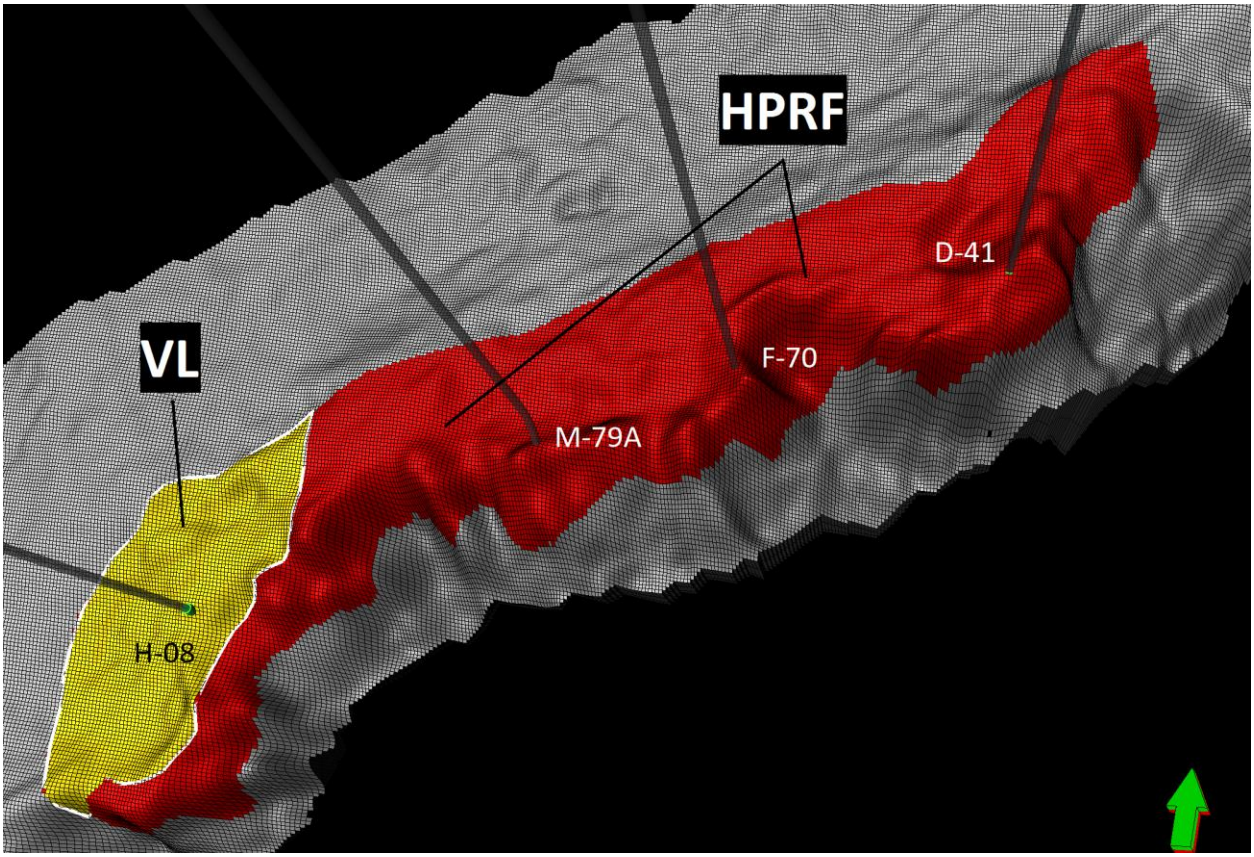

Figure 5.3.11: The two distinct reservoir zones, Vuggy Limestone (VL) and High Perm Reef Front (HPRF), are shown in the figure. The H-08 production well located in the VL area and the other three production wells are located in the HPRF area (M-79A, F-70 and D-41).

It is important to note that M-79A is nearly horizontal in the Abenaki 5 well while the other three production wells are vertical. As mentioned in the previous sections, one may expect gas recovery from a horizontal well to be higher than vertical wells since the perforated zone is in

contact with more fractures. As will be discussed in future sections, well performance indicated that this was not the case since these fractures also delivered more water to the well. The horizontal orientation of M-79A did however, increase the rate of water drain back and pressure recovery during shut in periods.

Porosity/permeability relationship for each reservoir region (VL and HPRF) was determined from conventional and sidewall cores. These relationships were applied to porosity maps to generate permeability for each reservoir region and zone. The following Figure 5.3.12 shows the generated permeability maps in X and Y directions (PERMX & PERMY). As can be seen in the map, initial permeability in the VL region is considerably higher than the HPRF due to higher matrix porosities in this region. Initial permeabilities in the Y direction were assumed equal to X direction (PERMX). Initial permeabilities in Z direction (PERMZ) were assumed equal to PERMX/10 (horizontal permeability divided by 10).

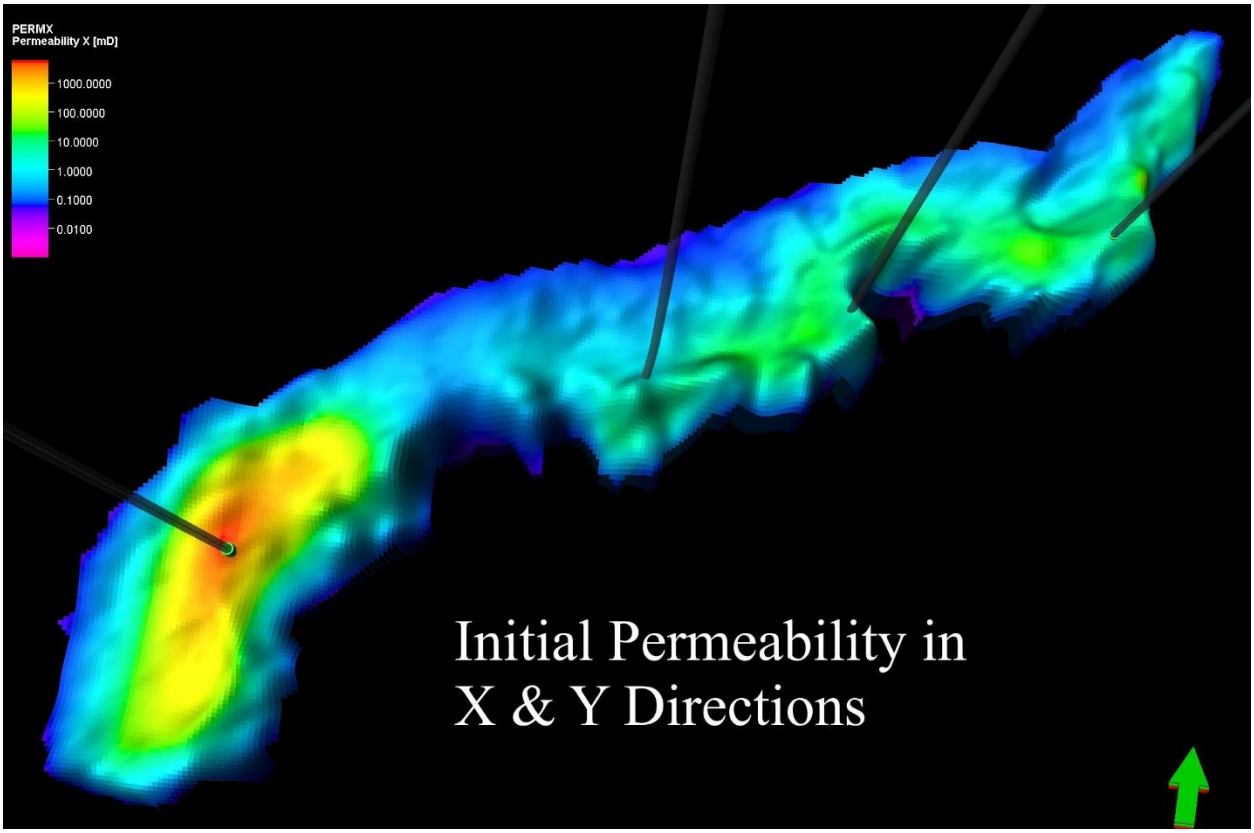

Figure 5.3.12: The above figure shows the initial permeability assigned in the X (horizontal) direction in the Abenaki 5 layer. The same permeability values were also assigned in the Y (vertical) direction.

In addition to the simulation modeling described earlier an analysis of the H-08 well test data was also conducted to improve reservoir characterization in the VL area. The CNSOPB's H-08 well test results and interpretations appear below. Pressure and flow rate data were plotted and the main build-up period was analyzed (Figure 5.3.13).

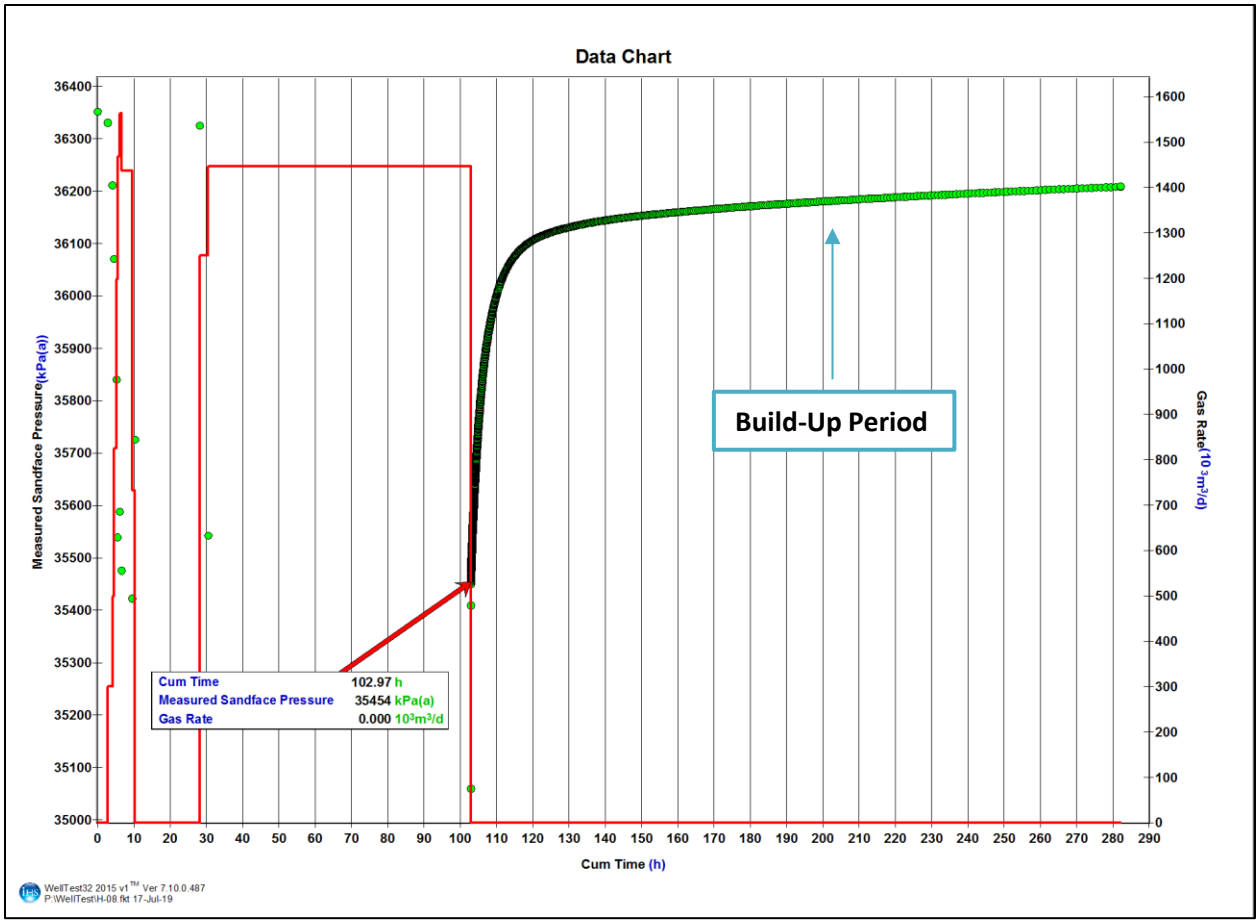

Figure 5.3.13: Analysis of H-08 pressure build up data.

After entering fluid properties, different models were tested to find the best type curve matches. Type curves are used in well test analysis as a method for quantifying well and reservoir parameters such as permeability, skin and wellbore storage by comparing the pressure change and its derivative of the acquired data to reservoir model prebuilt curve families. The best type curve matches (Figure 5.3.14 & 5.3.15) resulted from a composite radial model with a constant pressure outer boundary that consisted of four zones (Figure 5.3.16). The constant pressure boundary confirms the existence of an aquifer at the outer boundary. The innermost zone (34 m radius) has a very high average permeability (1640 mD). This high permeability confirms the existence of fractures and vugs. Permeability decreases significantly in the second, third and fourth zones. The

outermost region has a very low average permeability of 4 mD. These findings were honoured when assigning permeabilities to simulation grids in the H-08 area.

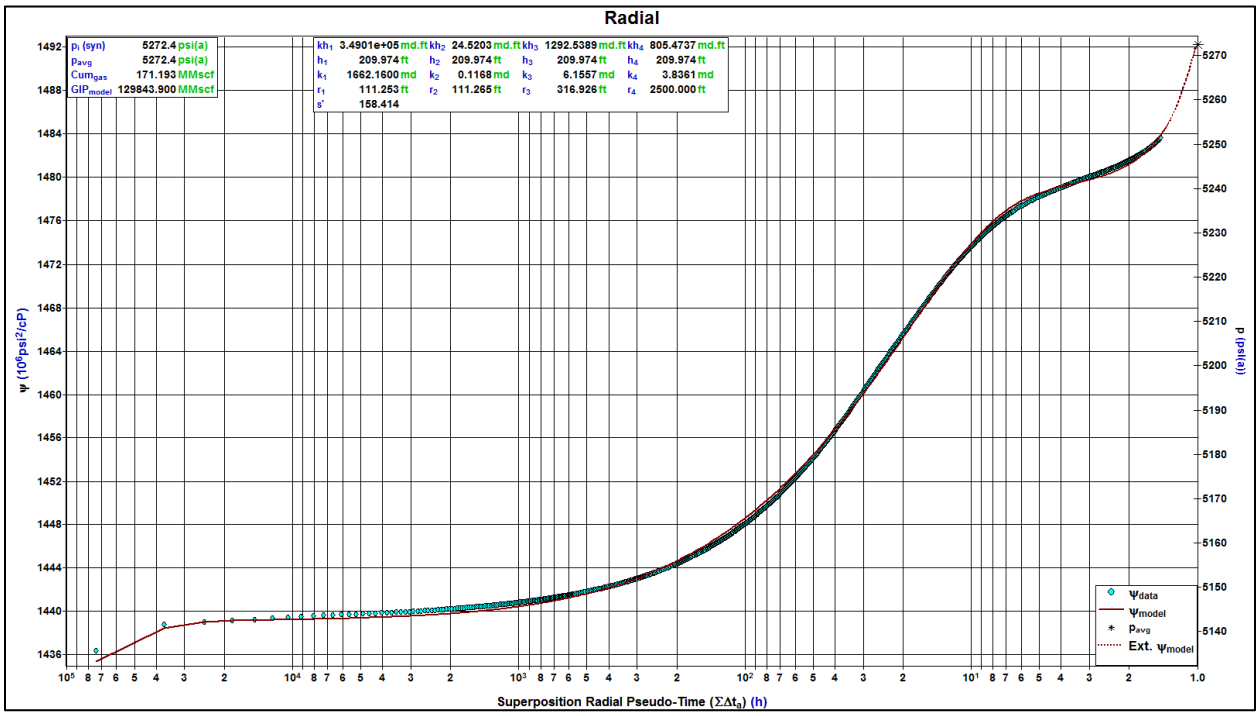

Figure 5.3.14: The above figure shows the radial match generated using a composite model for the H-08 build up period.

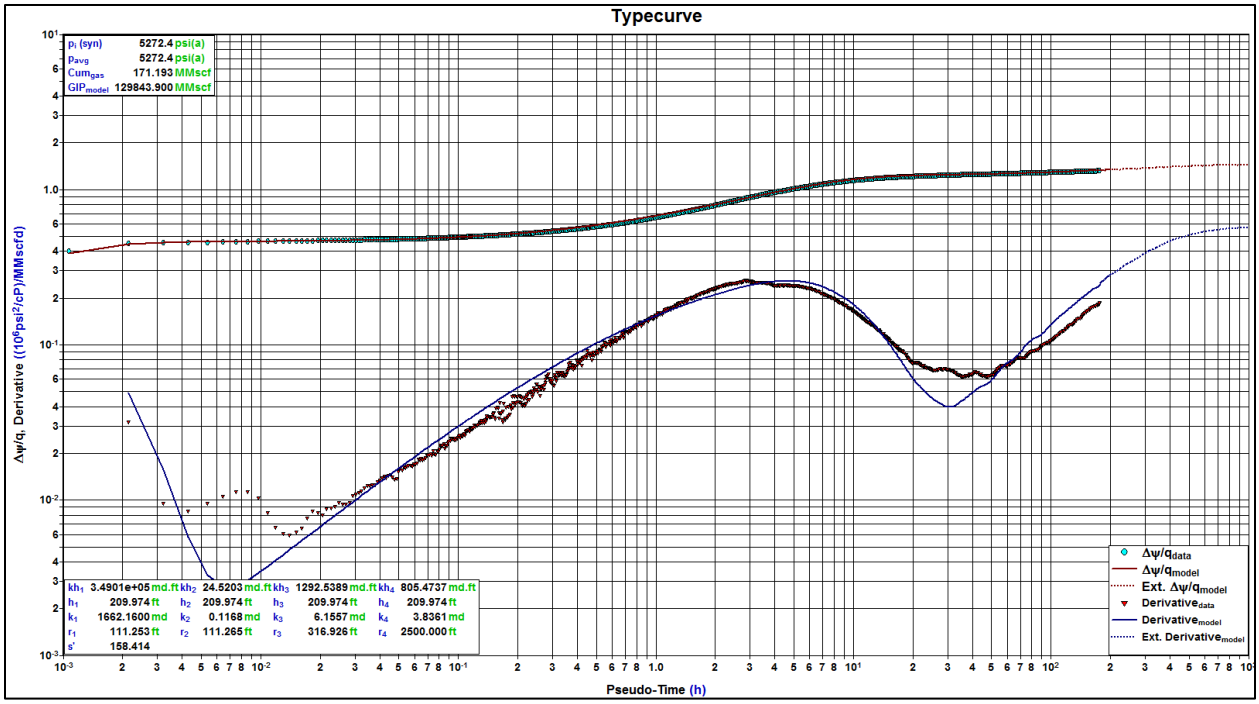

Figure 5.3.15: H-08 type curve match was used to estimate reservoir properties for the different layers using a composite model.

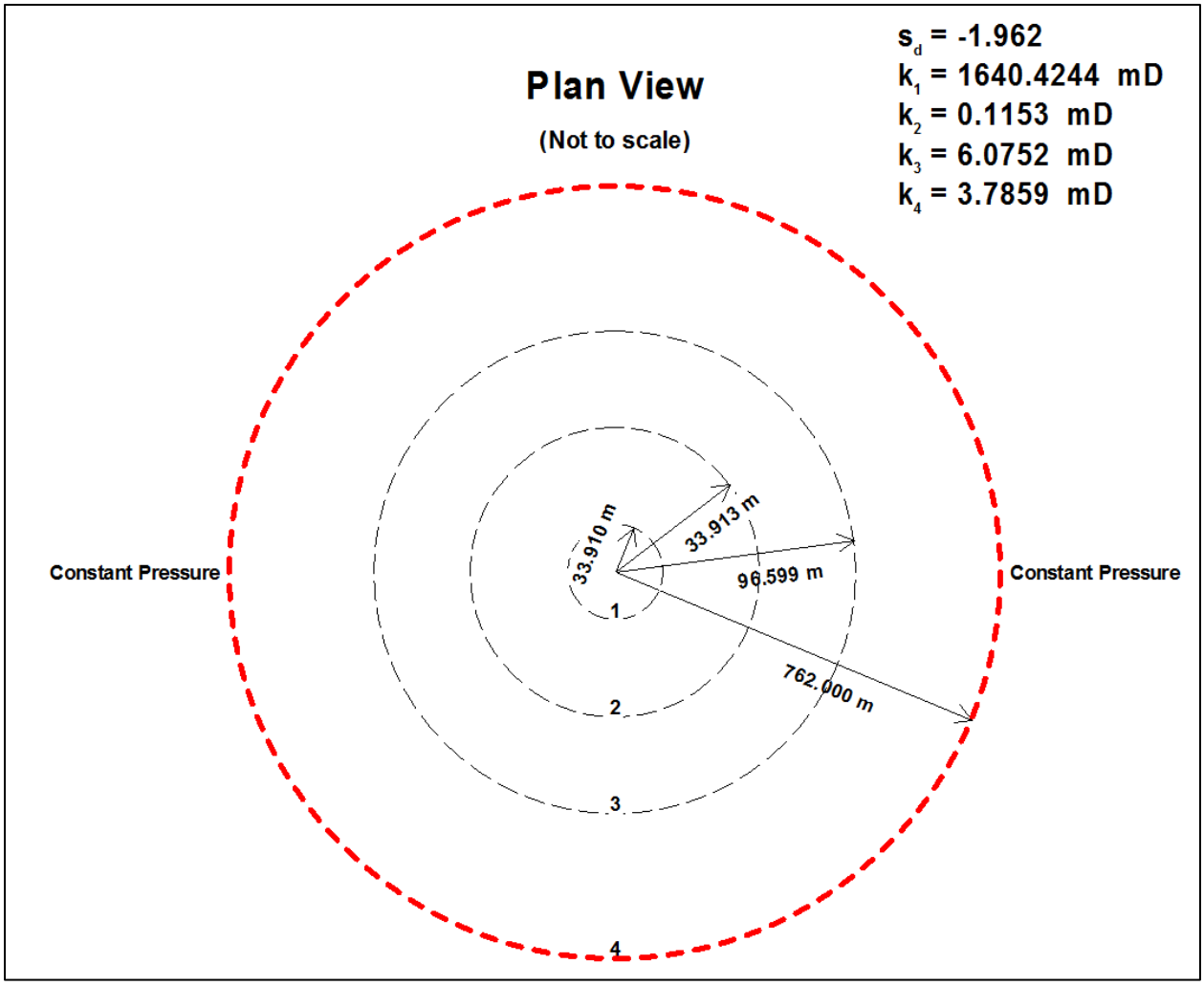

Figure 5.3.16: H-08 Composite Model. The four regions and their associated radiuses and permeability are shown in the figure. The best type curve match was obtained using this 4 layer composite model. This model resulted in an OGIP of approximately 3.7 E9m3 (130 Bcf) for H-08.

Special core analysis data such as capillary pressure and relative permeability were used to create 12 separate saturation regions in the simulation model. These saturation regions are shown in Figure 5.3.17.

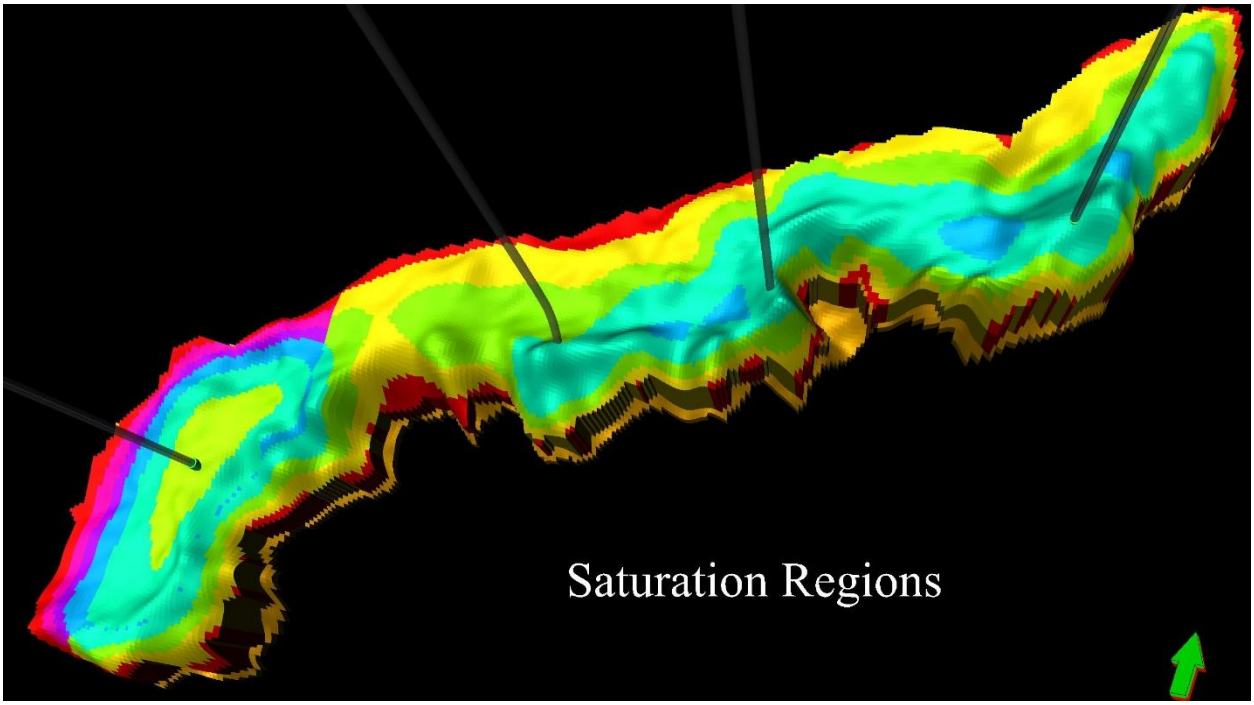

Figure 5.3.17: Saturation regions were assigned based on porosity ranges. Each of these saturations regions were then assigned a unique capillary pressure and relative permeability curves using special core analysis.

Capillary pressure and relative permeability curves were used to generate an initial water saturation model as shown in Figure 5.3.18.

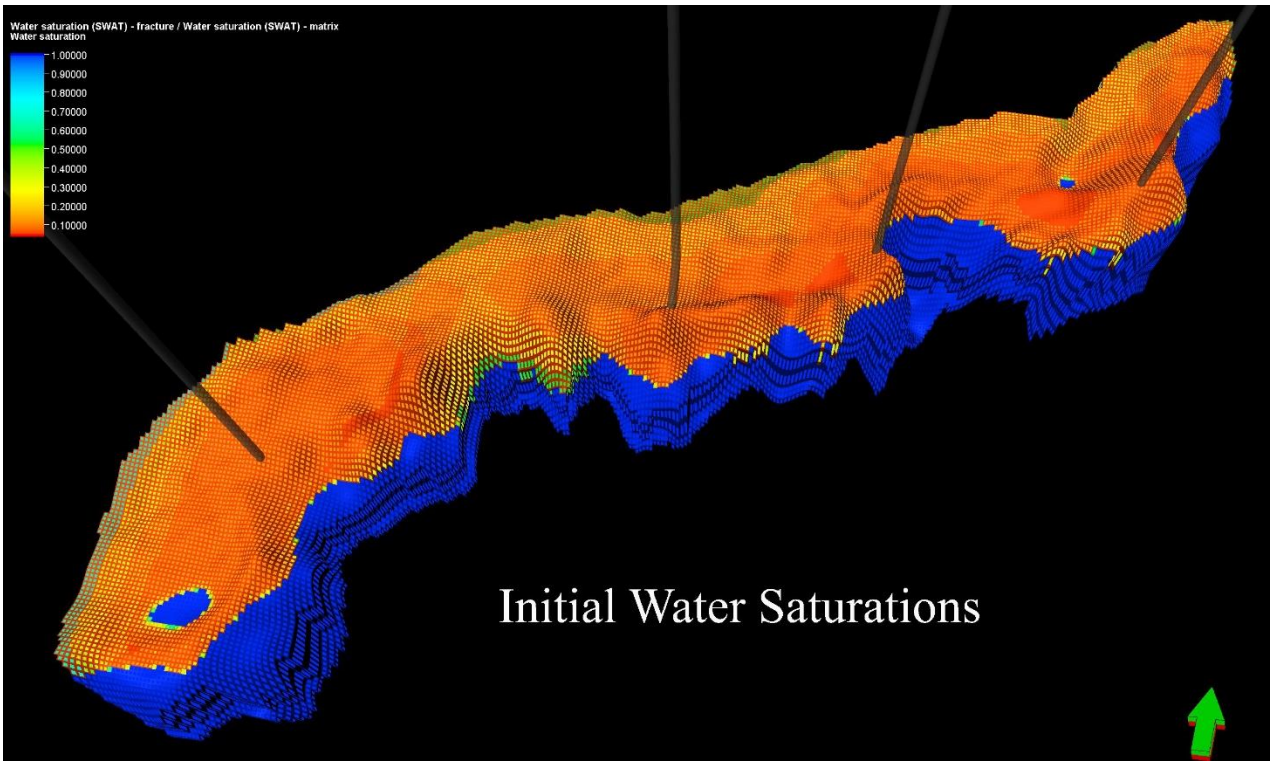

Figure 5.3.18: Abenaki 5 Initial Water Saturation Map.

The following pressure map (Figure 5.3.19) resulted from the model initialization described above. Initial pressure was in the range of 320 to 388 bars (4641 to 5627 psi) with a mean initial reservoir pressure of around 356 bars (5163 psi).

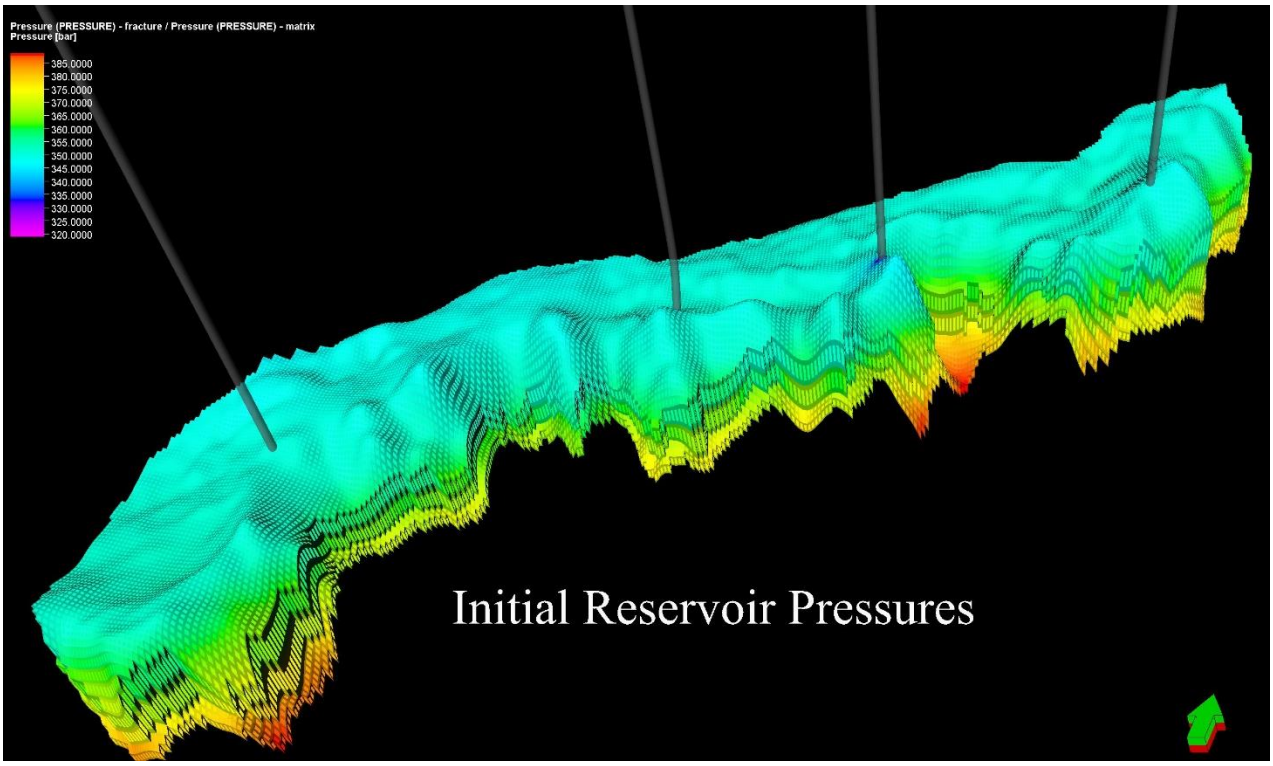

Figure 5.3.19: Abenaki 5 initial reservoir pressure map. Note pressure is consistent in each layer across the reservoir.

The size and strength of the aquifer was determined to be a significant uncertainty and a major risk to gas recovery from Deep Panuke. These were considered as key variables in the simulation modeling and sensitivity analysis.

5.4.Flow Simulation

The next step in building the simulation model was defining an initial project development strategy. The initial development plan strategy, in the 2006 DPA, assumed gas production rates as shown in Table 5.4.1 from the wells. The maximum water rate each well could produce, before the well had to be shut-in, was set to 3974.7 m3 (25,000) bbl/d and minimum gas rate from each well was assumed to be 0.42 E6m3/d (15 MMscf/d). These theoretical constraints were used by the operator in their depletion plan models. The CNSOPB conducted various sensitivity analyses around these constraints.

Table 5.4.1: Initial Development Plan Gas Rates (2006 DPA)

Well	Gas Production Rate E6m3/d (MMscf/d)
D-41	2.0 (70)
F-70	1.4 (50)
H-08	1.8 (65)
M-79A	2.5 (90)

The following charts show the results of the un-calibrated initial simulation runs for each well. Gas rate, Water to Gas ratio (WGR), cumulative gas production and, well pressures were plotted for the four Deep Panuke production wells.

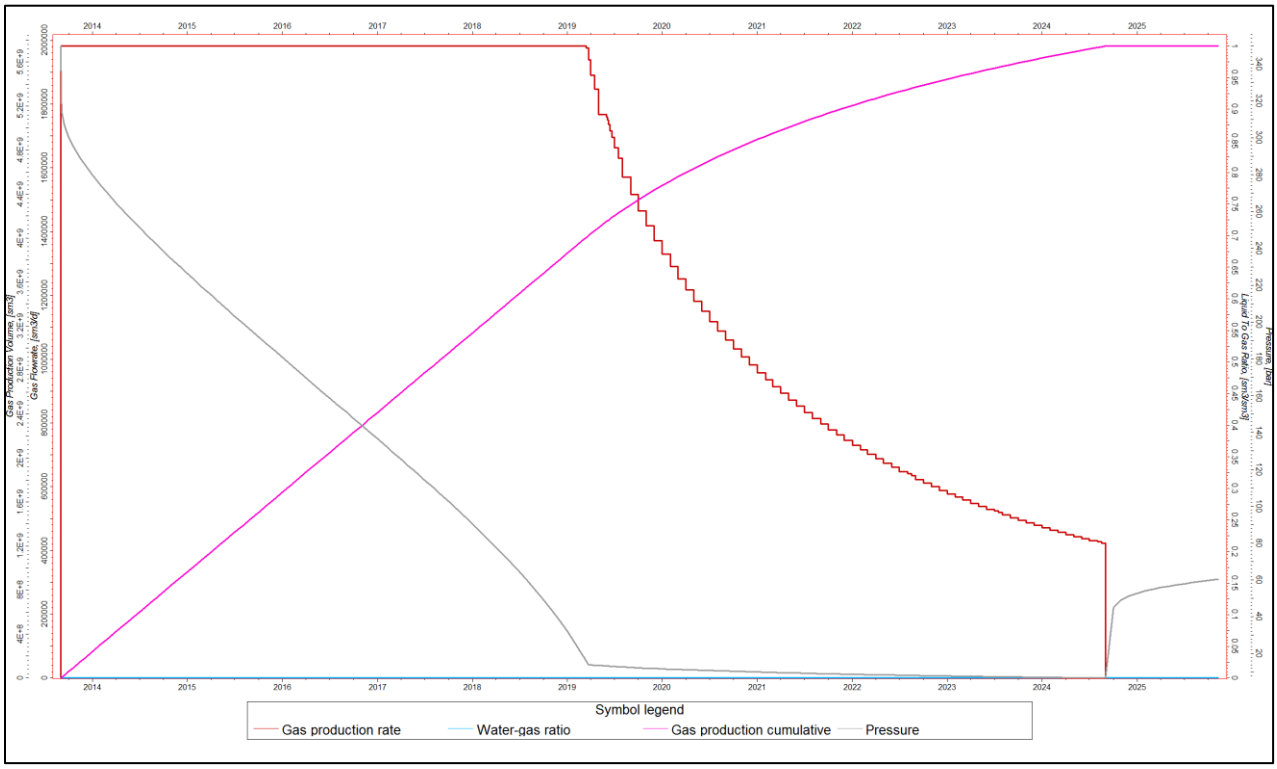

Figure 5.4.1: D-41 initial simulation results. The red line shows gas production rate. Pink line shows cumulative gas production. WGR is shown in blue and wellhead pressure is shown in gray.

D-41 well performance chart (Figure 5.4.1) indicates that a production rate of 2 E6m3/d (70 MMscf/d) could be sustained until Q1 2019. The gas rate would start declining in Q1 2019 and reach the minimum well gas rate of 0.42 E6m3/d (15 MMscf/d) in Q3 2024.

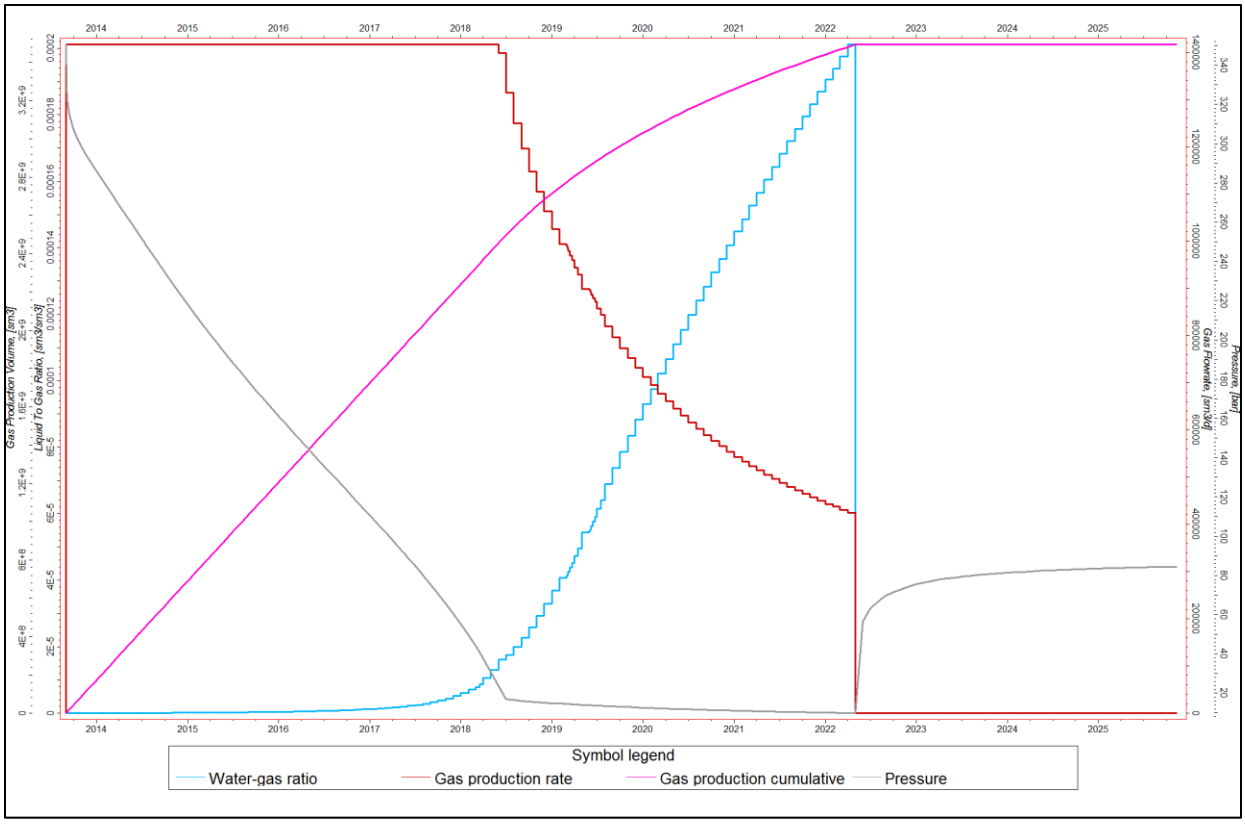

Figure 5.4.2: F-70 initial simulation results. The red line shows gas production rate. Pink line shows cumulative gas production. WGR is shown in blue and wellhead pressure is shown in gray.

F-70 well performance chart (Figure 5.4.2) shows that the production rate of 1.4 E6m3/d (50 MMscf/d) could be sustained until Q2 2018. The gas production rate started declining in Q2 2018 and reached a minimum rate of 0.42 E6m3/d (15 MMscf/d) in Q2 2022. The well was automatically shutdown, in the simulator, when the minimum gas rate was reached. The WGR trend demonstrated that water production from the well would start in early 2014 and reach a rate of approximately 87.4 m3 (550 bbl)/d in Q2 2022. Gas pressure build-up is also seen after the well is shut-in due to lower than 0.42 E6m3/d (15 MMscf/d) gas rate. This pressure build-up is associated with gas re-saturation of the near-wellbore region. This gas re-saturation suggests a continuous feed of gas from the matrix to fractures even after the well is shut-in. Also considering the WGR trend, water loading is not an issue for this well based on this initial un-calibrated simulation model.

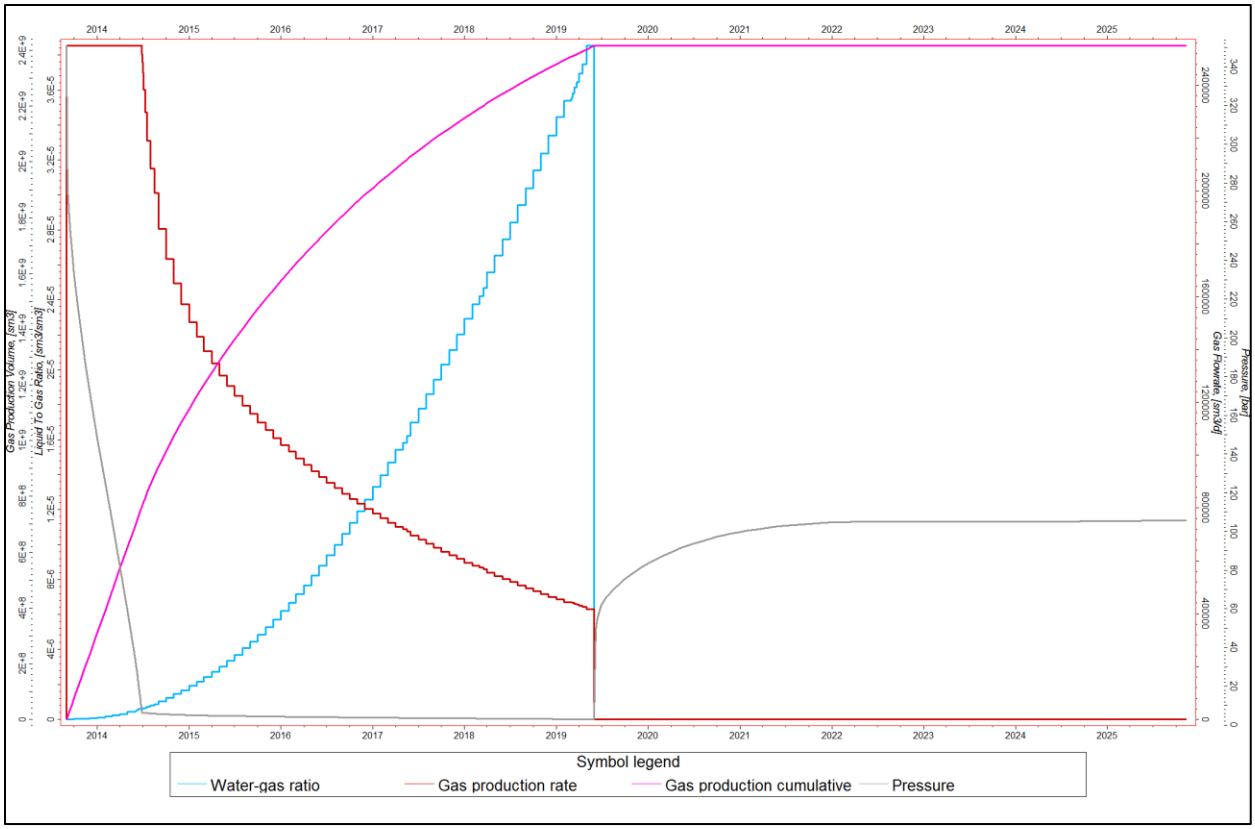

Figure 5.4.3: M-79A initial simulation results. The red line shows gas production rate. Pink line shows cumulative gas production. WGR is shown in blue and wellhead pressure is shown in gray.

M-79A well performance chart (Figure 5.4.3) indicates that a production rate of 2.5 E6m3/d (90 MMscf/d) could be sustained until Q2 2014. The gas rate would start declining and reach the minimum well rate of 0.4 E6m3/d (15 MMscf/d) in Q2 2019. WGR trend demonstrates that water production from the well would start in early 2014 and reach a water flowrate of approximately 100 bbl/d in Q2 2019. Gas pressure build-up is also seen after the well is shut-in due to lower than 0.4 E6m3/d (15 MMscf/d) gas rate. This pressure build-up is associated with gas re-saturation of the near wellbore region. This gas re-saturation shows a continuous feed of gas from the matrix to fractures even after the well is shut-in. Also considering the WGR trend, water loading is never an issue for this well based on this initial un-calibrated simulation model.

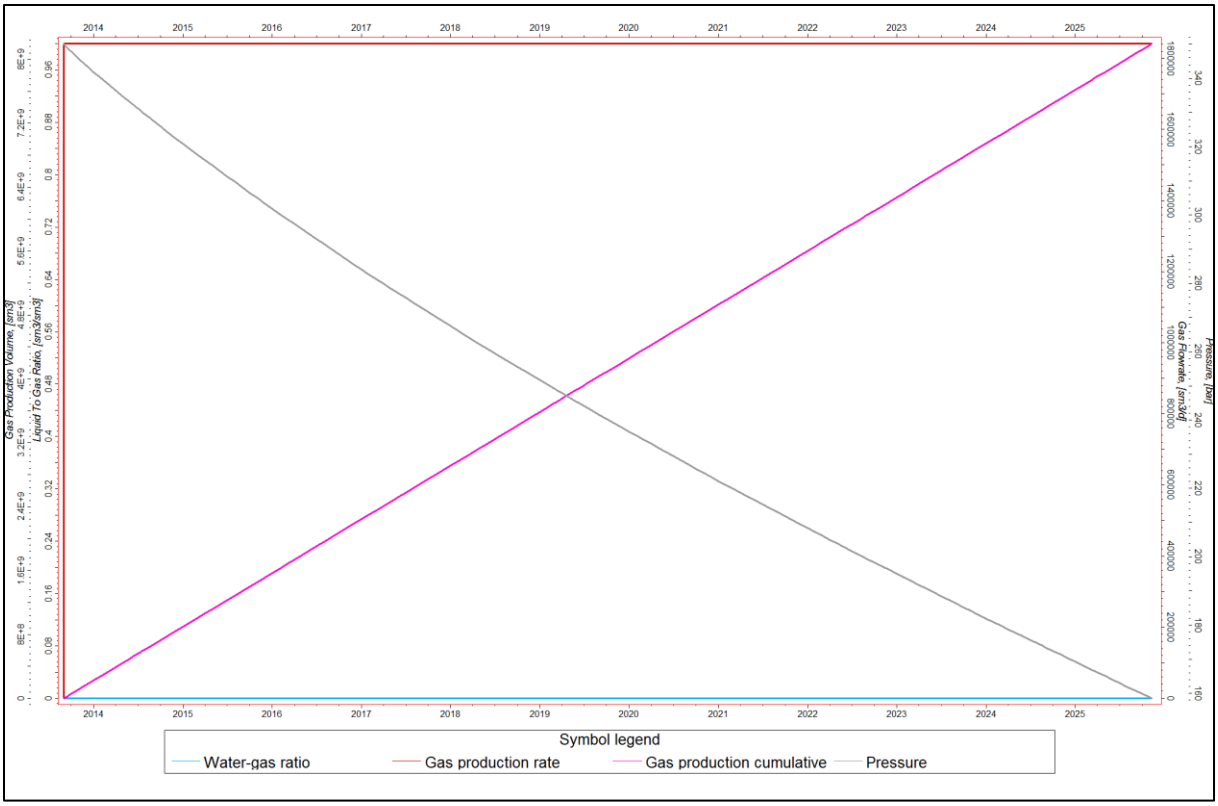

Figure 5.4.4: H-08 initial simulation results. The red line shows gas production rate. Pink line shows cumulative gas production. WGR is shown in blue and wellhead pressure is shown in gray.

H-08 well performance chart. (Figure 5.4.4) indicates that a production rate of 1.8 E6m3/d (65 MMscf/d) could be sustained until Q2 2026 (final simulation run date). The gas rate would not start declining until the simulation run reaches its final date and there was no water production from the well during the simulation run period.

Figure 4.4.5 shows a comparison of cumulative gas production from the four production wells to the end of 2025. As can be seen in this figure, based on the initial simulation run, H-08 produces significantly more gas than the three HPRF wells (D-41, M-79A & F-70). This is mainly related to the higher permeability and porosity of the VL area in the initial model. In the HPRF area, based on the initial simulation run, D-41 produces the most gas followed by F-70 and M-79A. This is

mainly due to D-41 being higher in structure as well as how porosity and permeability are distributed in the near-wellbore region.

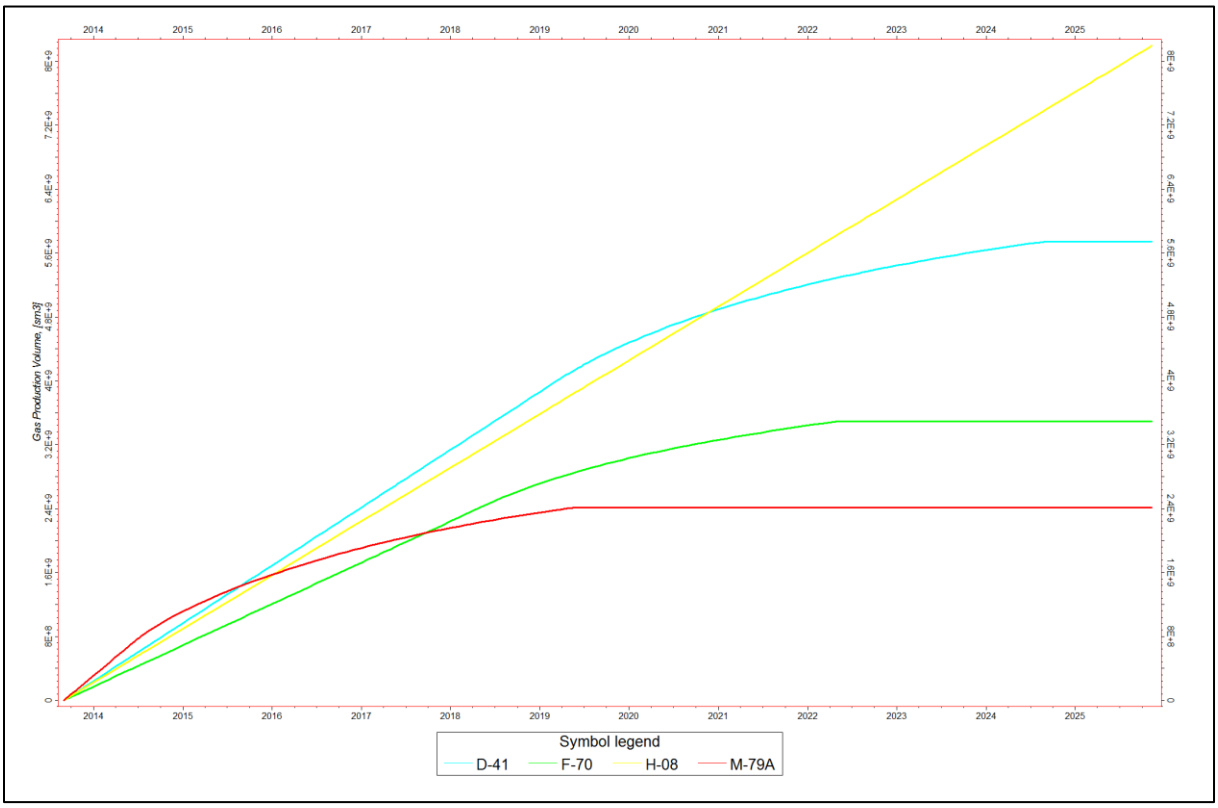

Figure 5.4.5: Cumulative gas production from the four production wells to end of 2025. H-08 produces the most gas and M-79A produces the least amount of gas based on the initial simulation model.

The following table (Table 5.4.2) shows cumulative gas production from each well to the end of 2025 resulting from the initial simulation run. These volumes are consistent with the operator's 2006 DPA recoverable gas estimates.

Table 5.4.2: Un-calibrated simulation model's cumulative gas production to end of 2025

Well	Cumulative Gas Production to Dec. 2025 E9m3 (Bcf)
D-41	5.7 (201)
F-70	3.5 (122)
H-08	8.1 (287)
M-79A	2.4 (85)
Total	**2.0 (695)**

A comparison of WGR trends from the initial model run for the four production wells is shown in Figure 5.4.6. Based on the results of these un-calibrated initial simulation models, M-79A was the first well that was expected to start producing water followed by F-70 and D-41. H-08 was not expected to produce any water until the end of 2025. Based on this initial simulation model results, none of the Deep Panuke wells were expected to have issues with water loading. The highest water rate was from F-70 and was approximately 79.5 m3 (500 bbl)/d, which was well below the technical water production capacity of the individual wells of 3974.7 m3 (25,000 bbl)/d.

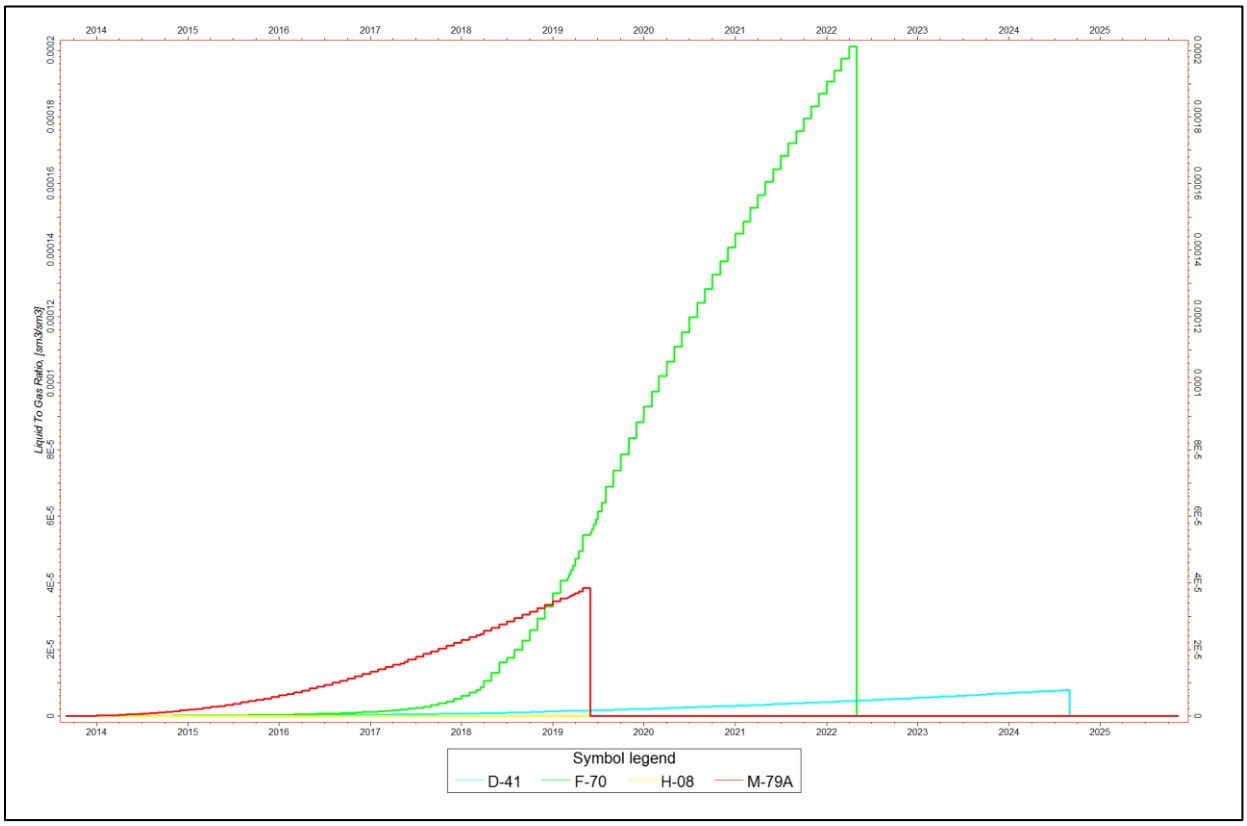

Figure 5.4.6: Well WGR profiles for the four production wells are shown. It can be observed that based on the initial simulation model, M-79A was the first well to produce water followed by F-70 and D-41. H-08 did not produce any water by the end of 2025. Water production was highest for F-70.

5.5. History Matching

Production from the Deep Panuke field started in August 2013 and ended in May 2018. Actual production data was used to calibrate and history match the simulation model. Reservoir characterization was periodically adjusted to improve history matching. It is important to note that the final calibrated reservoir characterization and simulation model results, summarized below, are based on a large number of simulation runs, extensive history matching and reservoir property refinements. In this report, the history matching process and simulation results are divided into two separate time-frames pre and post water production. This simulation model was regularly used to analyze the various depletion scenarios proposed by the operator to ensure economic recovery from the reservoir was maximized. A description of the major reservoir characterization modifications for each well is described below.

The accuracy of history matches and the ability of the reservoir simulation model to accurately predict recovery decreased after water production started from the wells. Figure 6.2.2 shows field level history matches from the start of production in August 2013 to May 2015. As can be seen in the figure, the history matches were reasonable up to the beginning of water production. It is unrealistic to expect a reservoir model to fully characterize complexity and heterogeneity of the reservoir and, for this reason, other methods including the use of extrapolations of observed data and established performance trends (decline analysis) were incorporated in forecasting performance.

5.5.1. Panuke H-08

Water production from H-08 started in June 2014. As shown in Figure 5.4.6, early water production from this well was not expected in either the operator or the CNSOPB's initial simulation models.

Figure 5.5.1.1 shows H-08's productivity since November 2014 when the well was returned to production after being shut-in from July 20, 2014, due to significant water breakthrough. It can be observed that the productivity of the well declined quickly after water production started. H-08 regained productivity after each shut-in period mainly because of water draining back into the reservoir during each was shut-in. The last 3 production cycles in late 2015 and early 2016 show that the well could only produce for a few hours to a few days. During these weak cycles, the well produced at very low rates and productivity declined very quickly due to excessive water production. Production from the well was shut-in after it became water loaded.

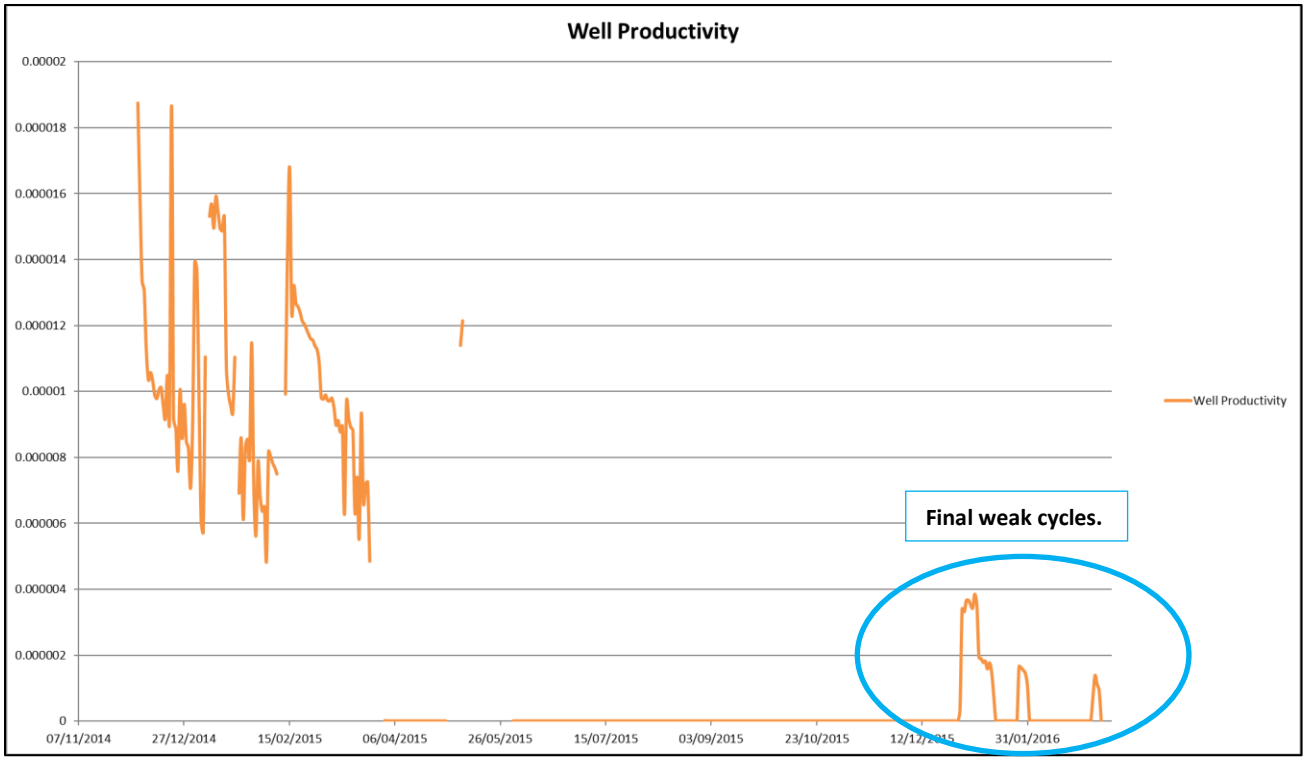

Figure 5.5.1.1: H-08 well productivity. It can be seen that productivity decreased dramatically after water production started. The increase in productivity is mainly associated with acid jobs and pressure build-ups after each shut-in period. Well productivity was significantly lower during the final production cycles.

Unexpected early water production from H-08 required many revisions to reservoir and aquifer characterizations in the VL area. Based on the un-calibrated initial simulation runs, this well was expected to recover the largest amount of gas compared to the other production wells. Reservoir properties such as porosity and permeability for both matrix and fractures in the H-08 area had to be adjusted to improve history matching. As shown in Figure 5.5.1.4, pressure and WGR matches were reasonable indicating that the revised reservoir description in the model is likely closer to the actual reservoir conditions. The following are the main revisions to the H-08 area's reservoir characterization:

- Abenaki 5 matrix porosity was reduced.
- Abenaki 5 matrix permeability was reduced in all directions (X, Y and, Z).

- The best method found to match water production early in the life of the well was to create a localized high transmissibility fault that goes through the low porosity/permeability interval (Tight Streak) between base of Abenaki 5 and 4. This fault was created by assigning high matrix and fracture permeabilities to local cells in the vicinity of H-08 perforations (Figures 5.5.1.2).
- In the final model, in order to get a match, the Abenaki 5 fracture permeabilities had to be an order of magnitude higher than matrix permeabilities.
- The VL region aquifer properties such as permeability, porosity and size were adjusted to allow better history matching of initial water production timing and intensity.

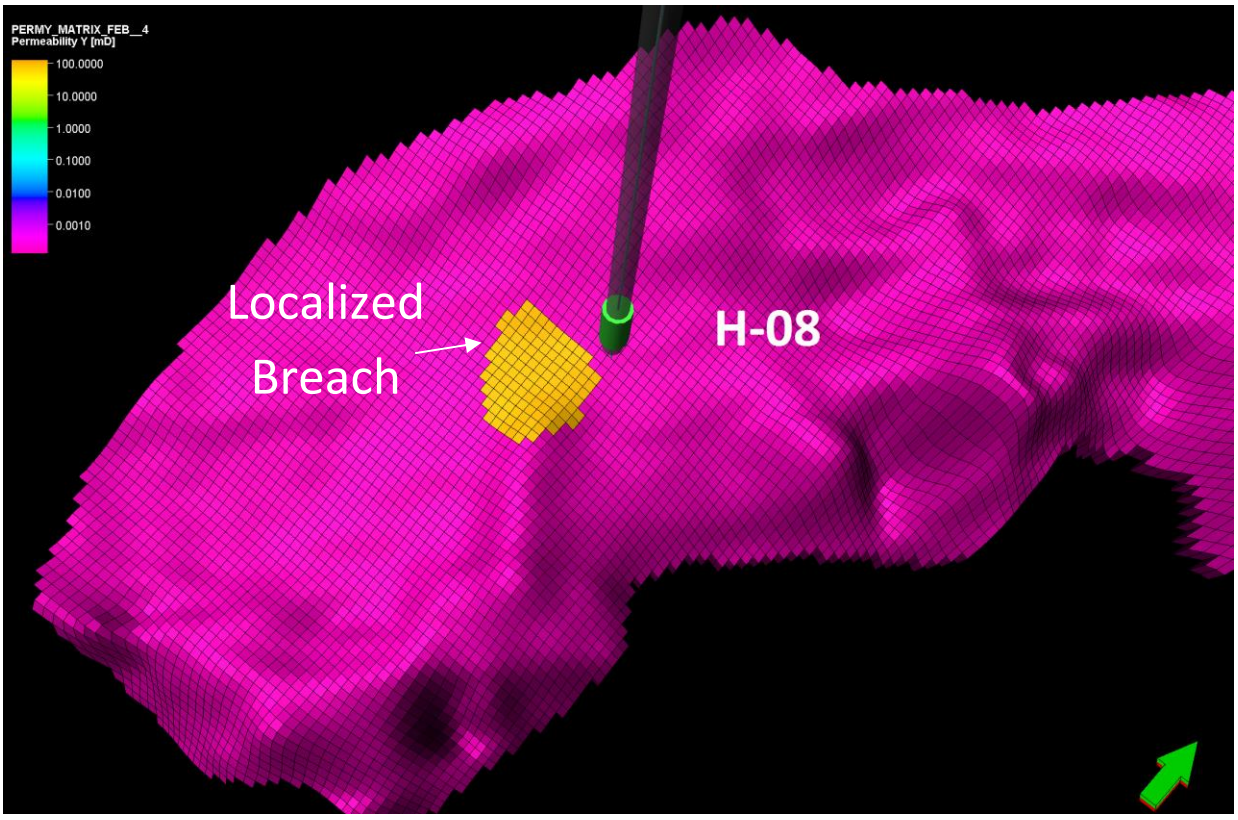

Figure 5.5.1.2: This figure shows how the model was adjusted to create a localized high transmissibility fault (yellow cells) in the Tight Streak to better match water production from the well.

H-08 was shut in from July 21, 2014, to December 3, 2014, after water production was observed. The WGR increased aggressively after production from H-08 resumed in December 2014. Although the revised simulation model predicted very high WGRs after production restart from the well, the WGR trend could not be matched precisely (Figure 5.5.1.3). This mismatch is mainly due to the complexity of the matrix-fracture system and the heterogeneity of the reservoir and the limited ability of the simulation modeling software to accurately model a complex dual porosity (matrix & fractures) reservoir.

Another strategy that the operator evaluated to increase gas recovery from the well was foam injection. The foam was expected to decrease the density of the standing water column to a degree that gas flow from the well could begin lifting water out of the well (foam-assisted lift). The foam was injected and well was re-started on January 26, 2016. The well was able to re-start, however gas production started to decline rapidly. Despite positive preliminary results from the foam-assisted lift, due to complications with the PFC's produced water system, foam injection was shut-in and well began to slug. The well water loaded and was shut-in on January 31, 2016. After months of laboratory tests and engineering analyses, it was determined that complications caused by foam injection were extensive and could not be resolved in a reasonable time and the cost of the modifications required to the water system would be much higher than the incremental revenue that would be realized from foam injection.

Figure 5.5.1.3: Panuke H-08 history match. The pressure and WGR matches were reasonable before water production from the well started. Match quality was lower after the start of water production.

5.5.2. MarCoh D-41

D-41 was the last Deep Panuke production well to begin producing water. D-41 did not start producing water until October 2016. This relatively late water production is mainly related to the well being structurally higher than the other wells and as a result has the greatest vertical standoff from the field wide gas-water contact. In addition, the Tight Streak acts as an effective barrier to vertical water encroachment in this part of the field. An acid treatment was performed in January 2018, after the well was shut-in due to excessive water production, in an effort to restart production and increase productivity. Figure 5.5.2.1 shows the productivity of the well from the beginning of gas production to end of production is June 2017. This figure shows that the productivity of the well was on a natural decline as the near-wellbore area was drained. It is also evident that the well regained some productivity after each shut-in.

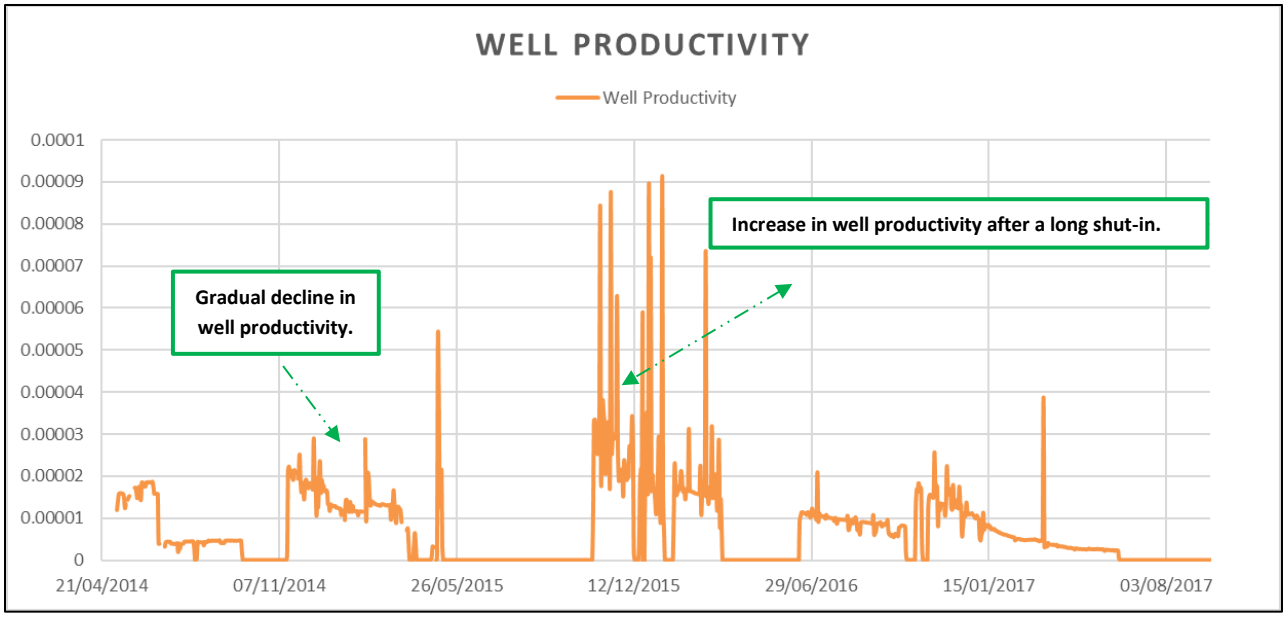

Figure 5.5.2.1: D-41 well productivity. It can be seen that well productivity naturally declined with production. It is also shows the well regained productivity after long shut-ins.

To observe changes in well productivity, an Inflow Performance Relationship (IPR) analysis was performed after one year of production. This method is used to assess well performance by plotting well production rate against the flowing bottomhole pressure. Figure 5.5.2.2 shows the initial and after one-year (October 2014) IPR curves. This comparison shows that productivity declined during the first year but not significantly. The Absolute Open Flow (AOF) decreased from close to 5.7 E6m3/d (200 MMscf/d) to around 4.5 E6m3/d (160 MMscf/d). AOF of a well is the rate at which well would produce against zero sand face back pressure. It is used as a measure of gas well performance because it quantifies the ability of a reservoir to deliver gas to the wellbore. Deliverability tests make it possible to predict flow rates against any particular backpressure, including AOF when the backpressure is zero.

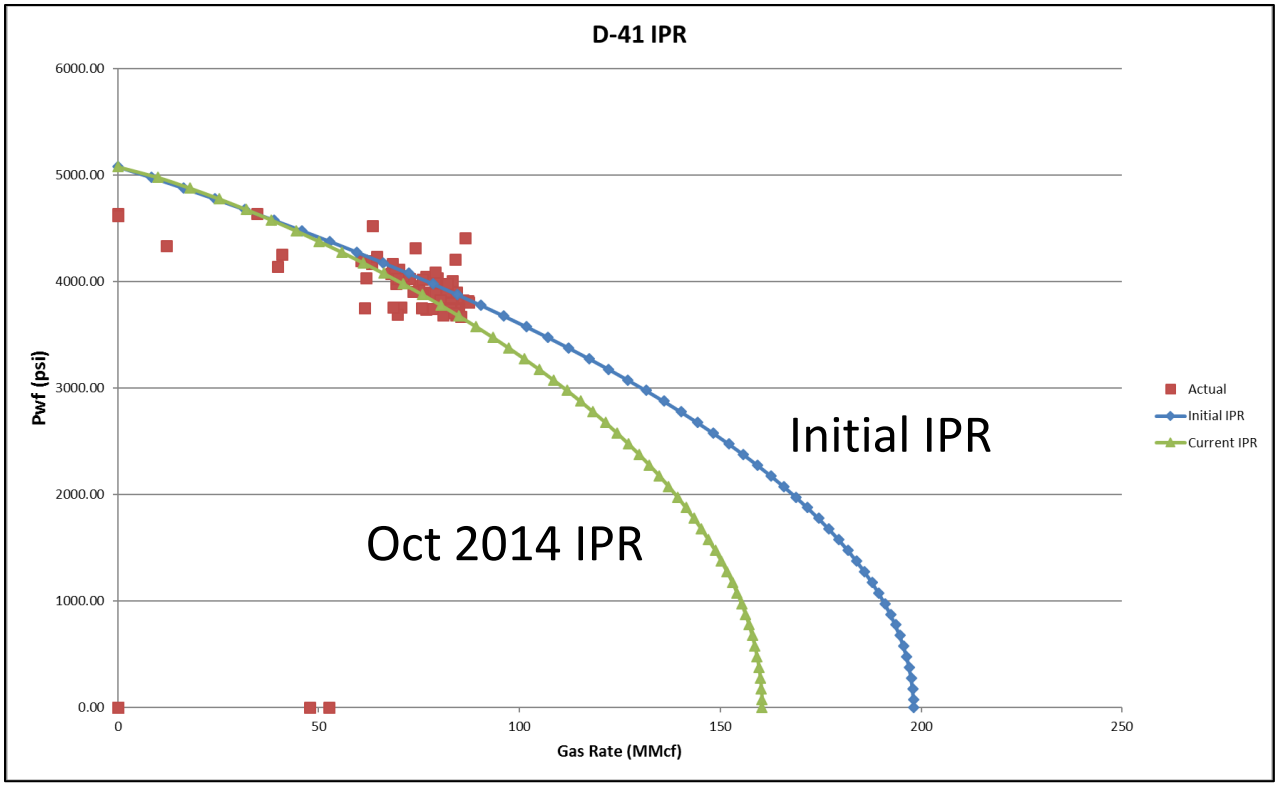

Figure 5.5.2.2: IPR analysis shows that the wells production capacity was decreased after a year of production.

Material balance analysis is an interpretation method used to determine original fluids-in-place (OFIP) based on production and static pressure data. The general material balance equation relates the original gas and water in the reservoir to production volumes and current pressure conditions. Material balance equations assume tank-type behavior at a given datum depth and the reservoir is considered to have the same pressure and fluid properties at any location in the reservoir. Gas material balance is a simplified version of the general material balance equation. When plotted on a graph of p/z (pressure/gas deviation factor) versus cumulative production, the equation can be analyzed as a linear relationship. For gas reservoirs connected to aquifers, the aquifer provides pressure support to the gas reservoir as it is depleted. In this case, the pressure decrease in the gas reservoir is balanced by water encroaching into the reservoir. As this happens, the pore volume of gas is decreasing and average reservoir pressure is maintained. Often this reservoir will show a flat

pressure trend after some depletion. D-41 material balance analysis shows that the well had started to feel the effects of the aquifer in January 2015 (Figure 5.5.2.3). Actual water production from the well, however, did not start until October 2016.

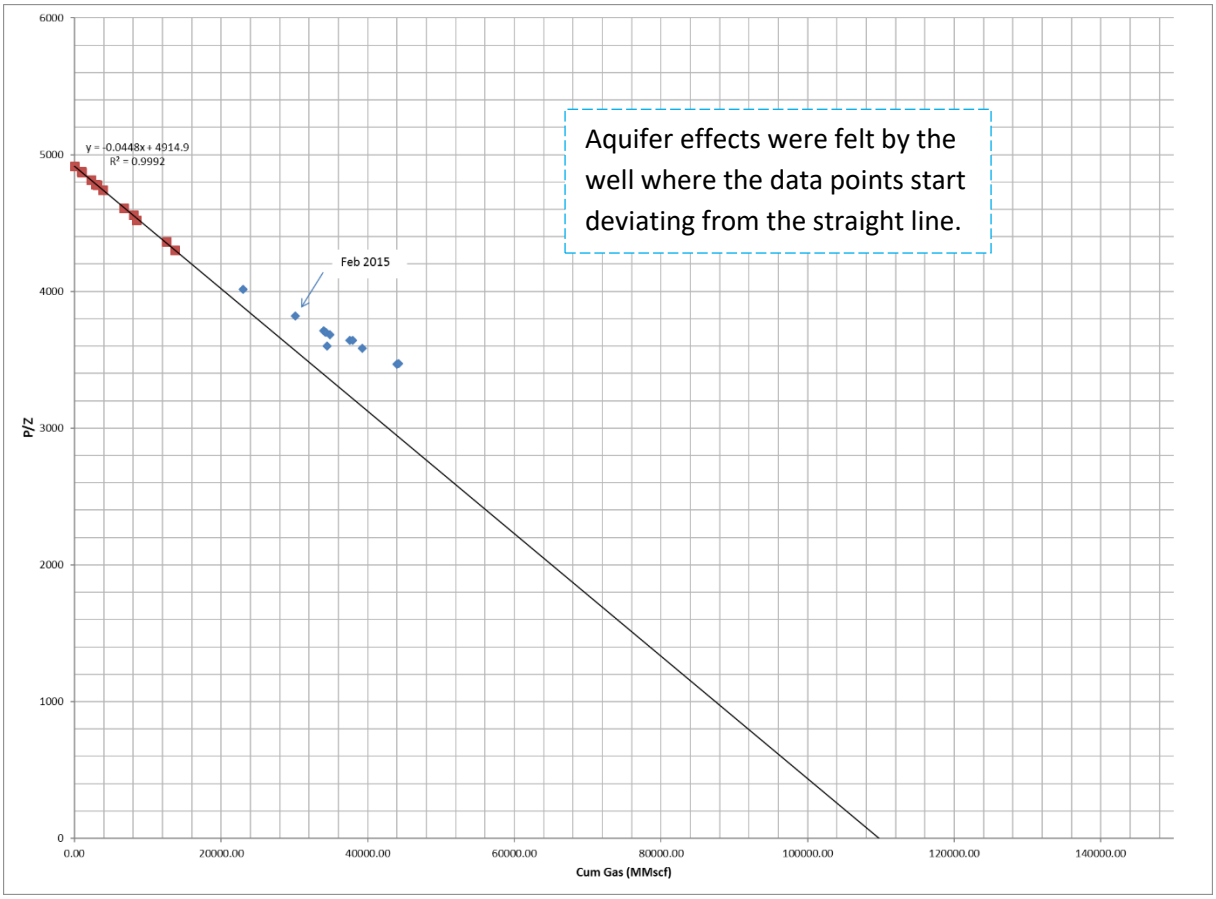

Figure 5.5.2.3: D-41 Material Balance Analysis. The data points clearly show that the well is receiving pressure support from an aquifer.

D-41 reservoir characterization had to be revised at different times during production to obtain a reasonable pressure history match. As shown in Figure 5.5.2.7, pressure history matches were reasonable prior to water production from the well. The following are the main revisions to D-41 area's reservoir characterization:

- Abenaki 5 matrix porosity was reduced as shown in Figure 5.5.2.4.

- Abenaki 5 matrix permeability in the Z direction was considerably higher than matrix permeabilities in the X and Y directions (Figures 5.5.2.5).
- Abenaki 5 fracture permeabilities (Figures 5.5.2.6) were an order of magnitude higher than the revised matrix permeabilities observed in figures 5.5.2.5.
- Considering the lack of water production from the well until later in the life of the field, the Tight Streak is acting as an effective barrier in this area and unlike the H-08 area, no permeability needed to be introduced in this model layer in the vicinity of D-41 to obtain a satisfactory history match.
- HPRF aquifer properties such as permeability, porosity and size were adjusted to match initial water production timing and intensity from all three High Perm Reef Front (HPRF) production wells (M-79A, F-70 & D-41).

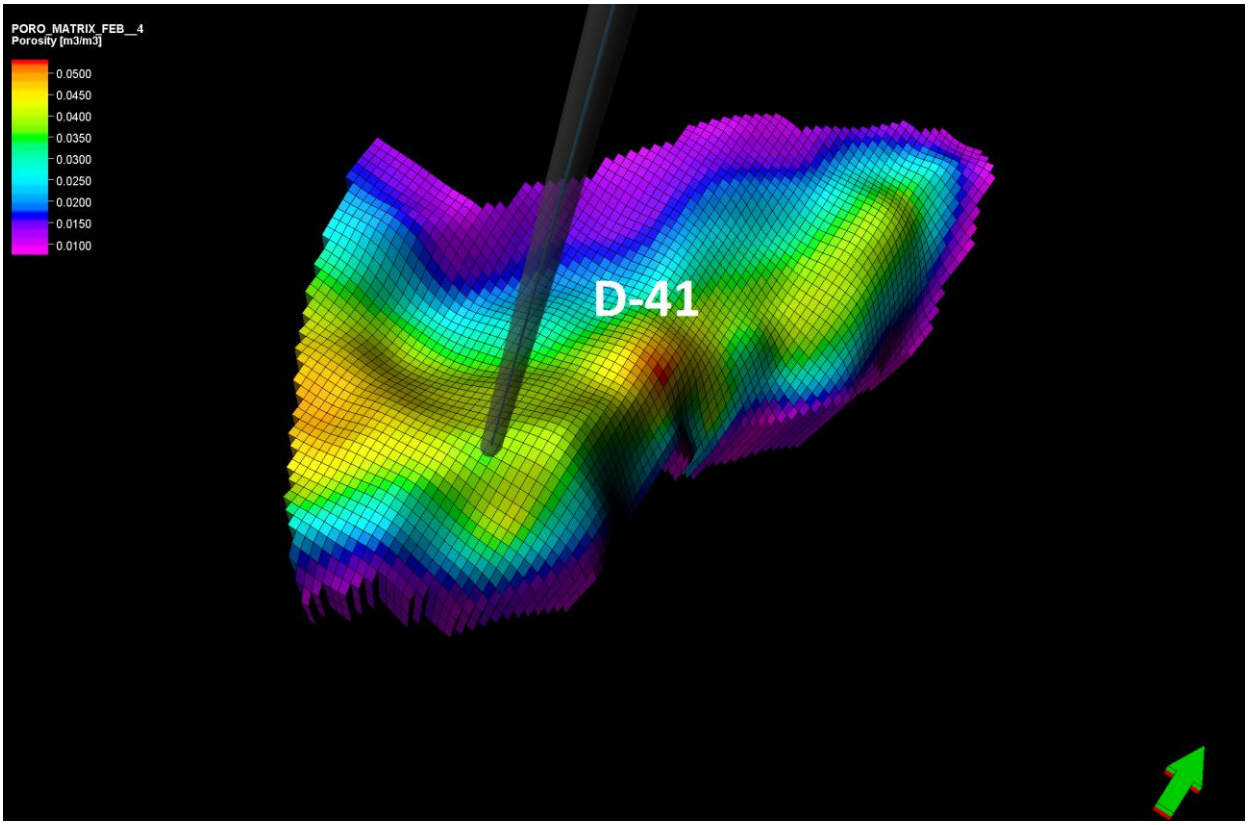

Figure 5.5.2.4: Abenaki 5 porosity in the D-41 area after the history matching process. Warm colours are higher porosity values.

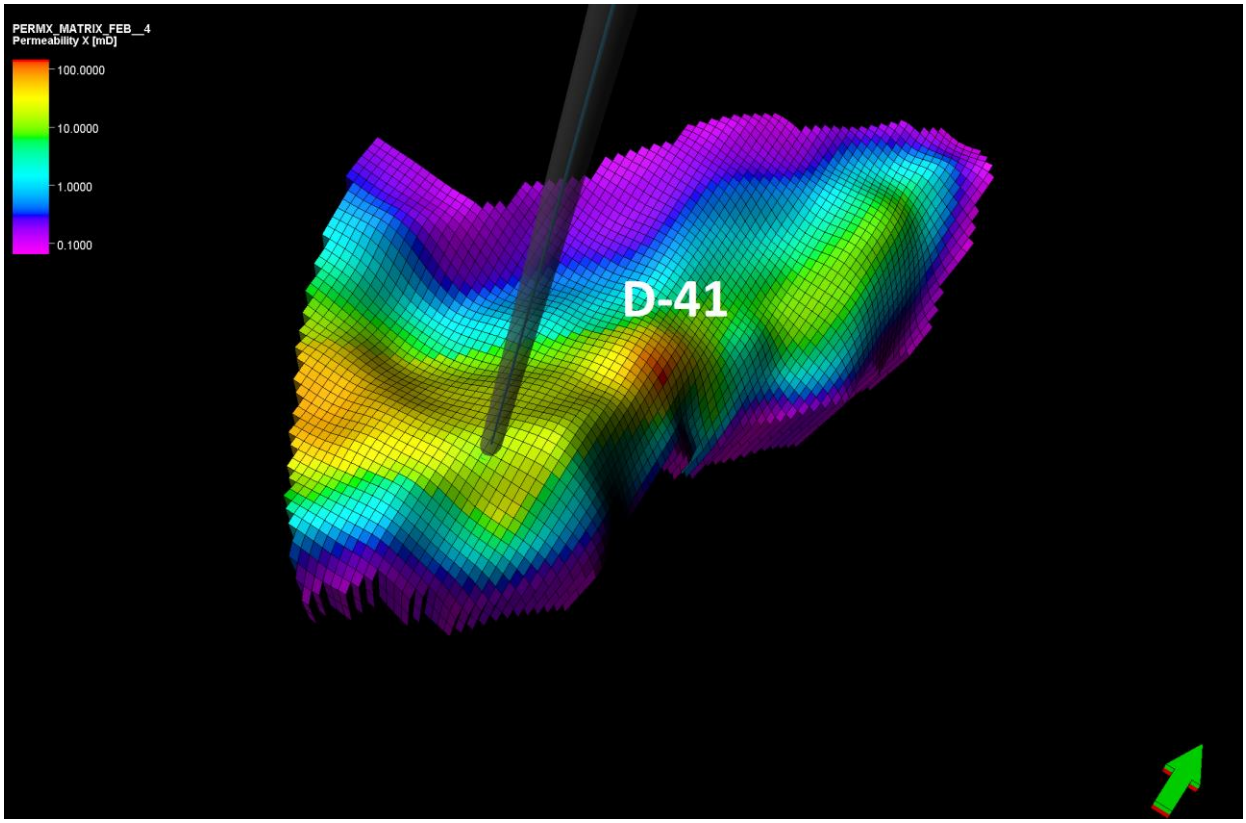

Figure 5.5.2.5: Abenaki 5 X direction matrix permeability in the D-41 area after the history matching process. Warm colours show higher permeability values.

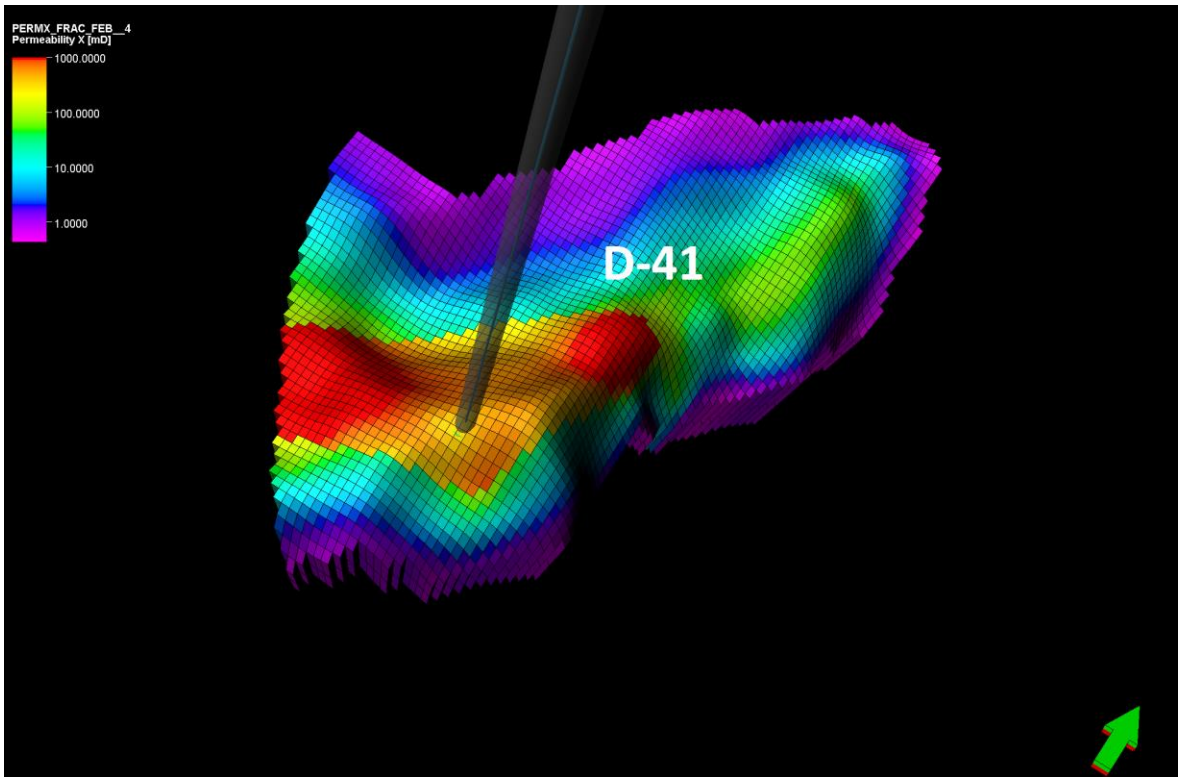

Figure 5.5.2.6: Abenaki 5 X direction fracture permeability in the D-41 area after the history matching process. Warm colours are higher permeability values.

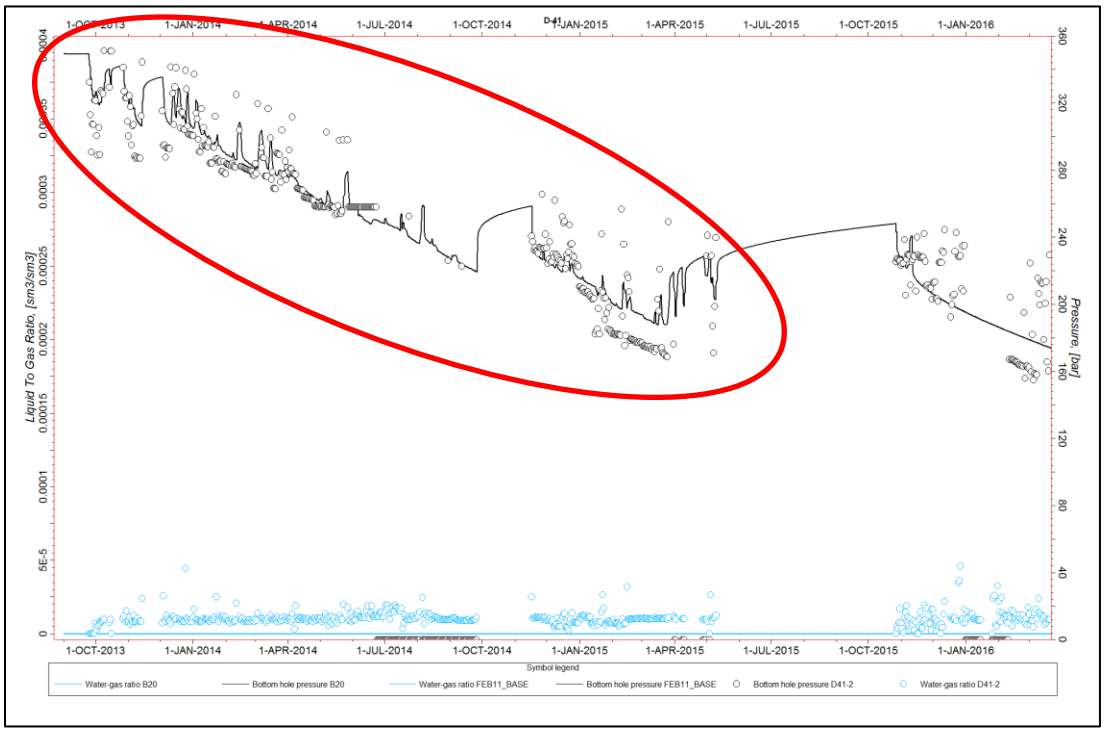

Figure 5.5.2.7: D-41 history match. The pressure match was reasonable. There was no water production from the well in the above period, which matched the simulation model.

5.5.3. Margaree F-70

Water production from the well started in August 2014. The well was then shut-in from September 26, 2014, to November 16, 2014 after an initial period of water production. An acid treatment was performed on this well in January 2015 which increased both gas and water productivity of the well. WGR continued to increase aggressively after production was resumed and the well stopped flowing gas due to high rates of water production in early May 2015. A second acid treatment was performed in November 2016 prior to a production restart. Production from the well was restarted and continued, despite rapidly increasing WGR, until March 2017 when the well had to be shut-in due to excessive water production. Top foaming the well was attempted to decrease the density of the standing water column in the well and enable the well to

lift water after being restarted. However, this technique was not successful and had to be discontinued due to complications with the produced water system. Subsequent attempts to restart production from F-70 were unsuccessful.

Figure 5.5.3.1 shows calculated WGRs and well productivities for F-70. The orange line shows well productivity and the blue line shows WGR. The acid treatment done in January 2015 is indicated on the graph. The trend shows well productivity to gas was considerably higher post-acid treatment. The trend also shows that the WGR trend also became more aggressive after the acid treatment. Both gas and water productivities at F-70 increased after each acid treatment. In addition, the well regained productivity from re-saturation of the near-wellbore areas and drain back of water after a prolonged production shutdown. Restart attempts after the final production period were unsuccessful which was an indication that the near-wellbore region continued to be saturated by water.

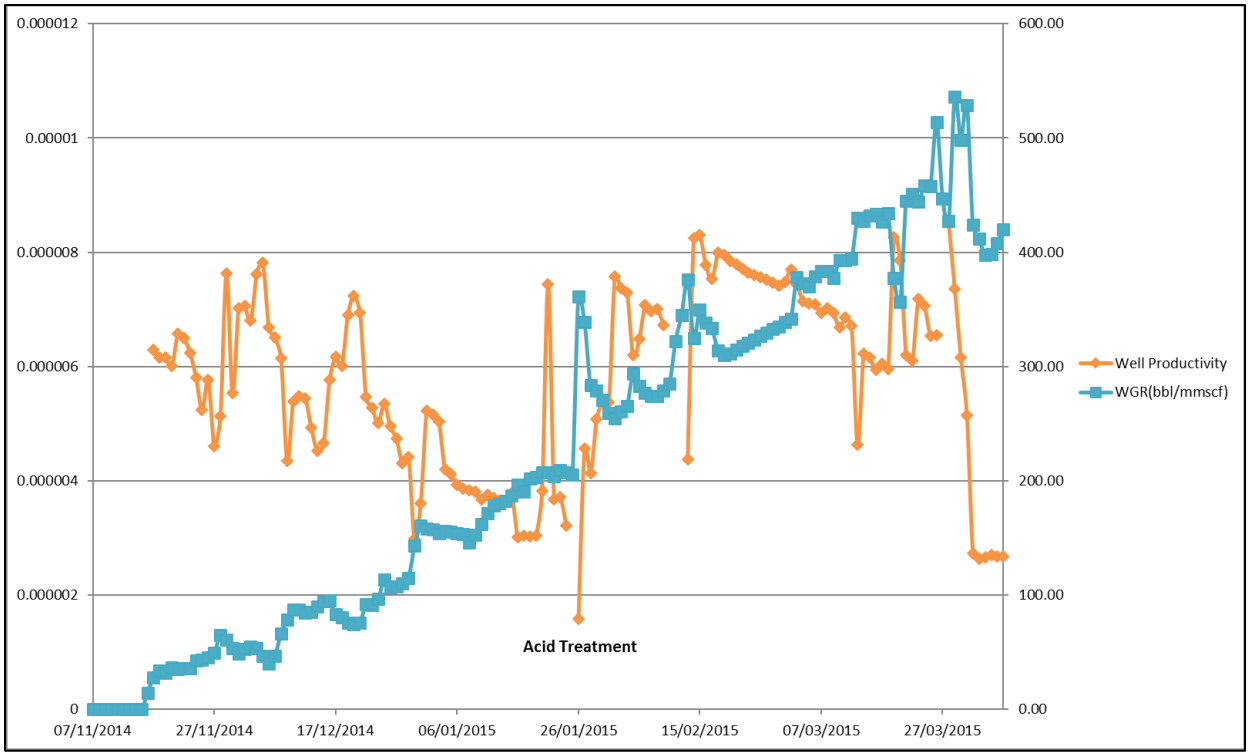

Figure 5.5.3.1: Effect of acid treatment on F-70 productivity and WGR. It can be seen that the productivity of the well and the WGR both increased after the acid treatment.

As mentioned above, F-70 was able to restart in late November 2016 after being shut-in for 7 months. Figure 5.5.3.2 shows that well productivities during this production period were generally lower than the period before the well was shut-in. It is also evident from the figure that well productivity declined quickly and the well became weaker with time.

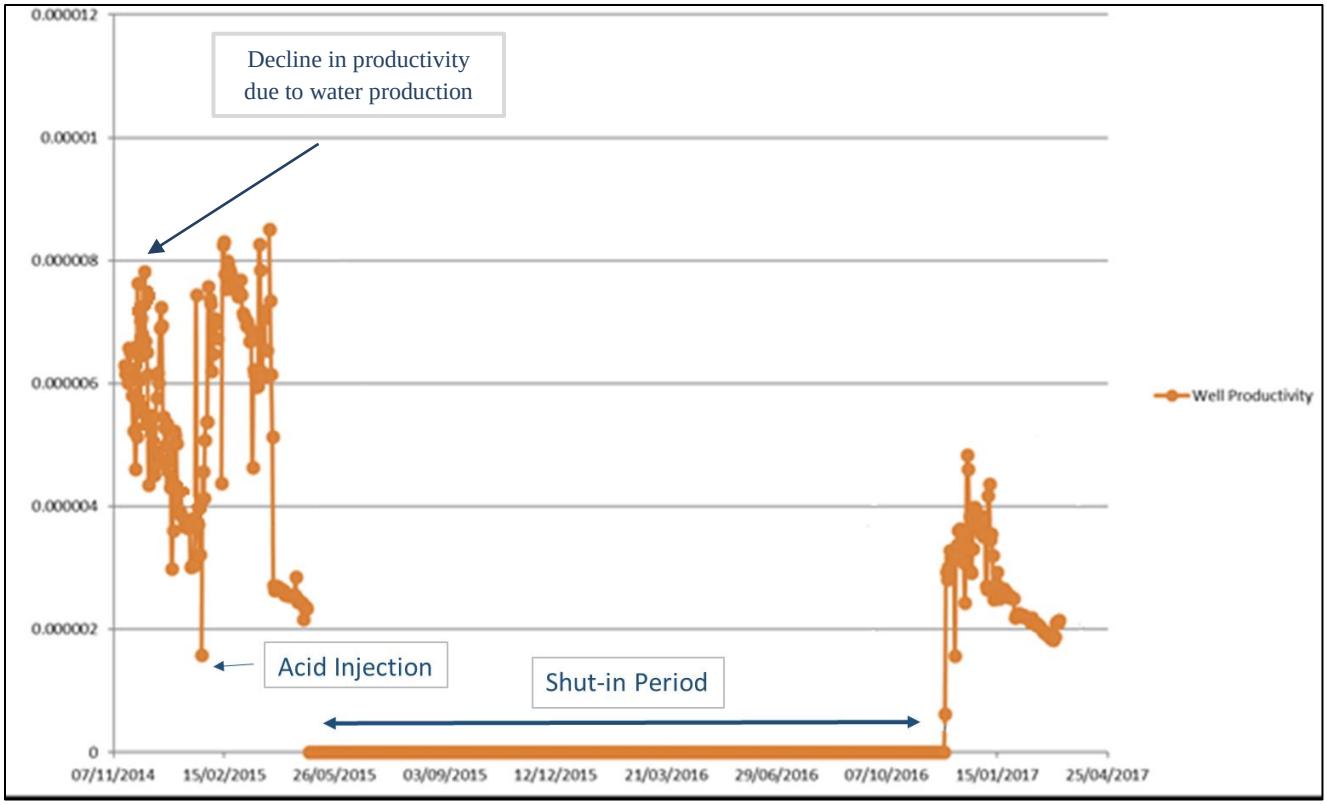

Figure 5.5.3.2: F-70 well productivity. It can be seen that productivity decreased dramatically after water production started. The increase in productivity is mainly associated with acid treatments and pressure build-ups after each shut-in period. The well regained some productivity after a 7 months shut-in period.

Based on the CNSOPB's initial un-calibrated simulation models, F-70 was not expected to produce any free water until late 2017. Early water production caused the CNSOPB to revise its reservoir and aquifer characterizations in the F-70 area to improve history matching. As shown in Figure 5.5.3.5 pressure and WGR matches were reasonable. The following are the main revisions to the F-70 area's reservoir characterization:

- Abenaki 5 matrix porosity in the F-70 area was reduced.
- Abenaki 5 matrix permeability was reduced in all directions (X, Y and, Z).
- Abenaki 5 matrix permeabilities in the Z direction were higher than matrix permeabilities in the X and Y directions.

- Abenaki 5 fracture permeabilities are an order of magnitude higher than matrix permeabilities.
- The best way to match early water production from the well was to create a local breach (localized high permeability fault/fluid conduit) near the F-70 well in the Tight Streak layer to allow vertical water encroachment. This breach was created by assigning high matrix and fracture permeabilities to cells near F-70 perforations (Figures 5.5.3.3, 5.5.3.4).

HPRF area aquifer properties such as permeability, porosity and size were adjusted to match initial water production timing and intensity.

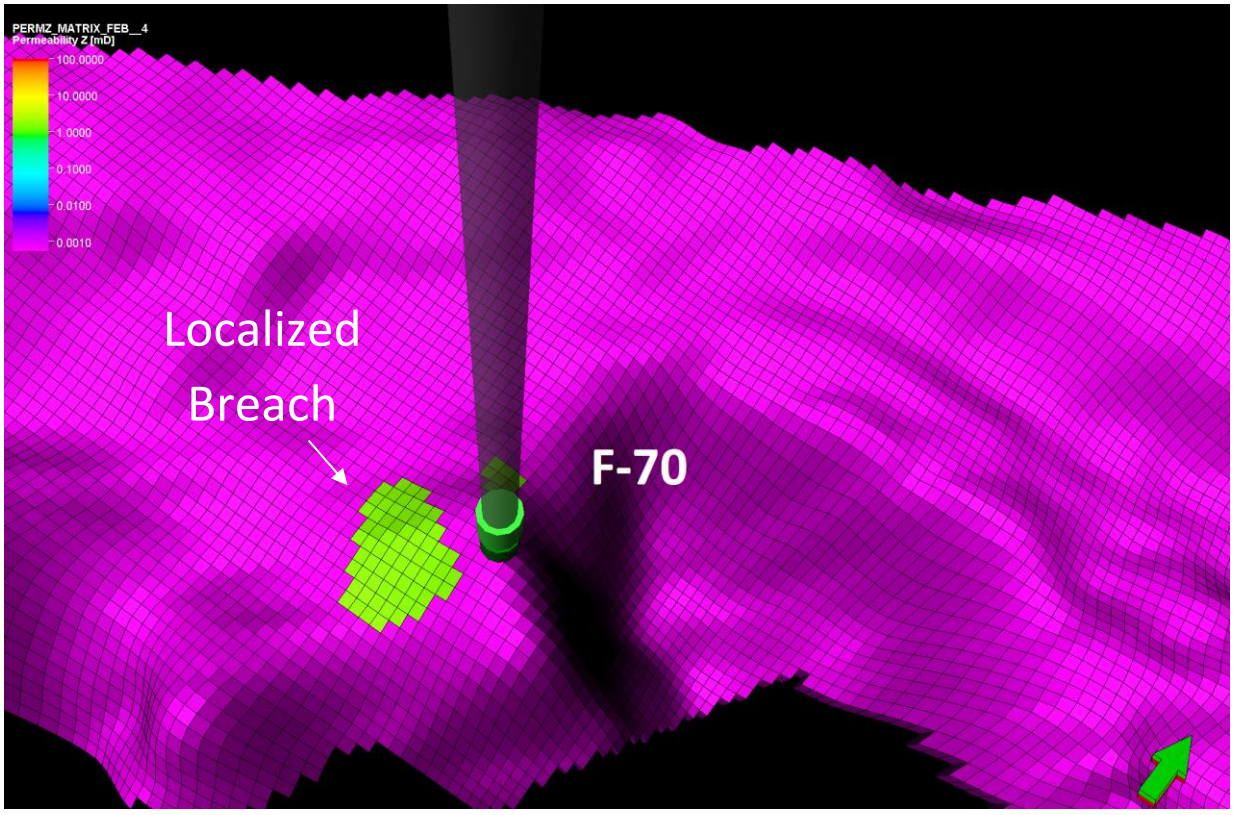

Figure 5.5.3.3: This figure shows the revision in the X direction matrix permeabilities of the cells in the Tight Streak layer (creation of a localized high transmissibility fault). These cells are shown in green colour. This revision was necessary to match water production from the well.

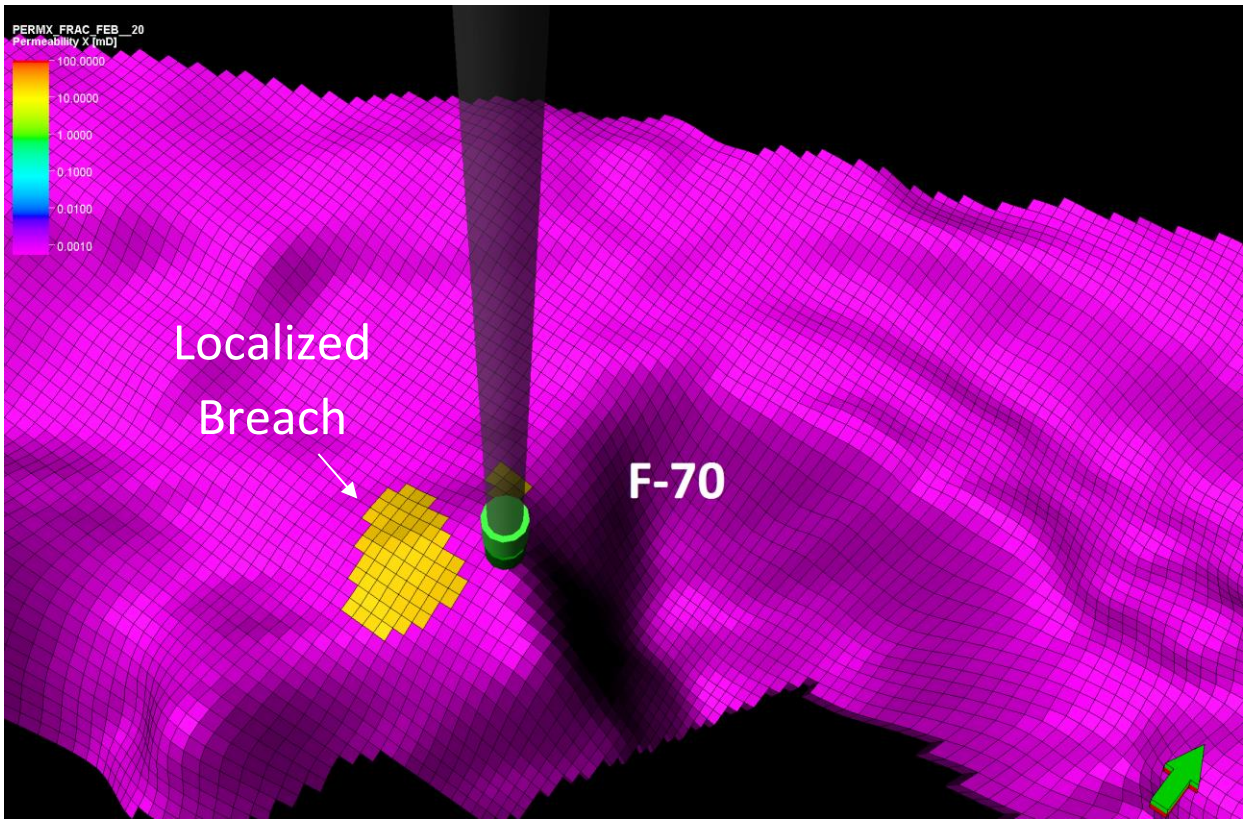

Figure 5.5.3.4: This figure shows the revision in the X direction fracture permeabilities of the cells in the Tight Streak layer (creation of a localized high transmissibility fault). These cells are shown in yellow. This revision was necessary to match water production from the well.

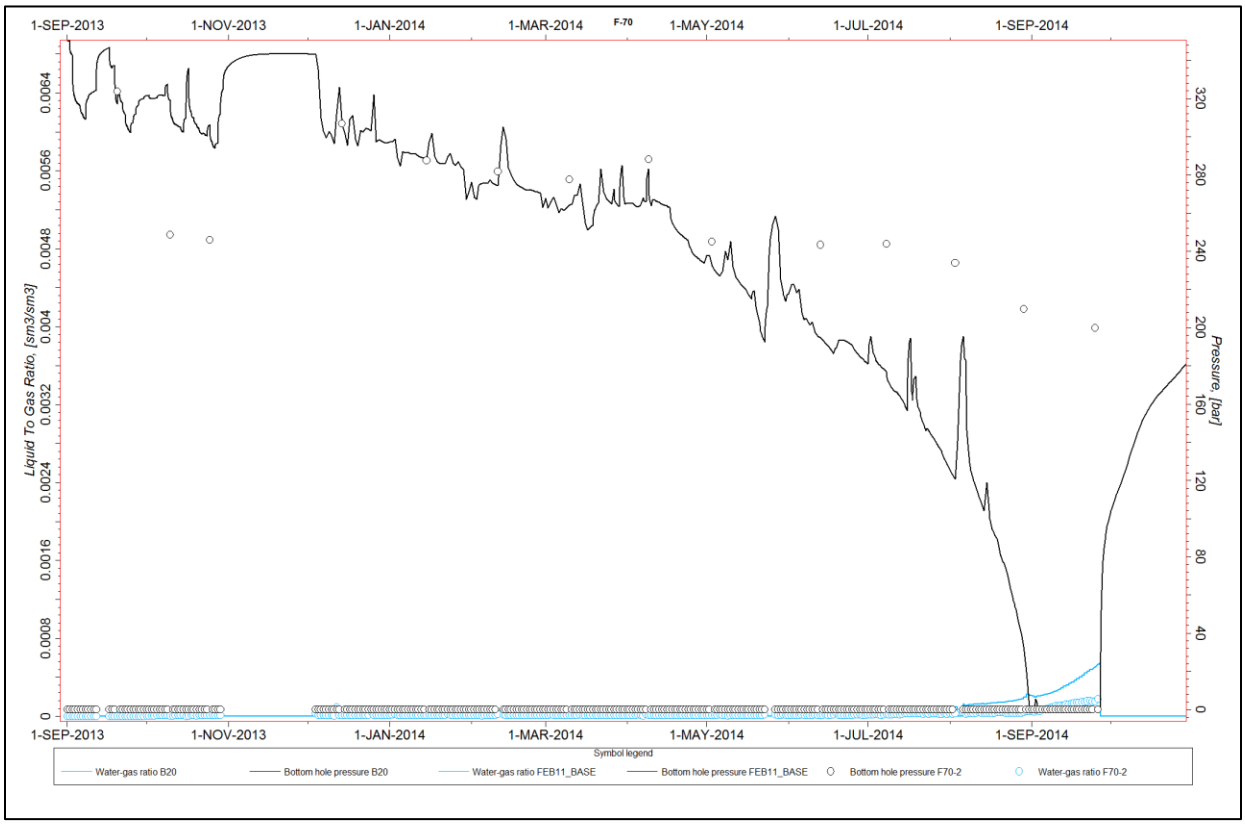

Figure 5.5.3.5: Pressure match was reasonable until the start of water production.

5.5.4. Panuke M-79A

Water production from this well started in August 2014 and increased very rapidly. The well was shut-in from September 16, 2014, to November 29, 2014 after this initial period of water production. The WGR continued to increase aggressively after production was resumed and the well had to be shut-in again on December 25, 2014. The next production period was from January 8, 2015, to February 5, 2015. The WGR increased very rapidly during this production period. The next production cycle was from March 12, 2015, to April 28, 2015 and the well had to be shut-in due to high WGR at the end of this production cycle. M-79A remained shut-in until December 7, 2015. On December 7, 2015, production resumed and the well produced water-free for several

days before the WGR started increasing rapidly and the well water loaded and stopped producing on January 11, 2016. The period of water-free production at the beginning of this production cycle was an indication that the near-wellbore region had re-saturated with gas. This gas re-saturation was also evident in the simulation model results. The next production cycle started on August 8, 2016, but could only be maintained until August 24, 2016. The duration of this production cycle was considerably shorter than the previous production cycles. M-79A produced for several more cycles. Each production cycle typically lasted from 2 - 4 weeks. Table 5.5.4.1 shows the number of days of production and cumulative gas production for each of these cycles.

Acid treatments were conducted by the operator to ensure perforations were not plugged and to increase the productivity of the well. The first acid treatment was performed in November 2014 after a sudden stop of production from the well due to a perforation blockage. Based on the success observed from this initial acid job in increasing well productivity, the operator continued with acid treatments until March 2016. The second acid treatment was performed on January 8, 2015. This acid treatment was also successful. Three additional acid treatments were performed between March 2015 and March 2016. These acid treatments are believed to have resulted in incremental recovery of 127.4 E6m3 (4.5 Bcf) of gas from the well.

As mentioned above, water production from the well started in August 2014. An IPR analysis was conducted in September 2014 to investigate the impact of water production on the well's productivity. Figure 5.5.4.1 shows both the August 2014 and September 2014 IPR curves. This data shows that the production capacity of the well was severely impacted and Absolute Open Flow (AOF) of the well decreased from 7.1 E6m3/d (250 MMscf/d) to 2.8 E6m3/d (100 MMscf/d) in a single year.

Table 5.5.4.1: M-79A Production Cycles

Production Cycle	# of Days of Production	Cumulative Production E6m3 (MMscf)
1	29	49.7 (1755)
2	26	28.9 (1019)
3	28	23.5 (831)
4	48	34.4 (1215)
5	36	31.7 (1119)
6	17	11.8 (416)
7	13	10.3 (363)
8	27	16.2 (572)
9	33	27.6 (976)
10	16	12.5 (440)
11	25	18.0 (634)
12	10	7.0 (247)

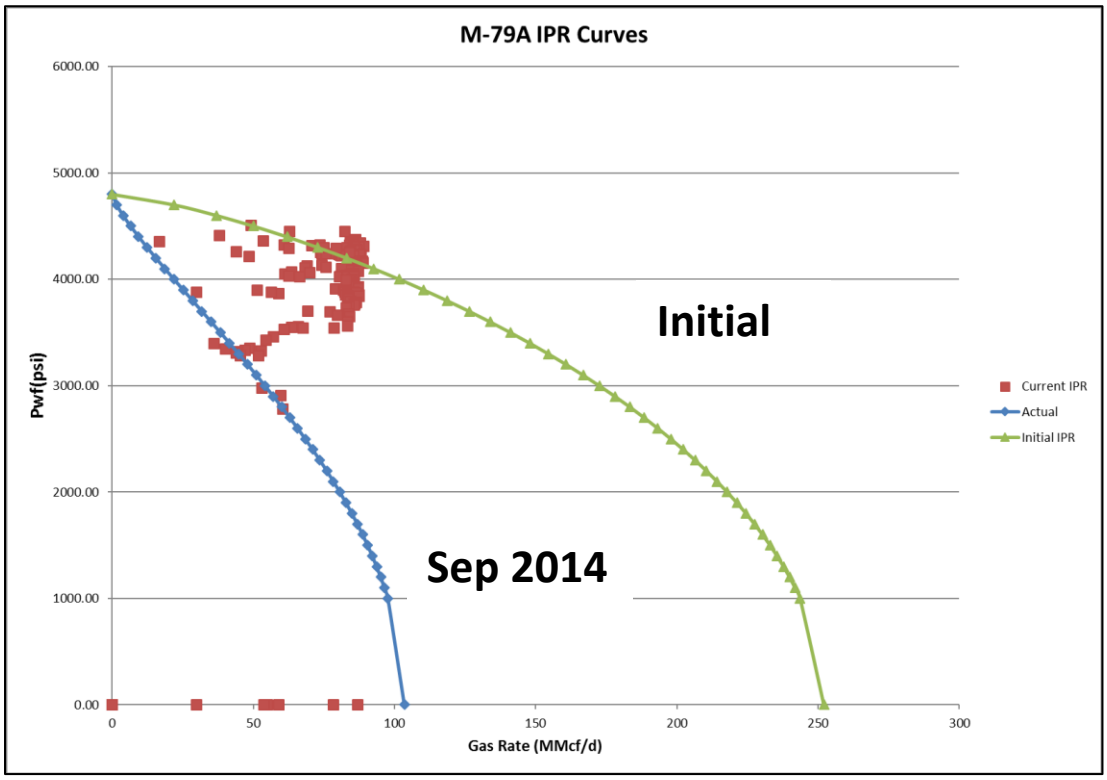

Figure 5.5.4.1: M-79A IPR Curves. The September 2014 curve shows that wells production capacity was significantly reduced after water production from the well started.

Figure 5.5.4.2 shows the number of days of production from the well during each production cycle. This trend confirms that in general the well became weaker and produced for fewer days over time. It is important to note that the data shown on the figure was affected by the acid jobs. The objective of these acid treatments was to eliminate possible downhole blockages from the perforated interval and to increase fracture conductivity resulting in improved gas flow. However, more conductive fractures, can result is a higher rate of water production since water also flows through the same fractures as the gas in a naturally fractured reservoirs such as those in the Deep Panuke field.

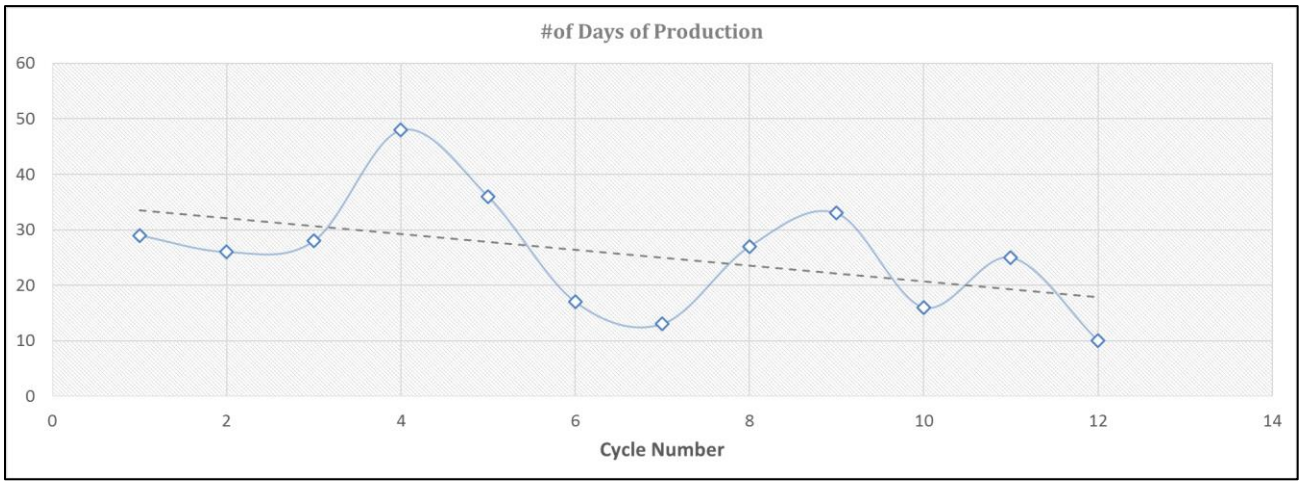

Figure 5.5.4.2: Number of days M-79A producing gas during each production cycle.

Figure 5.5.4.3 shows the trend of cumulative gas production from the well during each production cycle. This trend shows that in general, the well became weaker and produced less gas during each production cycle. It is important to note that some of these data points were affected by the acid jobs.

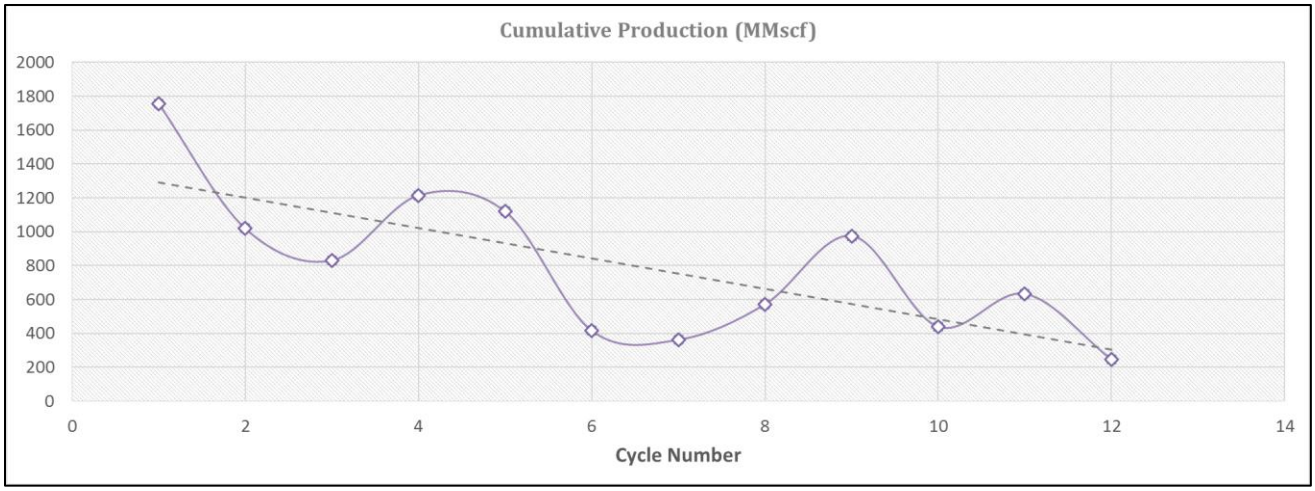

Figure 5.5.4.3: M-79A cumulative gas production during each production cycle.

Figure 5.5.4.4 shows flowing wellhead pressures during each production cycle. It can be observed that the flowing wellhead pressure decreased with time and declined more rapidly in later cycles. This is also an indication of the well losing its production capacity over time. For example, during the final production cycle (#12), shown on the chart, the well started producing at a much lower wellhead pressure and pressure declined at a much higher rate compared to previous production cycles.

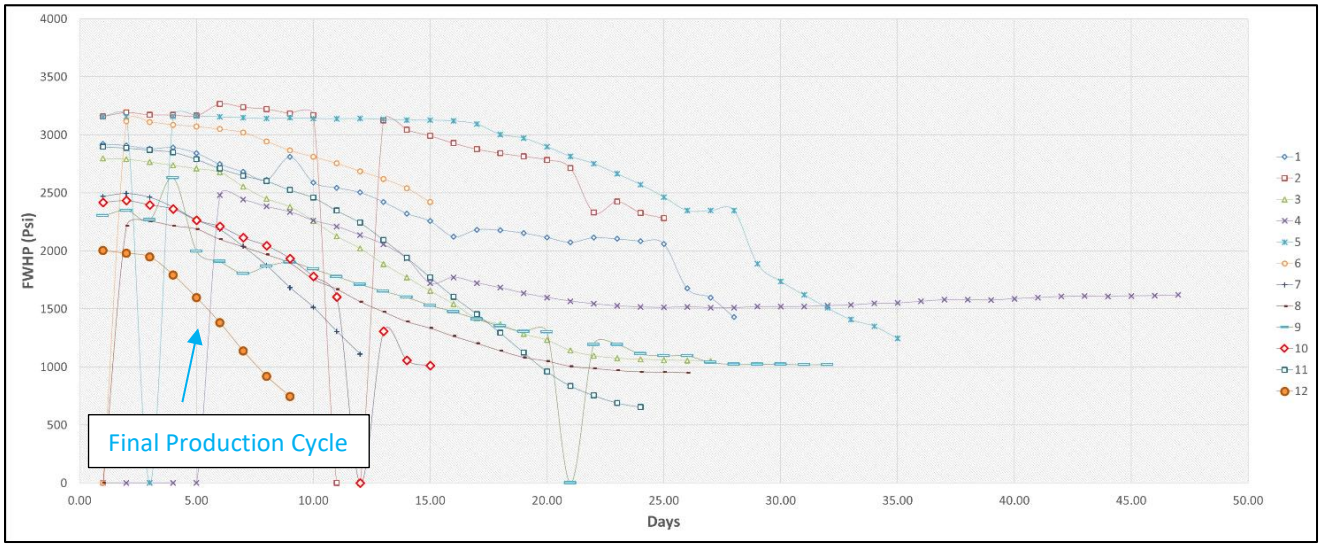

Figure 5.5.4.4: M-79A flowing wellhead pressure during each production cycle.

A data-mining model was created by the CNSOPB in April 2018 to predict the performance of M-79A in future cycles based on the well's previous performance and to assess expected recovery from future production cycles (Figure 5.5.4.5).

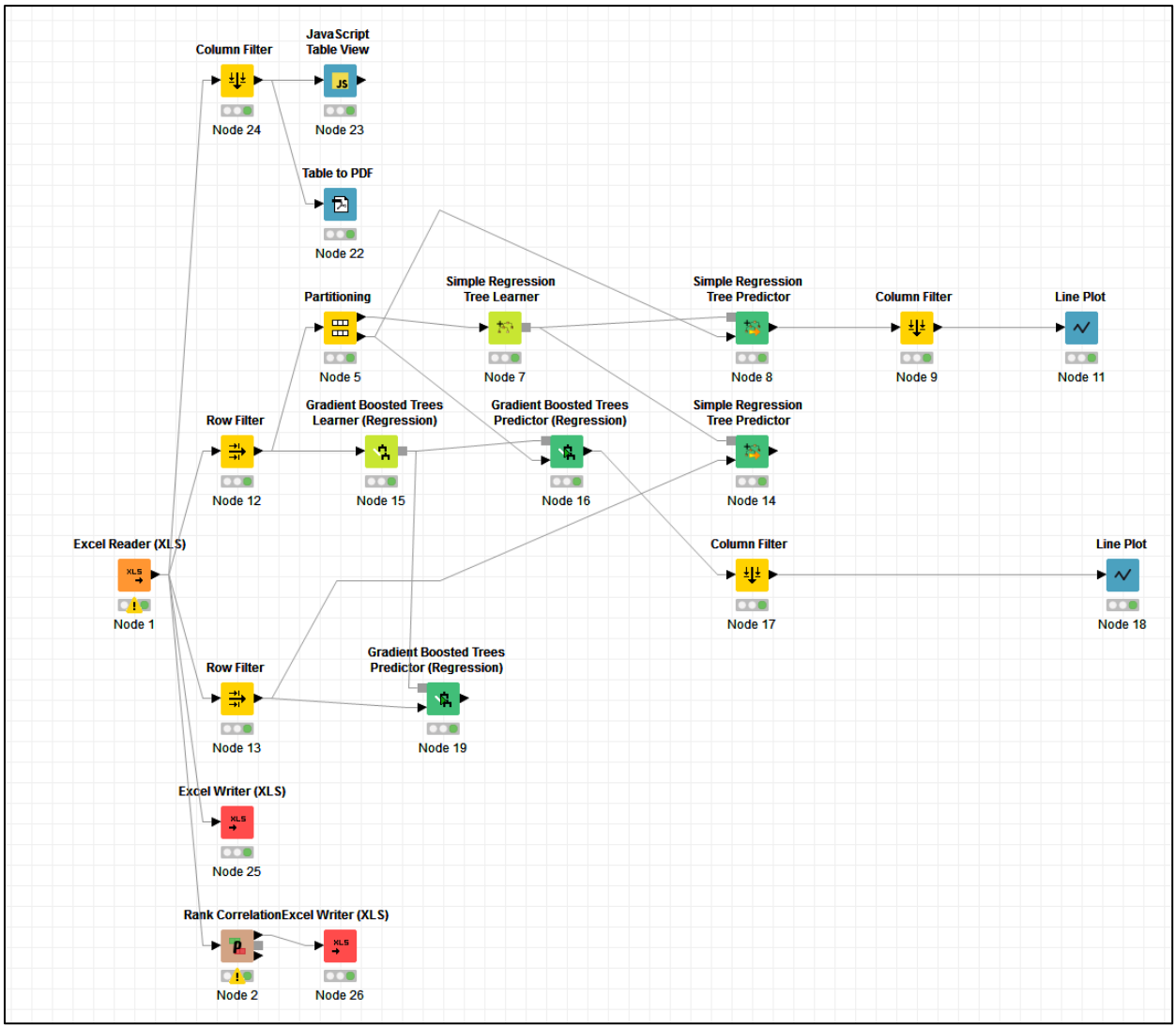

Figure 5.5.4.5: The CNSOPB's M-79A data mining model. This model was built to forecast the cumulative gas that would be produced during the next production cycle.

The following data were extracted from the above 12 production cycles and were used, along with the associated shut-in periods, to evaluate the variables that are expected to impact well performance during each production cycle:

- The number of days before pressure build-up started after the well was shut-in
- The number of days for pressure to fully build-up prior to each production cycle
- Maximum build up pressure prior to the start of each production cycle
- Initial flowing wellhead pressure for each cycle
- Number of days the well was shut-in after the well fully recharged
- Initial WGR after production from the well started
- Volume of Gas recovered from the well during each production cycle
- Number of days of production during each cycle
- Was an acid job associated with the production cycle?
- Had there been a plant trip during the production cycle?
- Was F-70 also on production during the production cycle?

Figure 5.5.4.6 shows values for the above variables for the 12 production cycles.

row ID	Dates	Shut-in Number	Days before pressure build up started	Days took for pressure to fully build up	Built up Pressure	Starting FWHP	Days well shut-in after fully recharged	Starting WGR after produciton started	Gas recoverd by subsequent run	Days of subsequent run	Acid Job Associated with subsequent run?	Plant Trip?	F-70 on Production
Row1	Sep 15 - Oct 29, 2014	Shut in 1	7	5	3237	3158	64	2	1019	26	y	n	y
Row2	Dec 25 - Jan 7, 2015	Shut in 2	10	3	3256	2796	3	94.43	831	28	y	n	y
Row3	Feb 5 - Mar 11, 2015	Shut in 3	28	4	3136	2500	4	135.8	1215.5	51	y	n	y
Row4	May 2 - Dec 5, 2015	Shut in 4	8	4	3065	3153	207	2.2	1112	37	n	n	n
Row5	Jan 12 - Mar 16, 2016	Shut in 5	43	7	3086	2486	16	115	92	4	y	n	n
Row6	Mar 21 - Aug 8, 2016	Shut in 6	0	0	3081	3116	141	7.11	416	16	n	y	n
Row7	Aug 25 - Sep 22, 2016	Shut in 7	15	7	3058	2471	7	145	363	13	n	n	n
Row8	Oct 6 -Jan 4, 2017	Shut in 8	64	10	2980	2215	17	251	572	27	n	n	y
Row9	Feb 1 -Mar 14, 2017	Shut in 9	26	5	2905	2304	11	158	975	33	n	n	n
Row10	Apr 17 -May 22, 2017	Shut in 10	23	7	2895	2418	7	127	439	16	n	n	n
Row11	Jun 8 -Dec 27, 2017	Shut in 11	45	20	2877	2897	138	3.21	633	25	n	n	n
Row12	Jan 22 -Apr 24, 2018	Shut in 12	83	9	2872	2003	5	210	572		n	n	n

Figure 5.5.4.6: Production cycle variables are shown in the above table. These variables were used in the data mining model to predict the cumulative production during the next production cycle.

The next step in predicting the performance of future cycles was to investigate which of the above variables plays a key role in well performance during each production cycle. A rank

correlation matrix tool was used for this purpose. This matrix tool calculates, for each pair of variables, a correlation coefficient. The resulting correlation is shown graphically in Figure 5.5.4.7.

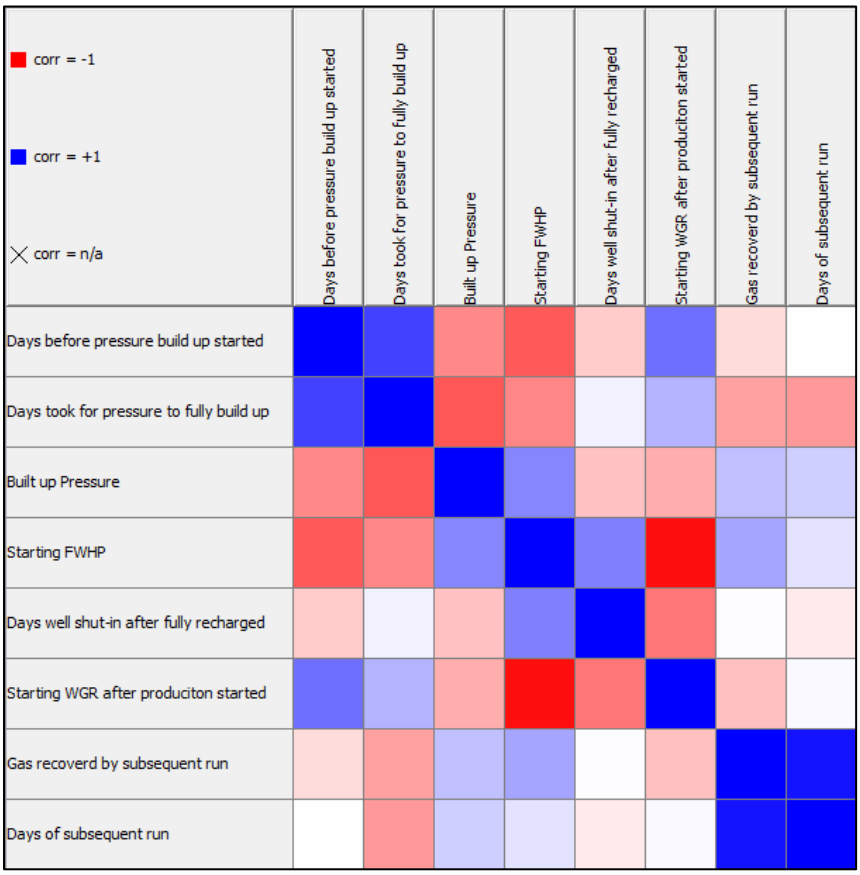

Figure 5.5.4.7: The above correlation matrix shows the degree of correlation between cumulative gas production during the production cycles and other variables. Blue shows positive correlation and red shows negative correlation. The variables with strong correlation were then used in the data mining model to predict cumulative gas recovery during the next production cycle.

The correlation values showed that gas recovery during each production cycle negatively correlated with the number of days it took for the well to build-up and positively correlated with initial flowing wellhead pressure when production was re-started. These two variables along with the other important variables, was there an acid job associated with the production cycle and had there been a plant trip during the production cycle, were used as input variables to the data mining model. The Gradient Boosted Model was used as the most suitable algorithm for this performance

prediction case. Gradient boosting is a machine learning technique for regression and classification problems, which produces a prediction model in the form of an ensemble of weak prediction models, typically decision trees. The input data was divided into model training and model testing sets. The testing set consisted of two data sets chosen randomly from the whole data set.

The above data shows that the created Gradient Boosted Model is predicting gas recoveries for each production cycle almost error-free and could be used to predict gas recovery from future gas production cycles from M-79A. This performance prediction model was used to determine the feasibility of continuing cyclic production from the well. Another benefit of using this data mining model to predict future gas recovery from the well was the challenges associated with using the simulation model to predict future gas production from the well after water production. Simulation model history matches were inaccurate during cyclic production mainly due to reservoir heterogeneity due to the complex nature of the reservoir.

The gas volume predicted to be produced from the well during the next cycle obtained from the above data-mining model was used to analyze the viability of producing the well for another cycle. It was determined that production for another cycle was uneconomic.

M-79A material balance analysis showed that the well had started to feel the effects of the aquifer in May 2014 (Figure 5.5.4.8). Actual water production from the well, however, did not start until August 2014.

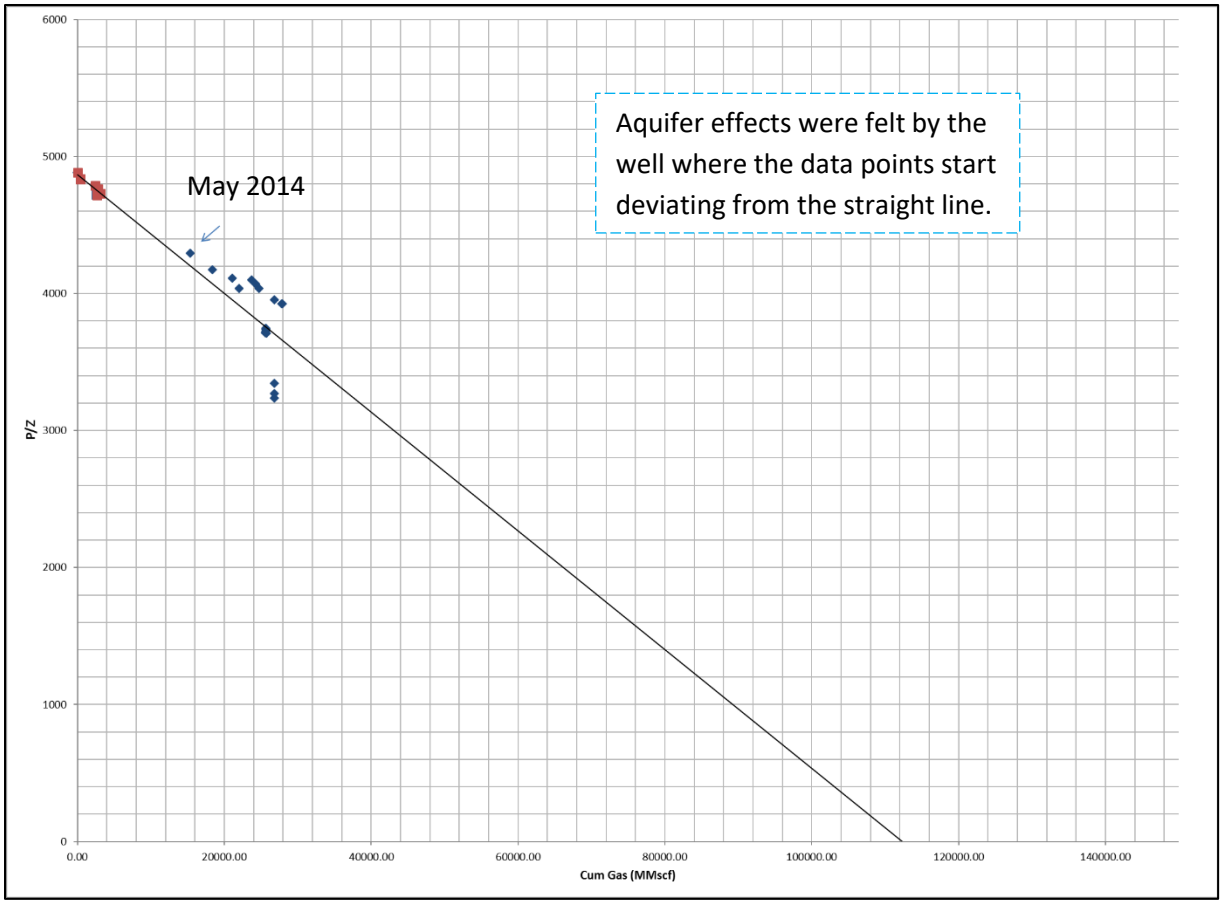

Figure 5.5.4.8: M-79A material balance analysis shows that the well received pressure support beginning in May 2014 due to its connection to the aquifer.

Early and ongoing water production from M-79A resulted in numerous updates to the CNSOPB's simulation model during production to improve history matching. As shown in Figure 5.5.4.11 the pressure and WGR matches were reasonable. The following are the main revisions to the M-79A area's reservoir characterization:

- Matrix porosity in the M-79A area was reduced.
- Matrix permeability was reduced in all directions (X, Y and, Z) in the M-79A area.
- Abenaki 5 matrix permeabilities in the Z direction were higher than matrix permeabilities in the X and Y directions.

- The best way to match water production early in well life was to create breaches (localized high permeability faults) near the M-79A wellbore in the Tight Streak layer to allow vertical water encroachment. These breaches were created by assigning high matrix and fracture permeabilities to the model cells near the M-79A perforations (Figures 5.5.4.9).
- Abenaki 5 fracture permeabilities are an order of magnitude higher than the matrix permeabilities (Figures 5.5.4.10).
- The properties of the aquifer in the HPRF, such as permeability, porosity and size were adjusted to match initial water production timing and intensity.

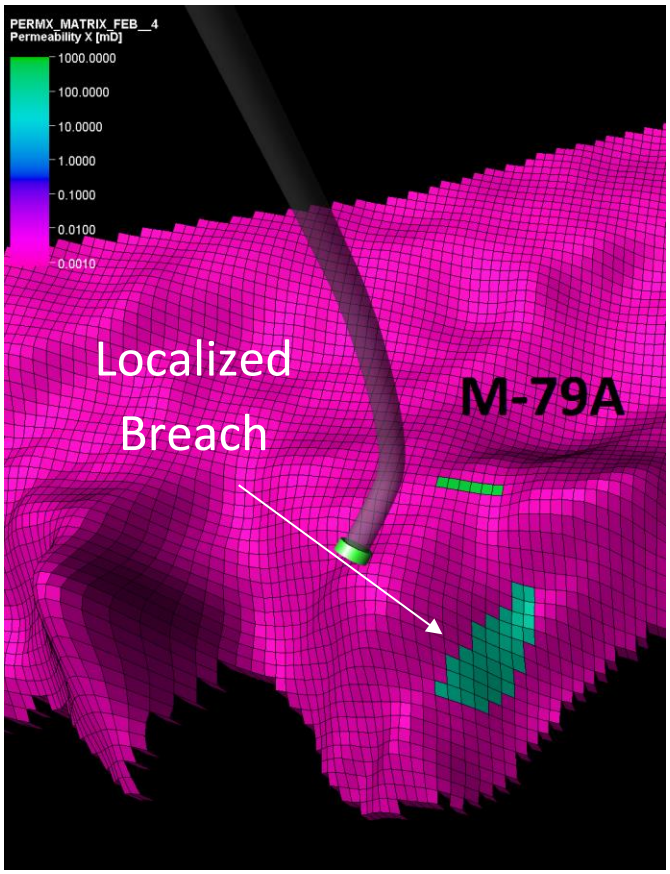

Figure 5.5.4.9: This figure shows the X direction matrix permeabilities in the Tight Streak layer. X direction matrix permeabilities were adjusted to match M-79A water production.

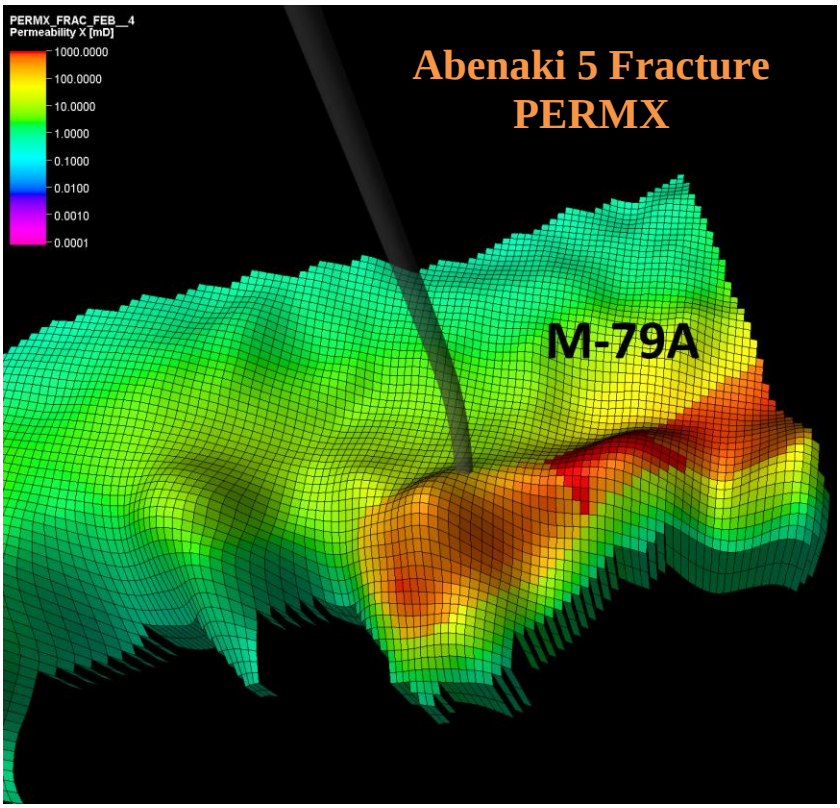

Figure 5.5.4.10: Abenaki 5 fracture permeability in the X direction was increased in the M-79A area as part of the history matching process. The above figure shows these revised permeabilities. Warm colours show higher permeabilities.

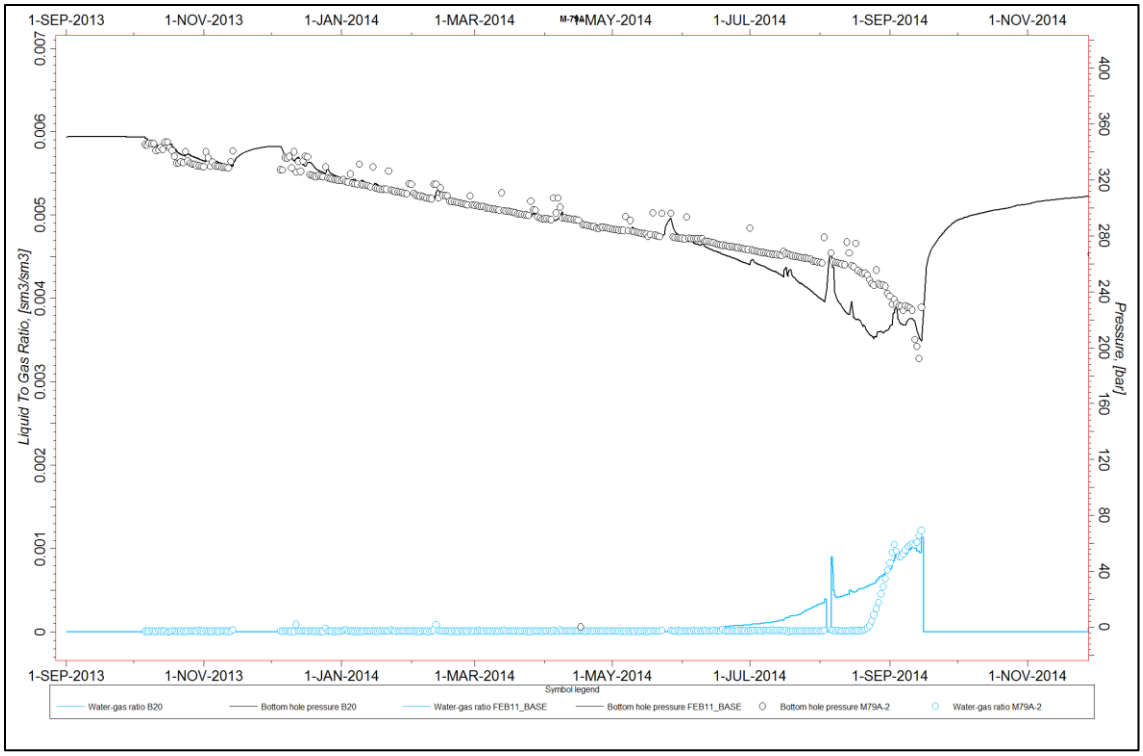

Figure 5.5.4.11: The figure shows there was a good pressure match in M-79A until the start of water production. Note when water production starts the points begin to separate from the lines.

6. Actual vs. Expected Well and Field Performance

Initially, there can be a large amount of uncertainty with un-calibrated simulation models. However, as production data is acquired these initial models and forecasts become more accurate with time and additional iterations.

6.1. 2006 DPA - Expected Deep Panuke Performance

The following table (Table 6.1.1) shows the operator's estimated OGIP and Recoverable Gas in Place (RGIP) for P90, P50, P10 and Mean cases (2006 DPA). The associated recovery factors are also shown for these cases in Table 6.1.2. Total expected recovery factors in the 2006 DPA ranged from 54 to 70 percent with a Mean recovery factor of 64 percent.

Table 6.1.1: Encana's OGIP and RGIPs (2006 DPA)

	Gross OGIP E9m3 (Bcf)				Gross RGIP E9m3 (Bcf)			
Reservoir Region	**P90**	**P50**	**P10**	**Mean**	**P90**	**P50**	**P10**	**Mean**
HPRF	16.5 (583)	23.7 (837)	32.2 (1,137)	24.0 (848)	9.7 (343)	16.0 (565)	23.9 (844)	16.5 (583)
VL	3.1 (109)	4.7 (166)	7.1 (251)	4.9 (173)	1.4 (49)	2.0 (71)	3.0 (106)	2.1 (74)
Total	21.3 (752)	28.6 (1,010)	37.4 (1,321)	28.9 (1,021)	11.5 (406)	18.2 (643)	26.2 (925)	18.6 (657)

Table 6.1.2: Encana's Expected Recovery Factors (2006 DPA)

	Recovery Factor			
Reservoir Region	**P90**	**P50**	**P10**	**Mean**
HPRF	59%	68%	74%	69%
VL	45%	43%	43%	43%
Total	54%	64%	70%	64%

In addition to above values, the operator used simulation models to generate raw and sales gas production profiles, which are presented in Figures 6.1.1 and 6.1.2.

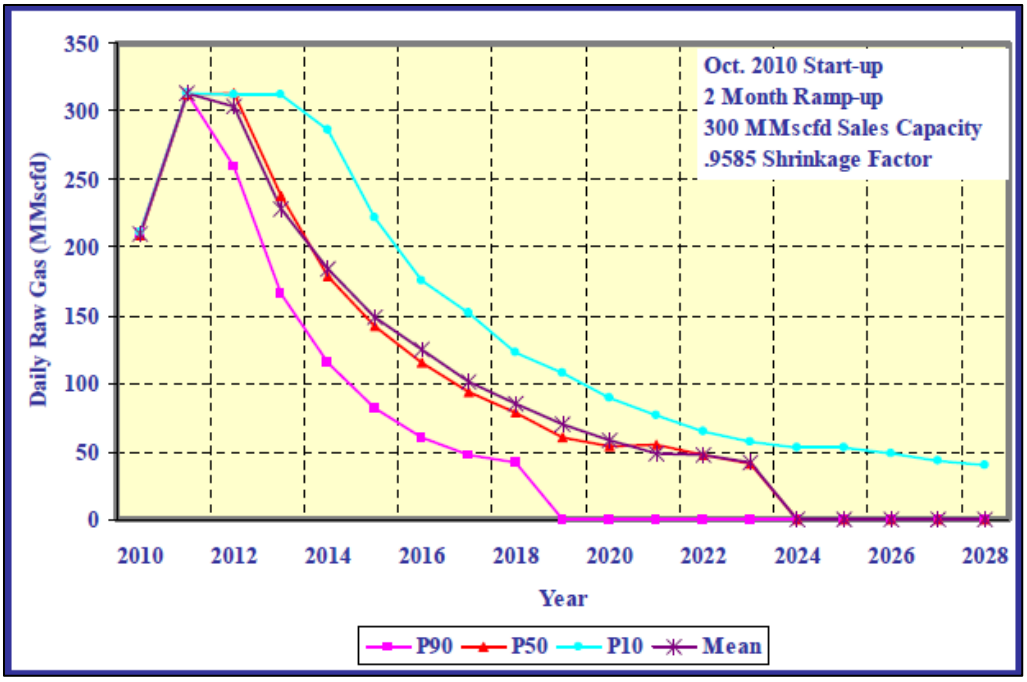

Figure 6.1.1: Deep Panuke raw gas production profiles (2006 DPA).

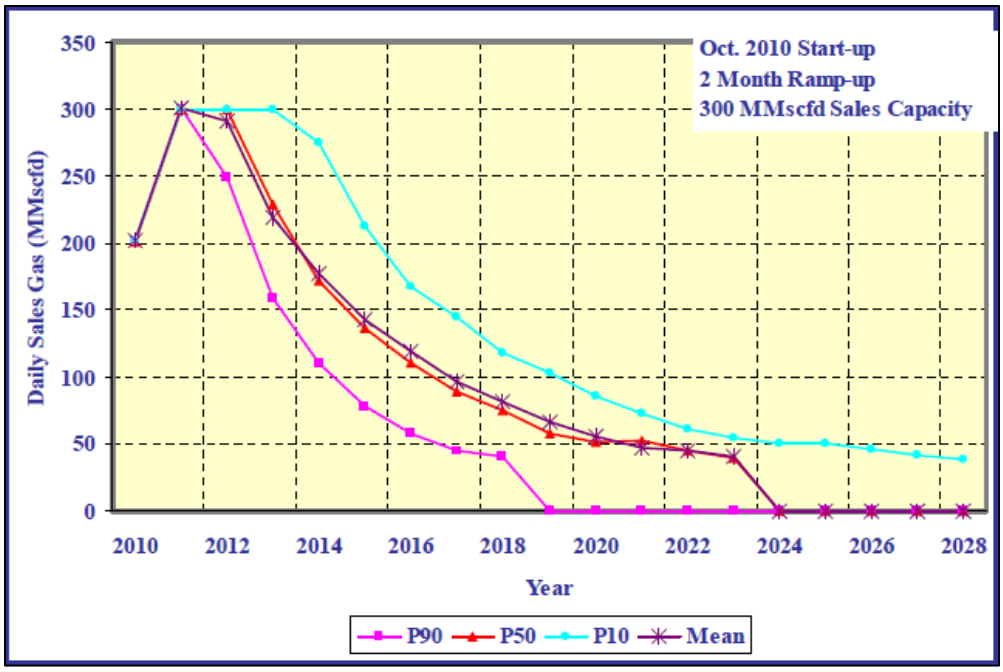

Figure 6.1.2: Deep Panuke Sales Gas Production Profiles (2006 DPA).

6.2. Actual Deep Panuke Performance

Figure 6.2.1 shows actual production from the Deep Panuke wells and the 2006 DPA expected (mean) production forecast. The Deep Panuke production wells produced from August 2013 until May 2018 with the largest gas volume produced from the HPRF wells (M-79A, F-70 and D-41). During the first half of 2018, only M-79A and H-08 were capable of production. Figure 6.2.1 shows that actual Deep Panuke production was significantly lower than the 2006 DPA expected production.

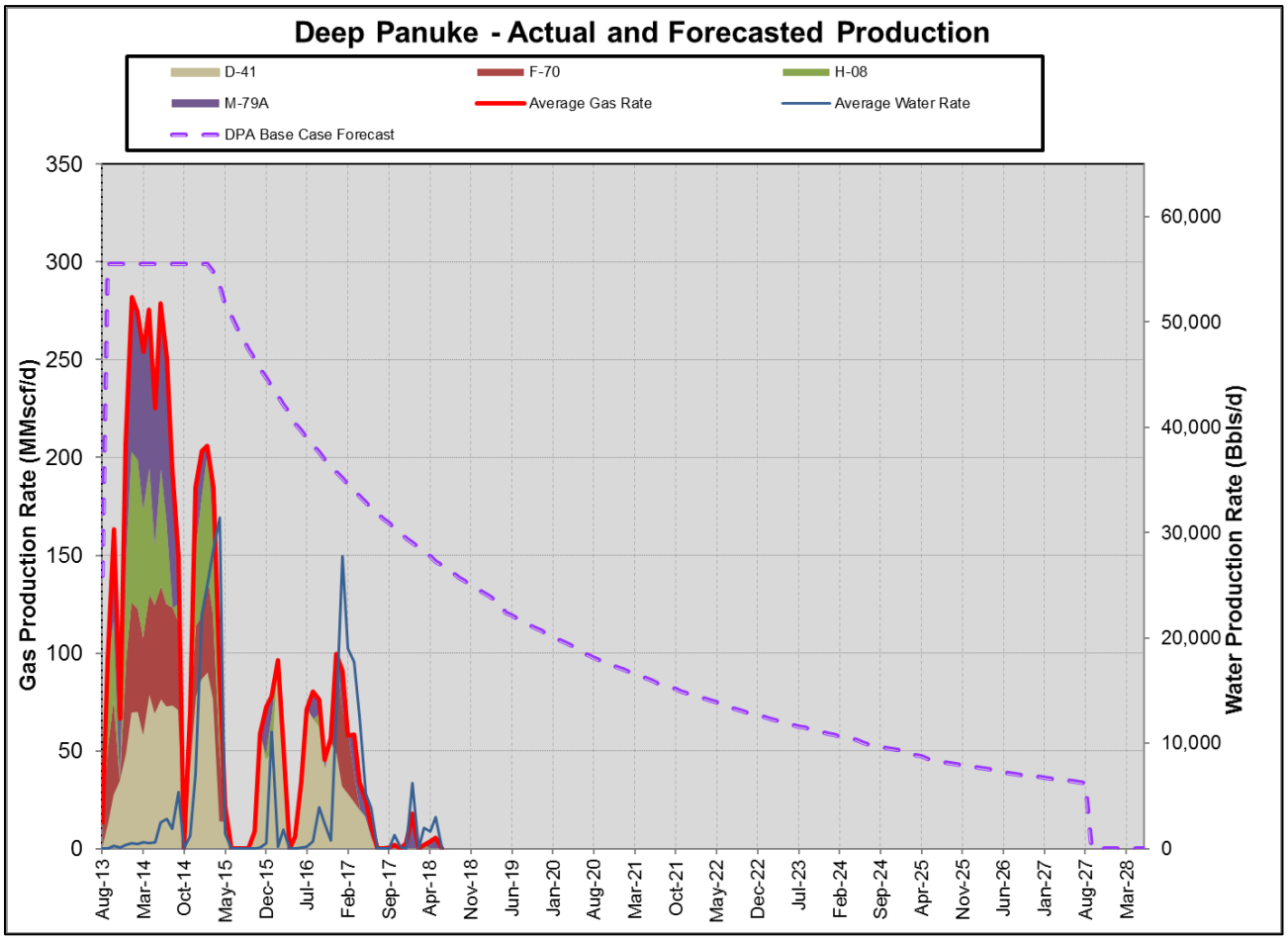

Figure 6.2.1: Deep Panuke actual production (red line) vs. 2006 DPA forecasted production (purple dashed line).

As described earlier in the report, well productivities were high during the initial water-free production period (August 2013 to May 2014) but deteriorated rapidly after water production commenced. Although higher production rates may result in earlier water production the CNSOPB's and the operator's simulation models both show that higher well production rates do not negatively impact total gas recovery. For reservoirs like Deep Panuke (i.e. highly fractured carbonate reservoirs connected to an aquifer), simulation modeling indicates that producing the wells at higher rates is the most effective production strategy and results in greater overall gas recovery.

The degree of connectivity between the Deep Panuke gas zone and the underlying aquifer had a major impact on reservoir performance. The presence of the low permeability "Tight Streak" between the Abenaki 4 and 5 was expected to act as an effective barrier to the aquifer. Simulation modeling indicated that there were likely a number of breaches or high permeability vertical faults/fractures in the Tight Streak in the vicinity of three production wells (H-08, M-79A and F-70) which accelerated water breakthrough (Figure 6.2.2). However, the connectivity between the aquifer and the gas zone in the D-41 area was more limited due to the lower density of fractures in this portion of the field, which resulted in greater overall gas recovery from the well.

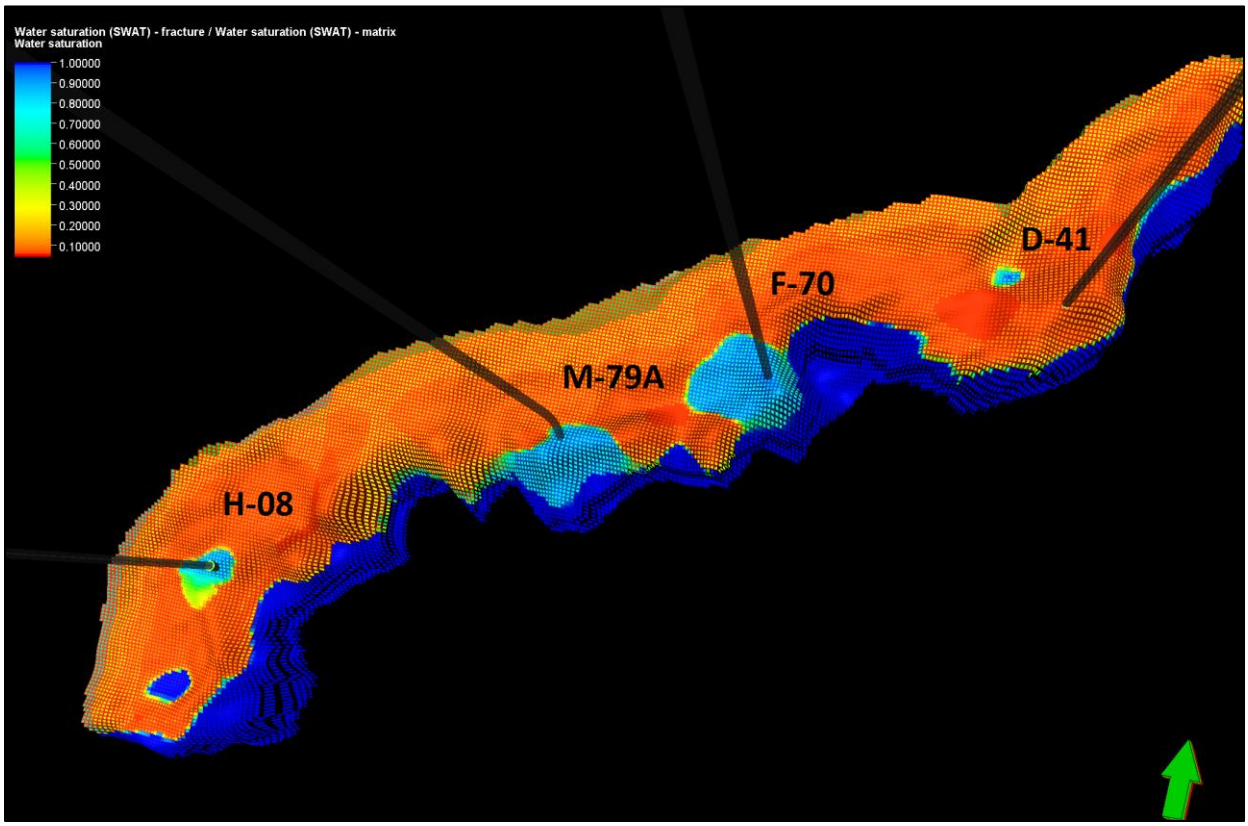

Figure 6.2.2: June 2015 water Saturation is shown in this figure. It can be seen that the F-70, M-79A and H-08 perforations are flooded while water has not reached the D-41 well yet.

7. CNSOPB Simulation Modeling Sensitivity Analysis

This section summarizes the results of the CNSOPB's simulation modeling sensitivity analysis. Due to the challenges of obtaining a reliable history match after water production and to simplify the analysis all wells are produced, in the model, at a rate of 2.4 E6m3/d (85 MMscf/d) with no shutdowns. Therefore, the results of these sensitivities should be observed qualitatively and not quantitatively. It is also important to note that D-41 is the only well that was capable of continuous gas production beyond 2015 while the other wells were only capable of intermittent (cyclical) production.

7.1. Vertical Matrix Permeability

Table 7.1.1 shows vertical matrix permeability multipliers and cumulative gas production for five permeability sensitivities. The cumulative gas production figure (Figure 7.1.1) and values (Table 7.1.1) show that increasing vertical matrix permeability (Cases 2-5) had only a minor impact on cumulative gas production. The severity and timing of water production are however affected by increasing vertical matrix permeability. As shown in Figure 7.1.2, water production starts earlier but is less severe as vertical matrix permeability increases. Water production from D-41 starts earlier and is more severe as vertical matrix perm increases. Decreasing matrix vertical permeability to half increases cumulative gas production from the reservoir by close to 10 percent. This is mainly due to delay in water production from all wells and less severe water production. Lower vertical matrix perm also decreases connectivity between the aquifer and the Abenaki 5 gas zone, which has a positive impact on overall recovery.

Table 7.1.1: Vertical Matrix Permeability multipliers

Case #	Vertical Matrix Perm Multiplier	Cumulative Gas Production E9m3 (Bcf)
1	0.5	6.9 (242)
2	2.9	6.3 (222)
3	5.3	6.4 (225)
4	7.6	6.4 (225)
5	10	6.3 (223)

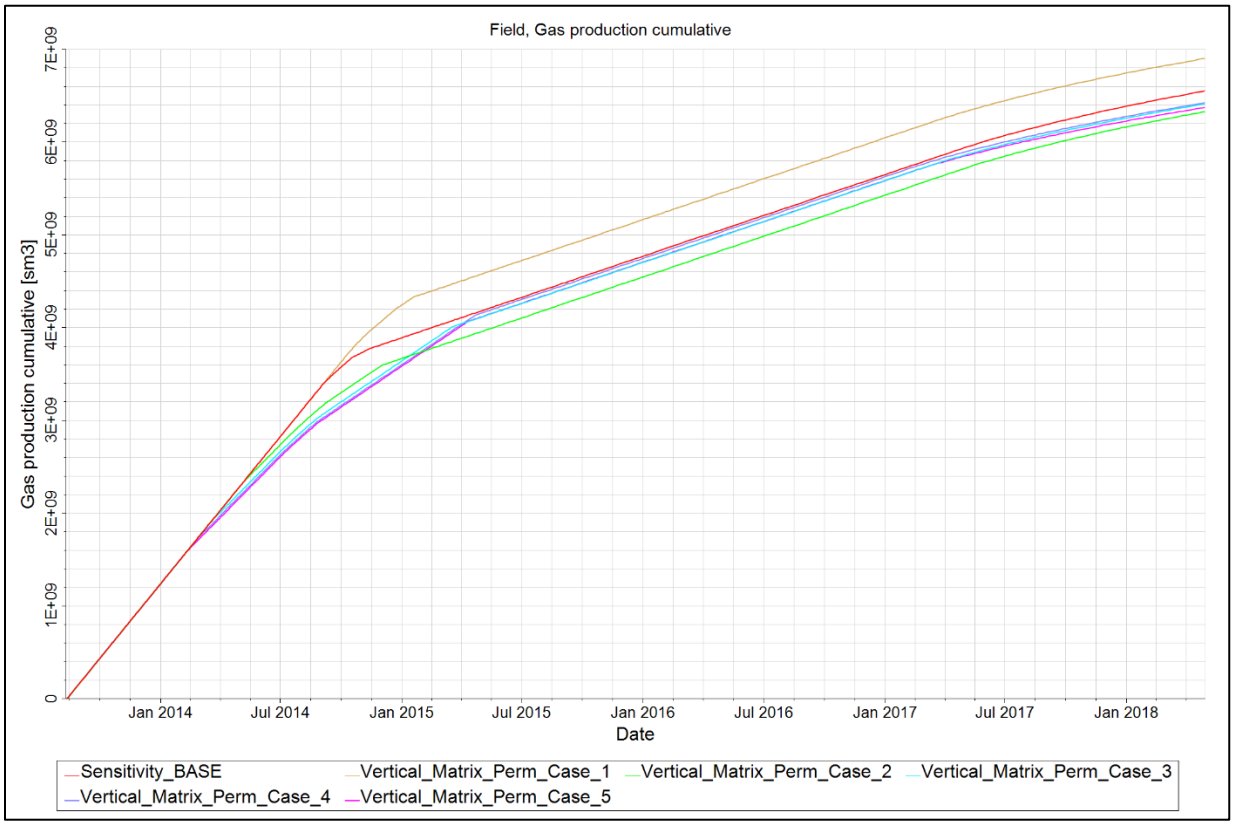

Figure 7.1.1: Cumulative gas production compared for various vertical matrix permeability sensitivity cases. It is shown that multiplying vertical matrix permeability by 0.5 will increase gas production mainly due to delays in water production and lower water production intensity.

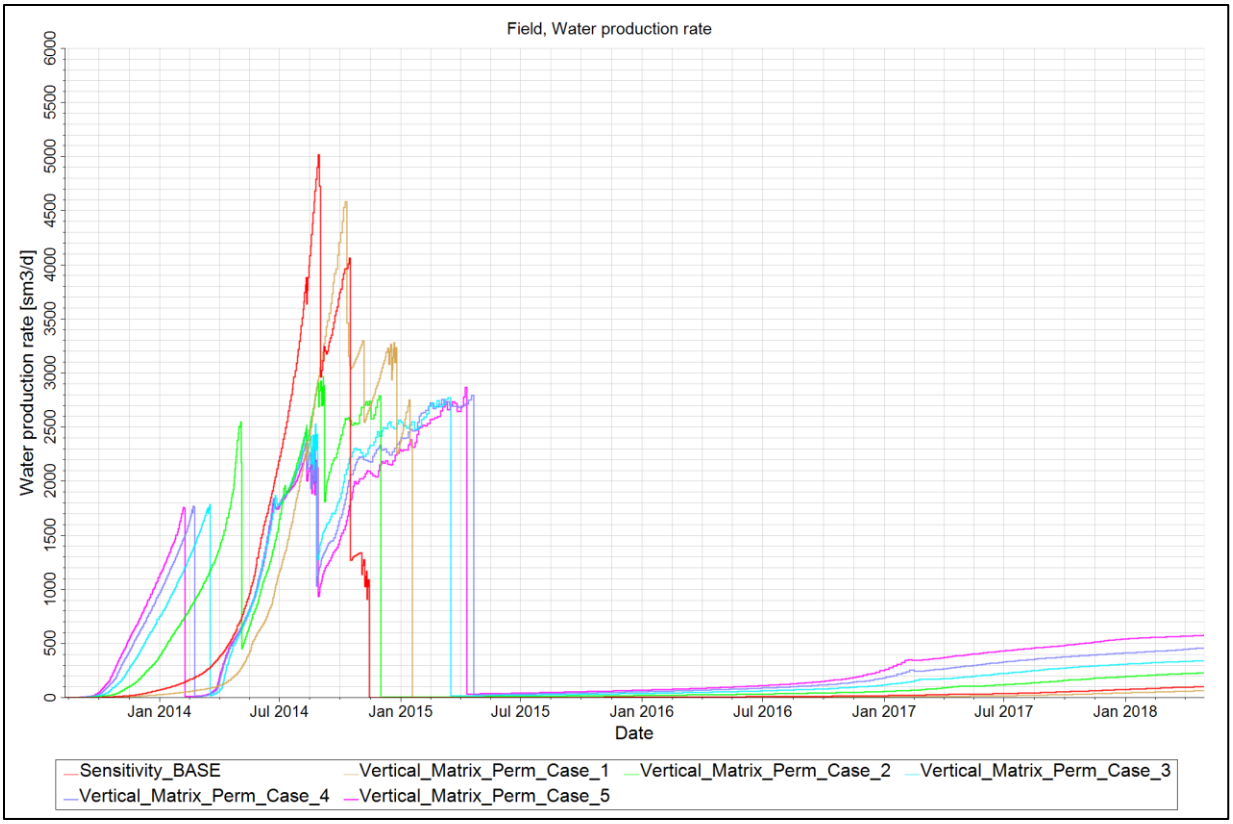

Figure 7.1.2: Water production rate comparison for various vertical matrix permeability sensitivity cases. This chart shows that decreasing vertical matrix permeability delays water production and decreases the intensity of water production.

7.2. Vertical Fracture Permeability

Table 7.2.1 shows the vertical fracture permeability multipliers and cumulative gas production for the five sensitivity cases. The cumulative gas production figure (Figure 7.2.1) and values (Table 7.2.1) show that increasing or decreasing vertical fracture permeability (cases 1-5) has little to no impact on cumulative gas production. The impact on the severity and timing of water production from the wells is also minimal as shown in Figure 7.2.2. These sensitivity results in conjunction with the result of vertical matrix permeability sensitivities discussed in 7.1 show that it is the vertical matrix permeability that has the greatest impact on the connectivity of the aquifer to the gas zone.

Table 7.2.1: Vertical Fracture Permeability multipliers

Case #	Vertical Perm Multiplier	Cumulative Gas Production E9m3 (Bcf)
1	0.5	6.2 (220)
2	2.9	6.2 (219)
3	5.25	6.2 (218)
4	7.6	6.2 (218)
5	10	6.1 (217)

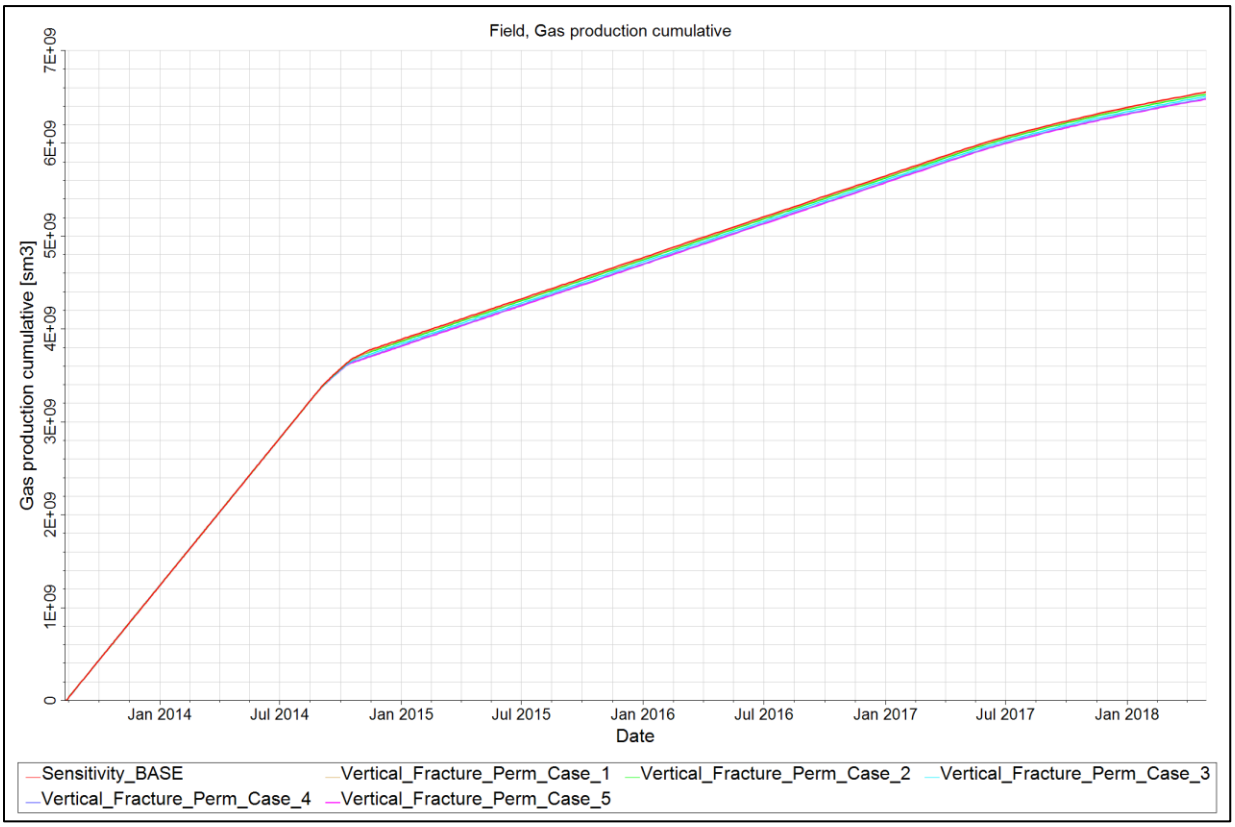

Figure 7.2.1: Cumulative gas production compared for various vertical fracture permeability sensitivities. Vertical fracture permeability has only a minor impact on gas production.

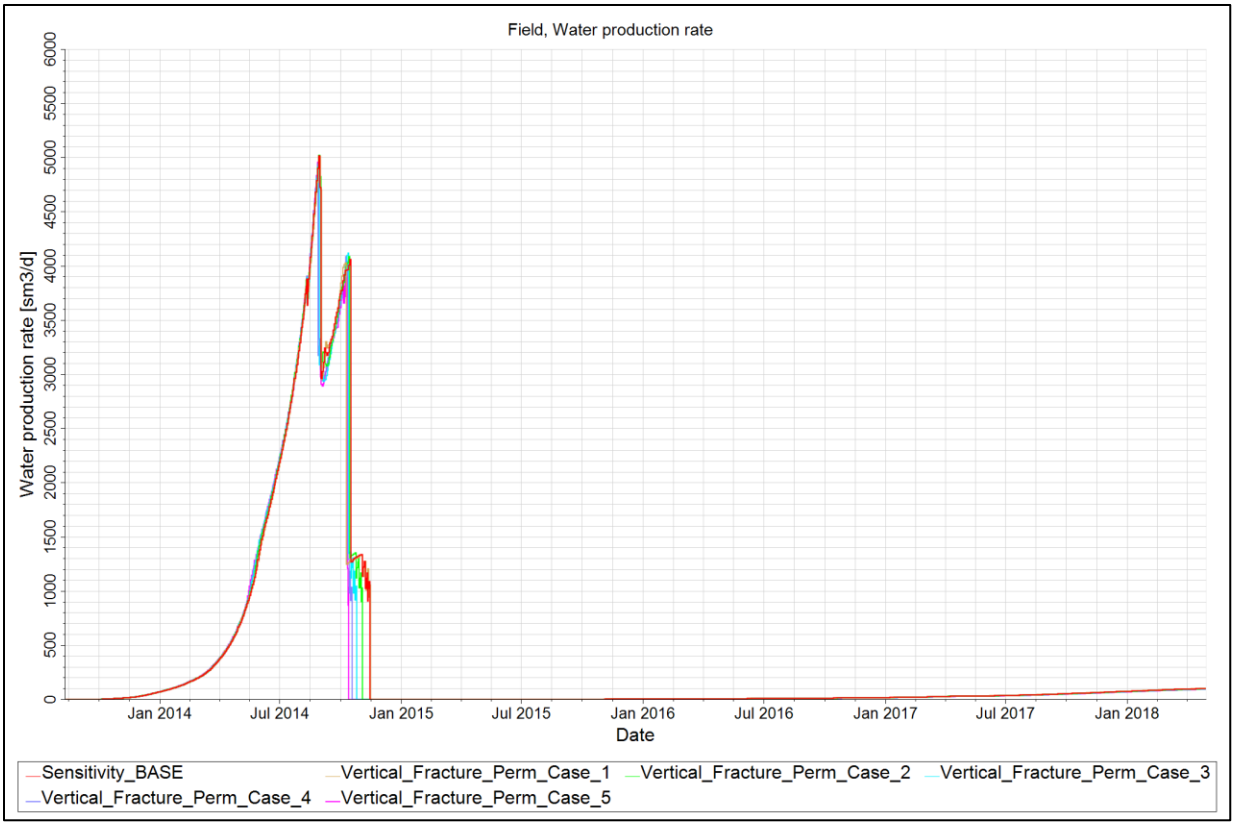

Figure 7.2.2: Water production rate compared for various vertical fracture permeability sensitivities. Vertical fracture permeability has only a minor impact on water production.

7.3. Perforation Length Increase

Table 7.3.1 shows three cases where the length of the existing well perforations was increased to evaluate the impact on gas recovery. The cumulative gas production figure (Figure 7.3.1) and values (Table 7.3.1) show that increasing the perforation length (Cases 1-3) had no impact on cumulative gas production or on the severity and timing of water production from the wells (Figure 7.3.2).

Table 7.3.1: Increase in Length of Perforations

Case #	Increase in Length of Perforations (m)	Cumulative Gas Production E9m3 (Bcf)
1	10	6.5 (230)
2	25	6.5 (230)
3	40	6.5 (230)

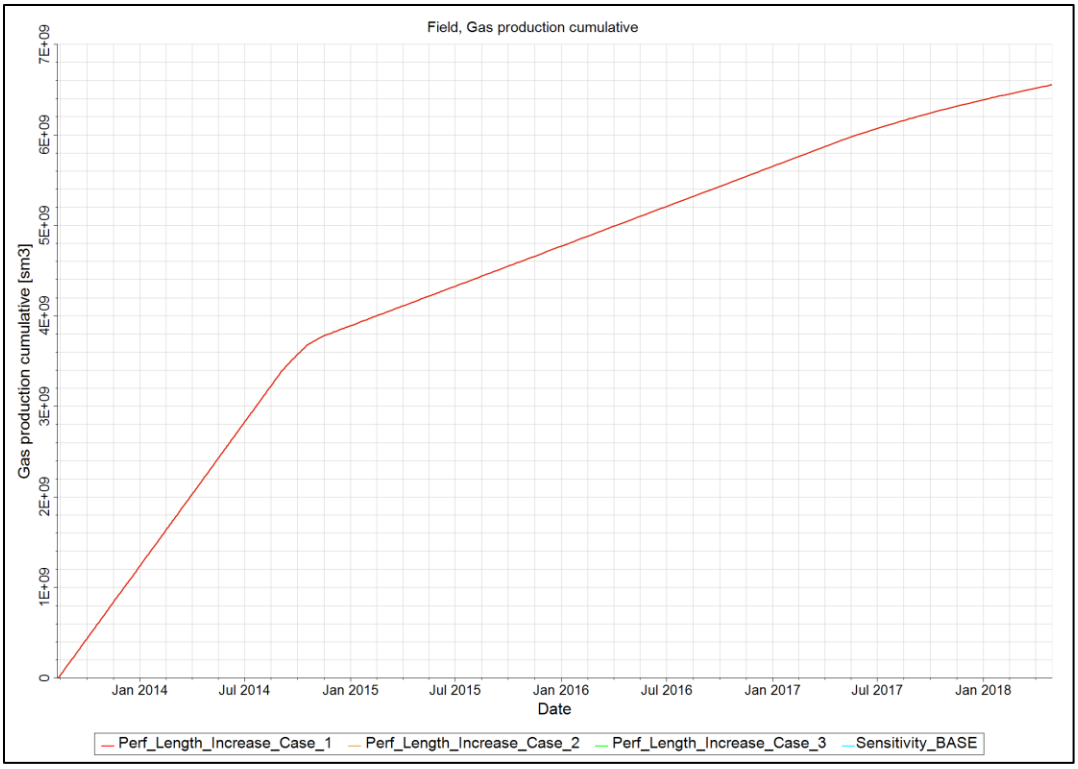

Figure 7.3.1: Cumulative gas production compared for different perforation lengths. The perforation length increases have no impact on gas production.

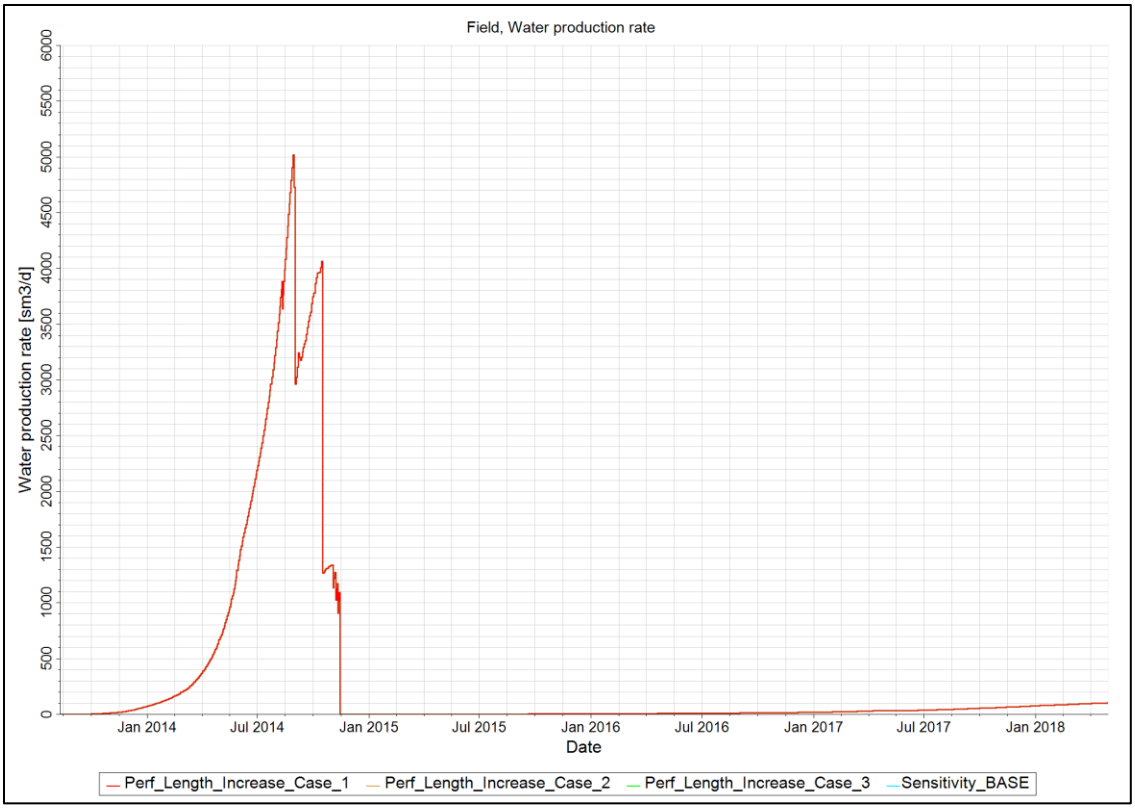

Figure 7.3.2: Water production compared for different perforation lengths. The perforation length increases have no impact on water production.

7.4. Perforation Length Decrease

Table 7.4.1 shows the three cases where the length of existing well perforations was decreased to evaluate the impact on overall gas recovery. The cumulative gas production figure (Figure 7.4.1) and values (Table 7.4.1) show that decreasing perforation length (Cases 1-3) had only minimal impact on cumulative gas production and on the severity and timing of water production (Figure 7.4.2).

Table 7.4.1: Decrease in Length of Perforations

Case #	Decrease in Length of Perforations (m)	Cumulative Gas Production E9m3 (Bcf)
1	10	6.5 (229)
2	25	6.5 (229)
3	40	6.5 (229)

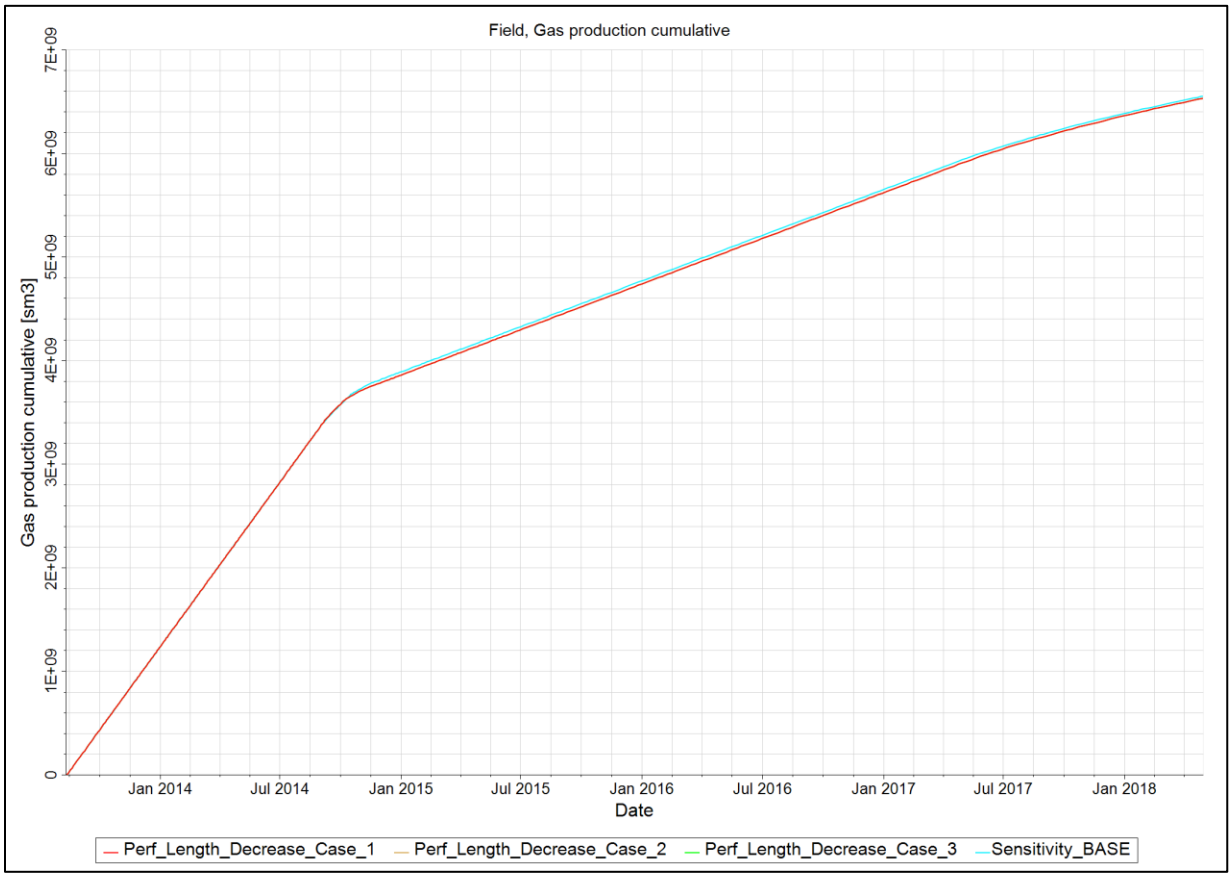

Figure 7.4.1: Cumulative gas production compared for various cases of perforation length decreases. Decreasing the length of the perforations has a minor impact on gas production.

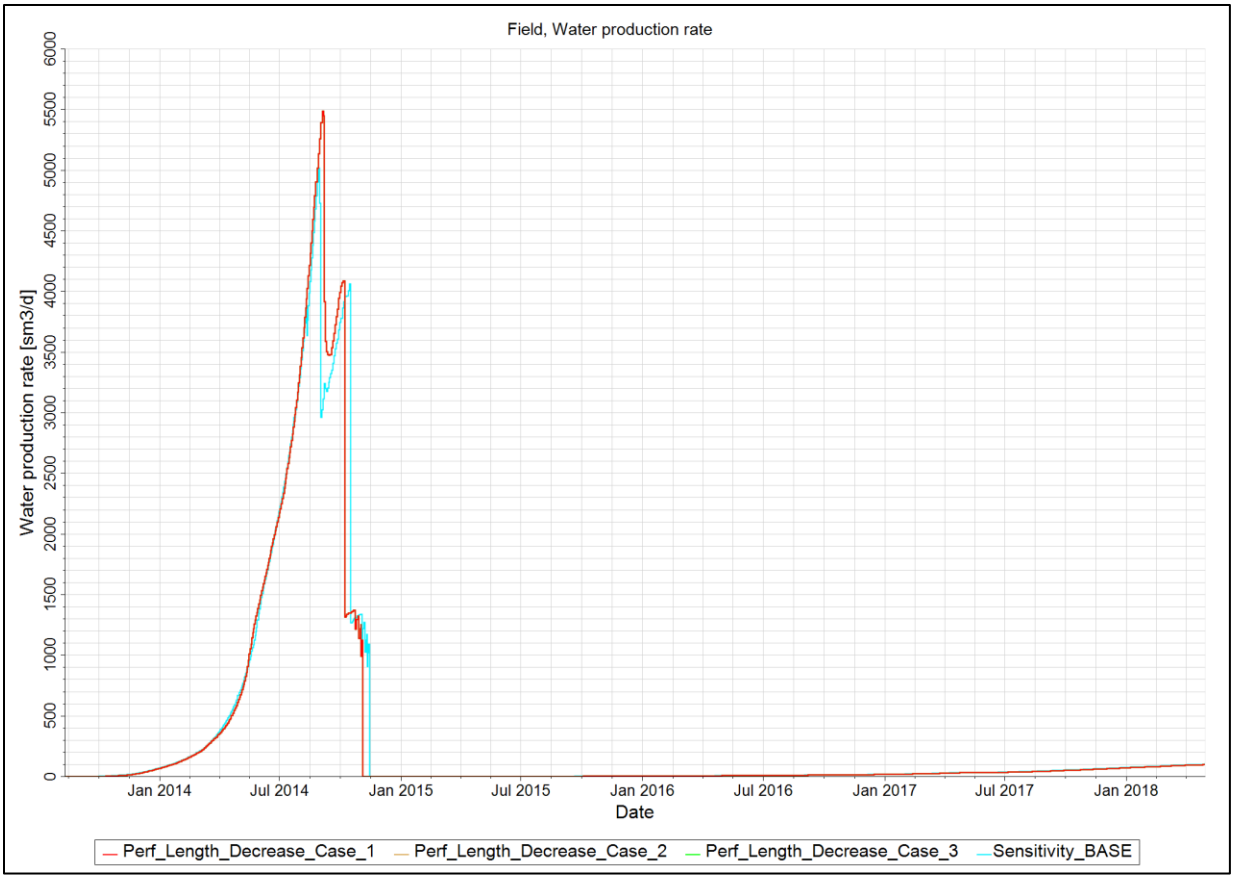

Figure 7.4.2: Water production compared for various cases of perforation length decreases. Decreasing the length of the perforations has only a minor impact on water production.

7.5. Rate Variability

Table 7.5.1 shows gas rate sensitivities and cumulative gas production for five rate sensitivity cases. The cumulative gas production figure (Figure 7.5.1) and values (Table 7.5.1) show that increasing the gas rate from 1.4 E6m3 (50 MMscf/d) to 2.5 E6m3 (87 MMscf/d) has a significant impact (31% increase) on cumulative gas production. The increases in cumulative gas production are relatively modest when the gas rate was increased from 2.5 E6m3/d (87 MMscf/d) to 3.5 E6m3/d (124 MMscf/d) (Figure 7.5.1). Increasing the gas rate caused earlier and more severe water production from the wells but also resulted in the greatest overall gas recovery, indicating that this method is the best production strategy for these types of reservoirs (Figures 7.5.1 & 7.5.2).

Table 7.5.1: Gas Rate Sensitivities

Case #	Gas Rate E6m3/d (MMscf/d)	Cumulative Gas Production E9m3 (Bcf)
1	1.4 (50)	5.0 (176)
2	1.9 (68)	6.0 (209)
3	2.5 (87)	6.5 (230)
4	3.0 (106)	6.6 (234)
5	3.5 (124)	6.7 (238)

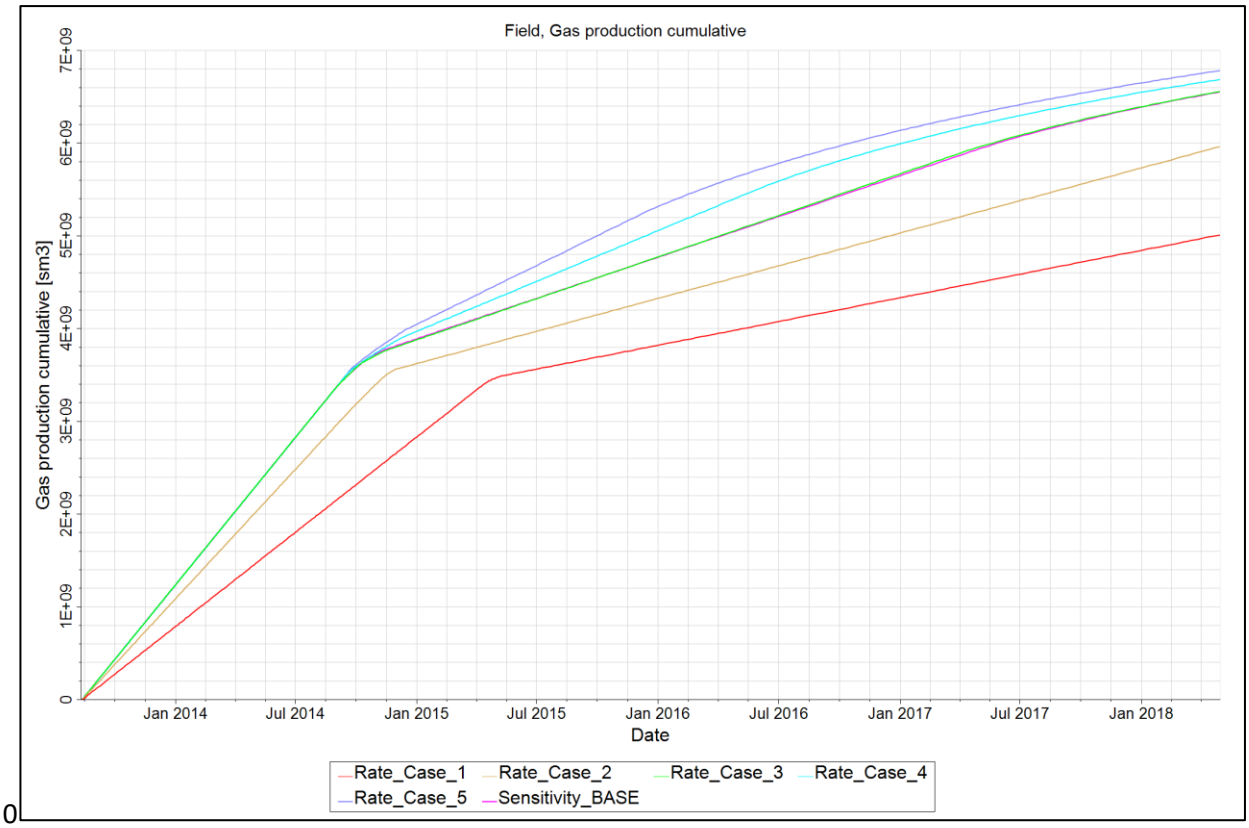

Figure 7.5.1: Comparison of cumulative gas production for five rate sensitivity cases. This chart validates the production strategy of producing the wells at high rates to maximize overall gas production.

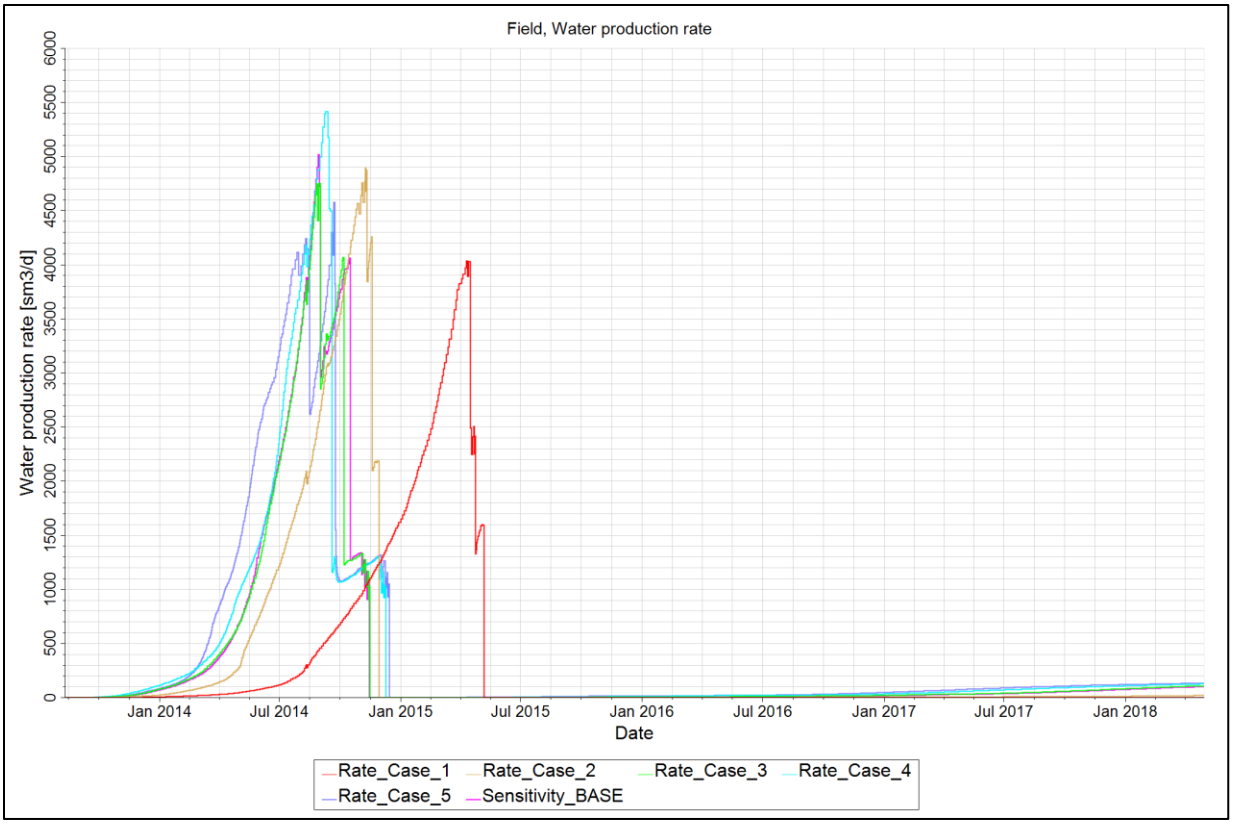

Figure 7.5.2: Comparison of water production for five rate sensitivity cases. This chart shows that water production is delayed when gas rate is lower. It was however shown in the previous chart that lower gas rate also decreases cumulative gas production from the field. While higher gas rates increase water production, this strategy also results in the greatest overall gas recovery.

Chaney Method was also used to calculate the critical gas rate that would cause water coning for the three vertical production wells. This method is used to determine the gas rate above which water conning in gas well is probable. Based on the analysis critical gas rates were the following (Table 7.5.2):

Table 7.5.2: Critical Water Coning Rate

Well	**Qc E6m3/d (MMscf/d)**
D-41	2.8 (100)
F-70	2.1 (75)
H-08	2.1 (75)

7.6. Additional Wells

The CNSOPB evaluated the option of drilling additional wells in different parts of the Deep Panuke field to assess the impact on overall gas recovery. A number of sensitivities were conducted and it was determined that the cost to drill and complete an additional production well(s) would significantly exceed the value of the incremental reserves that would be produced from the well. This analysis demonstrated that waste would not occur if no additional Deep Panuke production wells were drilled.

8. CNSOPB Resource Management Oversight

During the full life cycle of the Deep Panuke project, from the submission of the 2006 DPA to final decommissioning and abandonment, the CNSOPB ensured that the operator remained committed to sound resource conservation (waste prevention) practices and strategies. The operator was required to demonstrate to the CNSOPB on a regular basis that they had a comprehensive understanding of the petroleum resources under development and that their production activities maximized economic hydrocarbon recovery of the Deep Panuke resources and thus did not result in waste.

The CNSOPB's resource management oversight included independent geoscience and reservoir engineering models and studies, monitoring and surveillance of development and production activities and audits of the operator's resource management strategies and practices. In addition, advanced resource management tools and techniques were developed to monitor regulatory compliance against the numerous resource management documents submitted by the operator during the life of the project. The following are brief descriptions of some of the tools and methods used by the CNSOPB to ensure regulatory compliance and to verify waste of the resource did not occur.

8.1. Daily Monitoring and Surveillance

Section 80 of the *Nova Scotia Offshore Petroleum Drilling and Production Regulations* (Drilling and Production Regulations), requires operators to submit a daily production record, which includes but is not limited to gas and water production rates, WGR, tubing and subsurface pressures, flare volumes and fuel gas volumes.

The CNSOPB used various daily monitoring, surveillance and visualization tools and, dashboards to ensure any production anomalies were detected and discussed with the operator in a timely manner. The following are the key production parameters that were monitored for each Deep Panuke well on a daily basis:

- Daily gas production rate and production hours
- Daily condensate production rate and condensate to gas ratio
- Daily water production rate and WGR
- Daily wellhead and bottom-hole flowing pressures
- Daily wellhead and bottom-hole shut-in pressures and comparison charts
- Flared gas (percent of daily production)
- Acid gas injection rate, dilution gas, and acid gas compressor uptime
- Choke settings

The CNSOPB also monitored daily gas prices. These prices were used in various economic analyses and sensitivities to ensure economic hydrocarbon recovery was maximized (waste prevention). The general trend observed was that the prices were considerably higher during the winter months.

8.2. Monthly Monitoring and Surveillance

Section 85 of the Drilling and Production Regulations requires "*the operator to submit a report summarizing the production data collected during the preceding month*". To satisfy this requirement, the operator submitted monthly production reports to the CNSOPB while production was ongoing. The monthly production reports included the following data:

- Total field gas production

- Total field condensate production
- Total condensate and gas used as fuel
- Total gas flared
- Total acid gas injected and flared
- Total water produced from the field
- Dilution gas
- Sulphur production

The CNSOPB also used the monthly production data to analyze and monitor the performance of the field. The monthly data was used to perform decline analyses once the wells started declining. This decline analysis were used to predict remaining gas production.

8.3. Annual Production Reports

Section 86 of the Drilling and Production Regulations states that "*the operator shall ensure that, not later than March 31 of each year, an annual production report for a pool, field or zone is submitted to the Board providing information that demonstrates how the operator manages and intends to manage the resource without causing waste*".

These Annual Production Reports (APR) describe production activities and reviews the performance of the wells and pools in each producing field during the reporting period. This report is an important resource management document that is used by the CNSOPB to evaluate whether the field is being produced and managed in a manner that will not result in waste of the resource.

8.4. Reservoir Simulation Modeling

The reservoir simulation model described earlier in this report played a critical role in the CNSOPB's resource management oversight of the Deep Panuke project. It was regularly and actively used to ensure the operator's depletion plans and production strategies and practices did not result in waste by maximizing economic hydrocarbon recovery from the field.

8.5. Economic Analysis and End of Field Life Analysis

To ensure "waste" as defined in Section 159 of the *Canada-Nova Scotia Offshore Petroleum Resources Accord Implementation Act* (federal) does not occur, the CNSOPB is required to consider *"sound engineering and economic principle"* when making determinations related to the production operations, (e.g. well workovers, drilling of additional wells, cessation of production). In order to verify that the timing of production cessation for Deep Panuke would not result in waste, the CNSOPB conducted a detailed economic analysis which included a number of cost, commodity price and production sensitivities. The CNSOPB's economic analysis was conducted using both deterministic and probabilistic assessment methods. This economic analysis combined with an assessment of remaining reserves allowed the CNSOPB to ensure that the timing of production cessation for Deep Panuke would not result in waste.

8.6. Resource Management Plans

Section 16 of the Drilling and Production Regulations states that "*the development plan relating to a proposed development of a pool or field shall contain a resource management plan*". The Resource Management Plan (RMP) is the main document that describes how the operator intends to maximize economic hydrocarbon recovery (prevent waste) during the life of the project. During the life of the project as new data is acquired (e.g. production data, well test data, updated

simulation models etc.) the operator is required to ensure that this new data is analyzed and incorporated into the RMP to enhance the understanding of the reservoir and to ensure waste does not occur. The following are some of the main elements that are typically included in an RMP:

- Geological and geophysical description of the field(s)
- Petrophysical interpretations and analysis of each pool in the field(s)
- Reservoir engineering analyses and data
- In-place and recoverable reserve estimates
- Project depletion plan including the number of wells and contingent wells
- Well design of the production wells and a review of potential workovers
- Description of the production and export systems
- Expected overall operating efficiency
- Development and operating cost data

In addition to the initial RMP, Section 86 of the Drilling and Production Regulations, requires the operator to provide an annual RMP update. This annual update includes any changes to the in-place and recoverable hydrocarbon volumes, updated reservoir characterization, changes in production behaviour and any updates to the depletion plan. Economic information such as operating and capital costs are also included in these annual RMP updates.

8.7. Resource Management Meetings

Regular formal and informal meetings were scheduled with the operator's reservoir management team to discuss updates to the reservoir description, review changes in well and field performance, discuss well workovers, resource management strategies and depletion planning.

8.8. Resource Management Audits

The CNSOPB's resource conservation officers conducted audits of the operator's resource management strategies and practices including their reservoir simulation models. The scope of these audits included the following:

- A detailed review of the Deep Panuke reservoir simulation model.
- Assessment of resource management strategies and practices including supporting documentation.
- Valuation of reserve estimations.
- Evaluation of production forecasting methods and production forecasts.
- Review of production optimization methods.
- Assessment of reservoir modeling procedures and assumptions.
- Evaluate the drilling of additional production wells.
- Study of potential workovers.
- Evaluation of production rate sensitivities.
- Verification of bottom-hole pressure calculation methods.
- Audit of acid gas injection reservoir simulation model.

9. Conclusions and Lessons Learned

The key conclusions and lessons learned from the CNSOPB's Deep Panuke Resource Management Study are summarized below.

1. The recovery factor associated with water drive naturally fractured gas reservoirs such as Deep Panuke can be very low (as low as 20% of the original gas in place). Excessive water production is a common problem for these types of reservoirs. For fractured gas reservoirs, producing the wells at high rates is the most effective production strategy and while water production will likely increase it will also result in the greatest overall gas recovery.

2. The size of the aquifer and the degree of connectivity between the aquifer and gas zone were not well understood prior to the start of production due to the complex nature of the Deep Panuke reservoir and the relatively limited number of wells. In the 2006 DPA, the operator identified aquifer size and connectivity to the gas zone as major uncertainties that could have a significant impact on overall gas recovery.

3. The productivity of all production wells declined quickly after water production started. In general, once water production commenced and the wells began cycling, less gas was produced during each subsequent cycle and the duration of each cycle also decreased.

4. Simulation modeling is an important tool for managing fractured reservoirs such as Deep Panuke and predicting their performance. The uncertainties in the input data should be carefully considered when building a simulation model for fractured reservoirs. Typically, fracture properties are not well known. These uncertainties will decrease as production data

is obtained but at this stage, it may be too late to make significant changes to the depletion strategy (e.g. significantly increase water-handling capacity).

5. Using the simulation model to predict future gas production from the wells after the start of water production and during cyclic production was challenging mainly due to the complex nature of the reservoir and the fracture porosity system. To help mitigate these simulation modeling challenges, data-driven analytics and pattern recognition techniques were effective tools for analyzing and understanding the Deep Panuke reservoir.

6. During the life of the project as more production data was acquired it was determined that the four production wells were connected to a relatively modest volume of recoverable gas due to the complexity of the pore system and the connectivity to the underlying aquifer. The total cumulative production for the Deep Panuke field was 4.2 E9m3 (147.2 Bcf).

7. The CNSOPB's analysis confirmed that the operator's decision to not drill additional Deep Panuke production wells would not result in waste.

8. To match water production from H-08, F-70 and M-79A, a localized breach (high permeability fault/fracture), in the Tight Streak, was added near these wells to allow vertical water encroachment.

9. The horizontal orientation of M-79A did not result in a significant increase in gas recovery, compared to the other vertical production wells. However, the horizontal orientation of the well allowed water to drain back into the reservoir more easily and permitted the well to build pressure more rapidly after the well had water loaded during each production cycle.

10. Relatively late water production from D-41 was a result of the well's location higher on structure and the Tight Streak acting as a more effective barrier to vertical water encroachment, due to the lower density of fractures in this part of the field. As a result, D-41 had the highest overall gas recovery of any of the Deep Panuke production wells.

11. Acid treatments were generally successful at increasing well productivity. Foam injection was also used in an effort to decrease the density of the accumulated water column in the wells and improve gas recovery. These treatments were not as effective as acid treatments at increasing gas recovery.

10. Glossary

Acid gas
A gas that can form acidic solutions when mixed with water. The most common acid gases are hydrogen sulfide (H2S) and carbon dioxide (CO2) gases.

Bcf
Billion cubic feet.

Development Plan Application (DPA)
A plan submitted to the CNSOPB to obtain approval for developing an offshore oil or gas field.

Drill Stem Test (DST)
A procedure to determine the productive capacity, pressure, permeability or extent (or a combination of these) of a hydrocarbon reservoir.

Formation Micro Imager (FMI)
A logging tool used to generate an electrical image of the borehole.

Gas sweetening
The removal of H2S from sour gas.

Gel treatment
A method used to reduce permeability in the reservoir treatment volume in which the gels are ultimately placed to disconnect flow of water to perforations.

Inflow Performance Relationship (IPR)
Relation between the production rate and flowing bottom hole pressure.

Mcf
Thousand cubic feet.

mD
Millidarcies.

MMscf
Million standard cubic feet.

Modular Dynamics Formation Tester (MDTs)
Logging tool used for measurements of formation pressure, vertical and horizontal permeability of the formations near the wellbore and collection of formation fluid samples.

M&NP
Maritimes & Northeast Pipeline, which transfers natural gas to areas in Nova Scotia, New Brunswick, Maine and the Northeast U.S.

Original Gas in Place (OGIP)
The amount of gas first estimated to be in a reservoir.

Original fluids-in-place (OFIP)
The total amount of all fluids first estimated to be in a reservoir.

PERMX
Permeability in the x-direction.

PERMY
Permeability in the y-direction.

PERMZ
Permeability in the z-direction.

Plug back
A single operation in which a deeper zone is abandoned in order to attempt a completion in a shallower zone.

Production Logging Tool (PLT)
Logging tools used to evaluate the behavior of fluids in or around the borehole during production or injection.

Recoverable Gas in Place (RGIP)
The amount of gas that can be produced using currently available technology and industry practices regardless of any economic or accessibility considerations.

Resource Management Plan (RMP)
A plan that must be submitted to the CNSOPB to describe an operator's approach and commitment to resource management and conservation.

Tcf
Trillion cubic feet.

11. References

Pow, M., Allan, V., Mallmes, R., & Kantzas, A. (1997). Production of Gas from Tight Naturally fractured Reservoirs with Active Water. Annual Technical Meeting. doi:10.2118/97-03

Reiss, L. (n.d.). The Reservoir Engineering Aspects of Fractured Formations. Golf-Racht, T. D. (2011). Fundamentals of fractured reservoir engineering. Amsterdam: Elsevier.

Heinemann, Z., & Mittermeir, G. (2014). Natural Fractured Reservoir Engineering (Vol. 5). Warren, J., & Root, P. (1963). The Behavior of Naturally Fractured Reservoirs. Society of Petroleum Engineers.

Maysami, M., Gaskari, R., & Mohaghegh, S. D. (2013). Data Driven Analytics in Powder River Basin, WY. SPE Annual Technical Conference and Exhibition. doi:10.2118/166111-ms

Rezaee, M., Rostami, B., Zadeh, M., & Mojarrad, M. (2013). Experimental Determination of Optimised Production Rate and Its Upscaling Analysis in Strong Water Drive Gas Reservoirs. International Petroleum Technology Conference. doi:10.2523/16938-abstract

Aguilera, R. (1999). Recovery Factors and Reserves in Naturally Fractured Reservoirs. Journal Of Canadian Petroleum Technology, 38(07). doi:10.2118/99-07-da

Hamon, G., Mauduit, D., Bandiziol, D., & Massonnat, G. (1991). Recovery Optimization In A Naturally Fractured Water-Drive Gas Reservoir: Meillon Field. SPE Annual Technical Conference and Exhibition. doi:10.2118/22915-ms

Armenta, M., & Wojtanowicz, A. (2002). Severity of Water Coning in Gas Wells. SPE Gas Technology Symposium. doi:10.2118/75720-ms

Beattie, D., & Roberts, B. (1996). Water Coning in Naturally Fractured Gas Reservoirs. Proceedings of SPE Gas Technology Symposium. doi:10.2523/35643-ms

Wassmuth, F., Green, K., & Hodgins, L. (2004). Water Shutoff in Gas Wells: Proper Gel Placement Is the Key to Success. SPE/DOE Symposium on Improved Oil Recovery. doi:10.2118/89403-ms

Deep Panuke Initial Development Plan. (March 2002).

Deep Panuke Development Plan Addendum. (November 2002).

Deep Panuke Volume 2 (Development Plan). (November 2006).